

Oak Ridge National Laboratory Assessment of the Electrical Substation-Grid Test Bed with Inside/Outside Devices and Distributed Ledger Technology



Emilio C. Piesciorovsky
Raymond Borges Hink
Aaron Werth
Gary Hahn
Annabelle Lee
Jason Richards
Yarom Polsky

April 2022



DOCUMENT AVAILABILITY

Reports produced after January 1, 1996, are generally available free via OSTI.GOV.

Website www.osti.gov

Reports produced before January 1, 1996, may be purchased by members of the public from the following source:

National Technical Information Service
5285 Port Royal Road
Springfield, VA 22161
Telephone 703-605-6000 (1-800-553-6847)
TDD 703-487-4639
Fax 703-605-6900
E-mail info@ntis.gov
Website <http://classic.ntis.gov/>

Reports are available to DOE employees, DOE contractors, Energy Technology Data Exchange representatives, and International Nuclear Information System representatives from the following source:

Office of Scientific and Technical Information
PO Box 62
Oak Ridge, TN 37831
Telephone 865-576-8401
Fax 865-576-5728
E-mail reports@osti.gov
Website <https://www.osti.gov/>

This report was prepared as an account of work sponsored by an agency of the United States Government. Neither the United States Government nor any agency thereof, nor any of their employees, makes any warranty, express or implied, or assumes any legal liability or responsibility for the accuracy, completeness, or usefulness of any information, apparatus, product, or process disclosed, or represents that its use would not infringe privately owned rights. Reference herein to any specific commercial product, process, or service by trade name, trademark, manufacturer, or otherwise, does not necessarily constitute or imply its endorsement, recommendation, or favoring by the United States Government or any agency thereof. The views and opinions of authors expressed herein do not necessarily state or reflect those of the United States Government or any agency thereof.

Electrification and Energy Infrastructures Division

**OAK RIDGE NATIONAL LABORATORY ASSESSMENT OF THE ELECTRICAL
SUBSTATION-GRID TEST BED WITH INSIDE/OUTSIDE DEVICES AND
DISTRIBUTED LEDGER TECHNOLOGY**

Emilio Carlos Piesciorovsky
Raymond Borges Hink
Aaron Werth
Gary Hahn
Annabelle Lee
Jason Richards
Yarom Polsky

April 2022

Prepared by
OAK RIDGE NATIONAL LABORATORY
Oak Ridge, TN 37831-6283
managed by
UT-BATTELLE, LLC
for the
US DEPARTMENT OF ENERGY
under contract DE-AC05-00OR22725

CONTENTS

LIST OF FIGURES	v
LIST OF TABLES.....	vii
ABBREVIATIONS	ix
ABSTRACT.....	x
1. INTRODUCTION	1
2. ELECTRICAL SUBSTATION-GRID TEST BED SYSTEM.....	3
2.1 ELECTRICAL SUBSTATION-GRID TEST BED ONE-LINE DIAGRAM.....	3
2.2 SOFTWARE STEPS AND APPLICATIONS	4
2.3 RT-LAB PROJECT FOR THE ELECTRICAL SUBSTATION-GRID TEST BED.....	5
2.4 ELECTRICAL WIRING FOR INSIDE AND OUTSIDE SUBSTATION DEVICES	12
3. ELECTRICAL PROTECTION AND MEASUREMENT SYSTEM	16
3.1 CALCULATION OF INVERSE TIME OVERCURRENT SETTINGS.....	16
3.2 POWER PROTECTION AND METERING SYSTEM.....	19
3.3 PROTECTIVE RELAY SETTINGS	19
3.4 POWER METER SETTINGS	25
4. TIME SYNCHRONIZATION SYSTEM.....	28
4.1 TIME FRAME SOURCES	28
4.2 COMMUNICATION AND SETTING OF THE SEL-2488 SATELLITE- SYNCHRONIZED NETWORK CLOCK	29
4.3 SYNCHRONIZED TIME PROTOCOLS	32
5. COMMUNICATION SYSTEM.....	33
5.1 IEC 61850 VS. DNP COMMUNICATION	33
5.2 SETTING OF THE IEC 61850 MAP FOR DEVICES	33
5.3 IEC 61850 MAPS FOR THE SEL-451 RELAYS AND SEL-735 POWER METERS.....	38
5.4 SETTING OF DNP MAP FOR THE SEL-734 POWER METERS	41
5.5 RTAC FOR THE SEL-734 POWER METERS	42
5.6 TELNET NETWORK COMMUNICATION.....	47
6. DLT SYSTEM.....	49
6.1 DLT INTRODUCTION.....	49
6.2 DLT EQUIPMENT AND DIAGRAM.....	49
7. TEST BED ARCHITECTURE AND WORKSTATIONS	52
7.1 TEST BED ARCHITECTURE.....	52
7.2 TEST BED WORKSTATIONS AND SERVERS	54
7.2.1 Host computer.....	55
7.2.2 HMI computer.....	55
7.2.3 DLT-SCADA computer.....	55
7.2.4 Traffic network computer	56
7.2.5 Control center and local HMI computers.....	57
7.2.6 VM Blueframe computer	57
7.2.7 The DLT master node	57
7.2.8 EmSense high-speed SV emulator device	57
8. BLUEFRAME OPERATING SYSTEM.....	58
8.1 OVERVIEW	58
8.2 OPERATION	58
8.3 SETTING UP BLUEFRAME.....	59
9. TEST BED RESULTS.....	61
9.1 OVERVIEW	61
9.2 RESULTS OF ANALOG SIGNALS	61

9.2.1	Analog signals for protective relays	61
9.2.2	Analog signals for power meters	64
9.3	RESULTS OF TIMING AND SYNCHRONIZED SOURCE	68
9.4	RESULTS OF THE IEC 61850 AND DNP MESSAGES	70
9.4.1	IEC 61850 for the SEL-451 protective relays.....	70
9.4.2	IEC 61850 for the SEL-735 power meters	72
9.4.3	DNP for the SEL-734 power meters.....	74
9.5	RESULTS OF ELECTRICAL FAULT TESTS	76
9.5.1	Electrical fault test events	76
9.5.2	Electrical fault event detection with DLT.....	78
10.	DISCUSSION AND CONCLUSIONS	80
10.1	ELECTRICAL SUBSTATION-GRID TEST BED DISCUSSIONS.....	80
10.2	CONCLUSIONS.....	83
11.	REFERENCES	85
APPENDIX A. Data floating points of protective relays and power meters.....		A-1

LIST OF FIGURES

Figure 1. Electrical substation-grid test bed with DLT and inside/outside devices for cyber event detection.	1
Figure 2. One-line diagram of electrical substation-grid test bed power system.	3
Figure 3. Software applications to build the electrical substation-grid test bed.	4
Figure 4. SM_Master (A) and SC_Console (B) subsystems.	6
Figure 5. Electrical substation-grid test bed system.	7
Figure 6. Current (A, B) and voltage (C, D) interfaces of SEL-451 relays.	8
Figure 7. Current (A, B) and voltage (C, D) interfaces of SEL-734 and SEL-735 power meters.	9
Figure 8. Trip/close (A) and pole state (B) interfaces and trip/close signal circuits (C, D) of breakers for the SEL-451 protective relays.	10
Figure 9. Data acquisition circuit to collect signals from inside (A, B) and outside (C, D) substation devices with OpWrite File block (E).	10
Figure 10. OpComm block (A) with scopes for inside (B, C) and outside (D, E) electrical substation devices.	11
Figure 11. Scope for the SEL-451 protective relays (A–C) and SEL-735 power meters (D–G).	12
Figure 12. Wiring of analog signals for the SEL-451 relays.	13
Figure 13. Wiring of analog signals for the SEL-734 and SEL-735 power meters.	13
Figure 14. Form 5 (2-Element, 3 Wire Delta) configuration of power meter.	14
Figure 15. Form 9 (3-Element, 4 Wire Wye) configuration of power meter.	14
Figure 16. Wiring of digital signals for the SEL-451 protective relays.	15
Figure 17. Inverse time overcurrent curve coordination of fuses and relays at SEL-734 (A) and SEL-735 (B) power meter locations.	18
Figure 18. Minimum CTI between fuses and relays with electrical faults located at SEL-734 and SEL-735 power meter bus locations.	19
Figure 19. General Global Settings for the SUB_SEL451_FED1 protective relay.	20
Figure 20. Breaker 1 settings for the SUB_SEL451_FED1 and SUB_SEL451_FED2 protective relays.	21
Figure 21. Line Configuration settings for the SUB_SEL451_FED1 and SUB_SEL451_FED2 protective relays.	21
Figure 22. Relay Configuration Enables settings for the SUB_SEL451_FED1 and SUB_SEL451_FED2 protective relays.	22
Figure 23. Time Overcurrent settings for the SUB_SEL451_FED1 and SUB_SEL451_FED2 protective relays.	22
Figure 24. Protocol Selection and Communications settings for the SUB_SEL451_FED1 and SUB_SEL451_FED2 protective relays.	23
Figure 25. IP Configuration settings for the SUB_SEL451_FED1 protective relay.	24
Figure 26. Telnet Configuration (A), IEC 61850 Configuration (B), and IEC 61850 Mode/Behavior Configuration (C) settings for the SUB_SEL451_FED1 and SUB_SEL451_FED2 protective relays.	24
Figure 27. General Settings for GRID_SEL_734_FED1 (A) and GRID_SEL_735_FED1 power meters.	26
Figure 28. Ethernet Settings of the GRID_SEL_734_FED1 power meter.	27
Figure 29. Ethernet Settings of the GRID_SEL_735_FED1 power meter.	27
Figure 30. Time synchronization system for electrical substation-grid test bed.	28
Figure 31. UTC vs. USA time zones (https://www.calculator.net/time-zone-calculator.html).	29
Figure 32. Steps to communicate with the SEL-2488 Satellite-Synchronized Network Clock.	29
Figure 33. Local Time Settings of the SEL-2488 Satellite-Synchronized Network Clock.	30
Figure 34. Manual Date/Time settings for the SEL-2488 Satellite-Synchronized Network Clock.	30

Figure 35. IP Configuration settings for the SEL-2488 Satellite-Synchronized Network Clock.	31
Figure 36. Front Panel settings for the SEL-2488 Satellite-Synchronized Network Clock.	31
Figure 37. The created CID project file.	34
Figure 38. Firmware Identifier number of the SEL-451 protective relay.	34
Figure 39. Steps to select the IED.	35
Figure 40. Steps to set the IED Properties.	36
Figure 41. Steps to set the GOOSE Transmit (Metered Values) message of the IED.	36
Figure 42. Steps to set the Dataset (Metered Values) of the IED.	37
Figure 43. Steps to submit the CID file to the IED.	38
Figure 44. CID datasets of SEL-451 protective relays (A) and SEL-735 power meters (B).	39
Figure 45. Steps to set the DNP map of SEL-734 power meters.	41
Figure 46. Steps to find the Firmware version of the SEL-3530-4 RTAC.	43
Figure 47. Steps to log in with RTAC Database (A) and create a new RTAC project (B).	43
Figure 48. Steps to insert an SEL-734 device (A) and connection type (B).	44
Figure 49. SEL-734 Settings based on RTAC AcSELeRator (A) and AcSELeRator Quickset (B) software.	44
Figure 50. Steps to add analog inputs for the SEL-734 device at RTAC project.	45
Figure 51. Steps to set the SCADA device at the RTAC project.	46
Figure 52. Steps to set analog inputs of SEL-734 power meters in the Tag Processor.	46
Figure 53. Steps to observe the device traffic with the controller.	47
Figure 54. IP address (A) and steps (B) for Telnet Network communication.	48
Figure 55. Overview of the DLT network.	50
Figure 56. Architecture of the electrical substation-grid test bed with protective relays and power meters using DLT devices to study future cyber events.	52
Figure 57. Electrical substation-grid test bed and workstations.	54
Figure 58. IEC 61850 data displayed by one of the Attestation Framework modules.	56
Figure 59. Architecture of a representative DLT, Blueframe platform, and IED devices with the physical connections in addition to the logical connections and communications.	58
Figure 60. Main page of SEL Blueframe Portal after the user logs in.	59
Figure 61. Disturbance Monitoring App with plans from a user.	59
Figure 62. API App.	60
Figure 63. Measured currents and voltages of the SUB_SEL451_FED1 (A) and SUB_SEL451_FED2 (B) protective relays from the HMI with <i>CTR</i> of 80 and <i>PTR</i> of 60.	62
Figure 64. SEL-735 power meters with a current gain of 1 V/2,000 A (A) and 1 V/200 A (B) in the RT-LAB project.	65
Figure 65. SEL-735 power meters with a voltage gain of 1 V/9,000 V in the RT-LAB project.	65
Figure 66. Measured currents and voltages of the GRID_SEL735_FED1 (A) and GRID_SEL735_FED2 (B) power meters from HMI with <i>CTR</i> of 225 and <i>PTR</i> of 449.	66
Figure 67. Measure currents and voltages of the GRID_SEL734_FED1 (A) and GRID_SEL734_FED2 (B) power meters from HMI with <i>CTR</i> of 225 and <i>PTR</i> of 449.	67
Figure 68. Steps to evaluate the time source from SEL-451 relay display.	69
Figure 69. GOOSE Dataset of SEL-451 relays generated with the AcSELeRator Architect software.	70
Figure 70. GOOSE messages of SEL-451 protective relays collected with Wireshark software.	71
Figure 71. IEEE-754 floating-point converter website.	71
Figure 72. GOOSE Dataset of SEL-735 power meters generated with the AcSELeRator Architect software.	72
Figure 73. GOOSE message of SEL-735 power meters collected with Wireshark software.	73
Figure 74. Steps to log in with the SEL-3530-4 RTAC (A) and capture SEL-734 power meter messages (B).	74
Figure 75. DNP message of SEL-734 power meter collected with Wireshark software.	75

Figure 76. SEL-451 protective relay event for the SEL-734_AG-FAULT test.....	77
Figure 77. SEL-451 protective relay event for the SEL-734_AB-FAULT test.....	77
Figure 78. SEL-451 protective relay event for the SEL-734_ABG-FAULT test.....	78
Figure 79. SEL-451 protective relay event for the SEL-734_ABC-FAULT test.....	78
Figure 80. Percent error of measured voltages (A) and currents (B) for inside and outside substation devices at the electrical substation-grid test bed.....	80
Figure 81. Phasor diagrams of measured currents and voltages for the SEL-451 protective relays (A, B), SEL-735 power meters (C, D) and SEL-734 power meters (E, F) from GOOSE and DNP messages at the electrical substation-grid test bed.....	82
Figure 82. Electrical fault detection of SEL-451 relay (A) vs. DLT (B) and relay time percent error (C).	83

LIST OF TABLES

Table 1. Software applications used to build the electrical substation-grid test bed	5
Table 2. Radial power system configuration with outside substation devices and maximum load currents.....	16
Table 3. Constants and factors of SEL-451 protective relays and 50/100 T fuses	17
Table 4. Electrical fault and pre-fault RMS current magnitudes for primary and backup protection devices.....	18
Table 5. Settings for the SEL-451 protective relays	20
Table 6. Protocols and IP address for the SEL-451 protective relays.....	23
Table 7. General Settings for the SEL-734 and SEL-735 power meters	25
Table 8. Protocols and IP address for the SEL-734 and SEL-735 power meters	25
Table 9. Logical Node, Attribute, Data Source, and Description values for the SEL-451 protective relays and SEL-735 power meters (IEC 61850)	40
Table 10. Exported DNP map for analog inputs and outputs of SEL-734 power meters	42
Table 11. Summary of DLT devices.....	51
Table 12. IP address and function of inside and outside substation devices	53
Table 13. IP address and function of main devices at the control center.....	54
Table 14. Results for the electrical substation-grid test bed	61
Table 15. Measured currents and voltages of SEL-451 protective relays	63
Table 16. Percent errors of measured phase primary currents and phase to neutral primary voltages for the SEL-451 protective relays.....	64
Table 17. Measured primary currents and voltages of SEL-734 and SEL-735 power meters.....	67
Table 18. Percent error of measured primary current and voltage of SEL-734 and SEL-735 power meters	68
Table 19. Home screen and level menu settings for the date/time of the SEL-735 power meters	69
Table 20. Comparison of calculated relay time vs. measured relay time for the SEL-451 relay	77
Table 21. Assessment of electrical fault event detection with the relay HMI and DLT computer.....	79
Table A. 1. Assessment of data floating points converted from hexadecimal to decimal values for the SEL-451 protective relays	A-1
Table A. 2. Assessment of data floating points converted from hexadecimal to decimal values for the SEL-735 power meters	A-2
Table A. 3. Assessment of data floating points converted to measured values for the SEL-734 power meters.....	A-3

ABBREVIATIONS

3L	three line
3LG	three line-to-ground
CT	current transformer
CTI	coordination time interval
DLT	distributed ledger technology
DNP	Distributed Network Protocol
GOOSE	Generic Object Oriented Substation Events
GUI	graphical user interface
HIL	hardware-in-the-loop
HLF	Hyperledger Fabric
HMI	human-machine interface
IED	intelligent electronic device
IRIG-B	Inter-Range Instrumentation Group–Time Code Format B
ITC	inverse time current
LL	line-to-line
LLG	line-to-line ground
LLTI	low-level test interface
MV	medium voltage
NTP	Network Time Protocol
PT	power transformer
PTP	Precision Time Protocol
RAM	random-access memory
RMS	root mean square
RTAC	real-time automation controller
SCADA	supervisory control and data acquisition
SLG	single line-to-ground
SV	sampled values
VM	virtual machine
VT	voltage transformer

ABSTRACT

The electrical substation-grid test bed was created to integrate GOOSE (Generic Object Oriented Substation Events) and/or DNP (Distributed Network Protocol) messages with time synchronized sources and distributed ledger technology (DLT). The objective was to study the impact of electrical faults and cyber events at an electrical substation with inside and outside substation devices. The electrical substation-grid test bed was based on the design of a 34.5/12.47 kV electrical substation (sectionalized bus configuration) with two power transformers, connected to radial power lines and load feeders. The electrical substation-grid test bed was installed at the Advanced Power System Protection lab space at the Grid Research Integration and Deployment Center, at the US Department of Energy's Oak Ridge National Laboratory. This test bed was created for the DLT task of the DarkNet project.

The electrical substation-grid test bed was created to simulate electrical faults and/or cyber events that could cause damage to the electrical infrastructure. In addition, tests were run that are usually not allowed to be performed in an operational electrical power grid because these test scenarios could trip circuit breakers and/or generate electrical fault situations that could damage equipment. The tests performed in the electrical substation-grid test bed were executed in a better way than in a real electrical substation and/or power grid because multiple tests could be run in a short period of time, and complex permits and safety/schedule restrictions like in a real electrical substation environment were not needed.

The electrical substation-grid test bed was created using real measurement, communication, and protection devices that are used by electrical utility companies to have the same conditions as in a real power grid or electrical substation. The electrical substation-grid test bed was based on using a real-time simulator and expansion box with amplifiers that were wired to electrical substation-grid devices. This hardware-in-the-loop included protective relays, power meters, Ethernet switches, remote terminal units, a synchronized timing network clock, DLT devices, workstations, and servers.

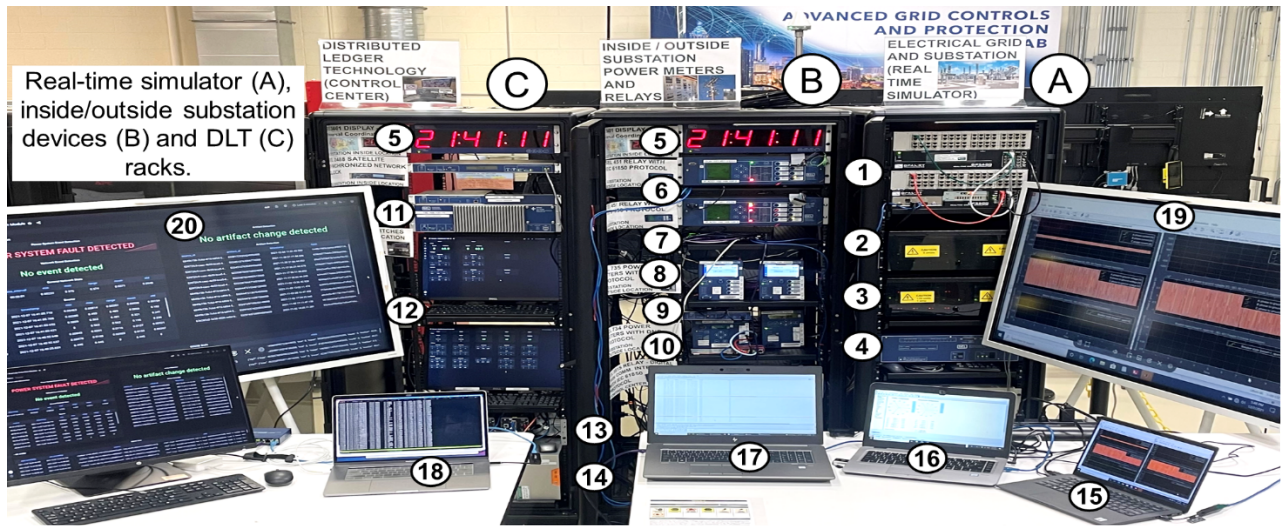
This report describes the design, installation, and assessment of the electrical substation-grid test bed that was similar to an operational electrical substation, integrating the power system protection, communication, and control systems. The results for the electrical substation-grid test bed were based on

- Verifying the analog signals for protective relays and power meters,
- Observing the synchronized time source frame at devices,
- Authenticating the GOOSE (IEC [International Electrotechnical Commission] 61850) and DNP messages from power meters and protective relays, and
- Verifying the trip conditions of protective relays at electrical faults with the power system fault event detection using DLT devices.

For future work, the electrical substation-grid test bed with protective relays and power meters using DLT and synchronized time source from DarkNet will be used to study the impact of cyber events at inside and outside substation devices. Advanced algorithms for detecting cyber events produced by undesirable protective relay settings will be studied to improve the detection and reliability of protection, control, and communication systems at power grids.

1. INTRODUCTION

This report describes the design, installation, and assessment of the electrical substation-grid test bed at the Advanced Power System Protection lab space at the Grid Research Integration and Deployment Center, at the US Department of Energy's Oak Ridge National Laboratory. This test bed was developed to create a real framework to study the scalability of distributed ledger technology (DLT) data architecture and vulnerability assessment in an electrical substation with inside and outside substation devices. The test bed had a real-time simulator rack (Figure 1A), inside/outside substation device rack (Figure 1B), and DLT communication rack (Figure 1C). The main goal of this test bed was to generate different power system scenarios, such as normal operation and electrical fault events. The electrical substation-grid test bed was created to perform electrical fault and cyber event tests for inside and outside devices with IEC (International Electrotechnical Commission) 61850 protocol and/or DNP (Distributed Network Protocol). Figure 1 shows the electrical substation-grid test bed.



Real time simulator (1), 5 A amplifiers (2), 1 A /120 V amplifiers (3), power source (4), clock displays (5), SEL 451 relays (6), ethernet switch (7), SEL 735 meters (8), SEL 3530-4 RTAC (9), SEL 734 meters (10), SEL 3555 RTAC (11), SCADA screens (12), CISCO ethernet switches (13), DLT devices (14), host computer workstation (15), HMI computer workstation (16), DLT-SCADA computer workstation (17), traffic network computer workstation (18), real-time simulation monitor (19) and event detection monitor (20).

Figure 1. Electrical substation-grid test bed with DLT and inside/outside devices for cyber event detection.

As shown in Figure 1, the electrical substation-grid test bed with DLT and inside/outside devices for cyber event detection was formed by the following systems:

1. The electrical substation-grid test bed system, represented by the utility source, power transformers (PTs), circuit breakers, power lines, buses, and loads
2. The electrical protection and measurement system, represented by the SEL (Schweitzer Engineering Laboratories)-451 protective relays (inside substation devices) and SEL-734 and SEL-735 power meters (outside substation devices)
3. The time synchronization system, given by the timing synchronized sources and time clock displays
4. The communication system with Ethernet switches, real-time automation controllers (RTACs), and firewalls

5. The DLT system with CISCO Ethernet switches and DLT devices

The electrical substation-grid test bed has four main workstations (i.e., computers) that are connected to the electrical substation network of the test bed.

1. The host computer that was used to run the tests generated the phase currents and phase to neutral voltages that were measured by the protective relays and power meters, and breaker pole states measured by the protective relays.
2. The human-machine interface (HMI) computer was used to set the protective relays and power meters. The HMI was also used to change relay settings during the event tests to study the effect of the event time and collected data at the electrical substation-grid test bed.
3. The DLT-supervisory control and data acquisition (SCADA) computer was used to collect the measurements from substation inside (protective relays) and outside (power meters) devices and detected cyber events.
4. The Blueframe computer was focused on retrieving and storing the artifacts from intelligent electronic devices (IEDs), such as power meters and protective relays.

2. ELECTRICAL SUBSTATION-GRID TEST BED SYSTEM

In this section, the one-line diagram of the power system, and inside/outside substation devices to be connected in the test bed are presented. The steps to create the electrical substation-grid test bed are described based on the software provide by the original equipment manufacturers and others, that are used to integrate the power meters (outside substation devices) and protective relays (inside substation devices) with the communication devices, and the real-time simulator. The RT-LAB simulation software platform project configuration for the electrical substation-grid test bed and the wiring circuits of the power meters and protective relays with the real-time simulator are presented.

2.1 ELECTRICAL SUBSTATION-GRID TEST BED ONE-LINE DIAGRAM

The power system was based on an electrical substation with two PTs of 10 MVA, and primary/secondary voltages of 34.5/12.47 kV. The electrical grid was a 12.47 kV power system that could be connected as a radial configuration. The electrical grid has power meters and fuses on feeders. The inside substation devices were two SEL-451 protective relays, and the outside substation devices were two SEL-735 power meters and two SEL-734 power meters. Figure 1 shows a one-line diagram of the electrical substation-grid configuration. The electrical substation was based on a sectionalized bus configuration [1]. This arrangement is based on two single bus schemes, each tied together with bus sectionalizing breakers. The sectionalizing breakers may be operated open or closed, depending on system requirements. This electrical substation configuration allows the removal of a bus or circuit breaker from the service to keep service with another circuit breaker and/or bus, if necessary. The sectionalized bus configuration allows a flexible operation, higher reliability than a single bus scheme, isolation of bus sections for maintenance, and the loss of only part of the substation for a breaker failure or a bus fault [1]. The sectionalized bus configuration is shown in Figure 2A. The electrical grid was connected to the substation feeders through two breakers. The power meters measured the phase current and phase to neutral voltages of fuse feeders. The electrical grid is shown in Figure 2B. The electrical substation and grid protection schemes were based on using overcurrent relays and fuses, respectively.

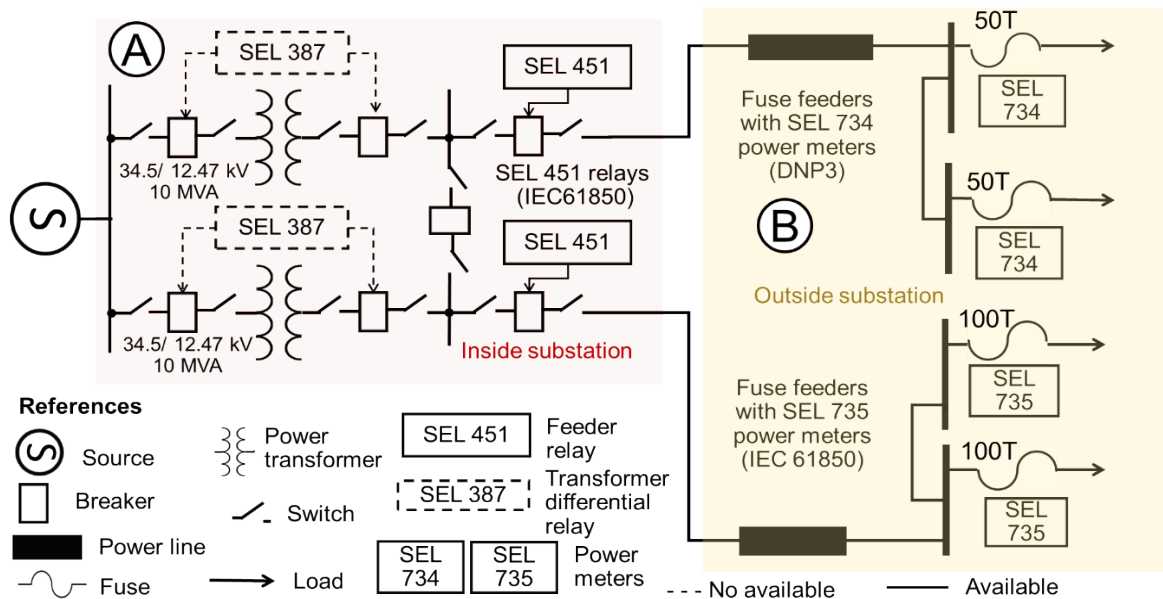


Figure 2. One-line diagram of electrical substation-grid test bed power system.

2.2 SOFTWARE STEPS AND APPLICATIONS

In this electrical substation-grid test bed, a real-time simulator with hardware-in-the-loop (HIL) was set with protective relays, power meters, remote terminal units, Ethernet switches, and DLT devices. The installation of the electrical substation-grid test bed required the integration of protection, control, and communication equipment with different software programs. Figure 3 shows the software used to install the electrical substation-grid test bed at the Advanced Power System Protection lab space at the Grid Research Integration and Deployment Center.

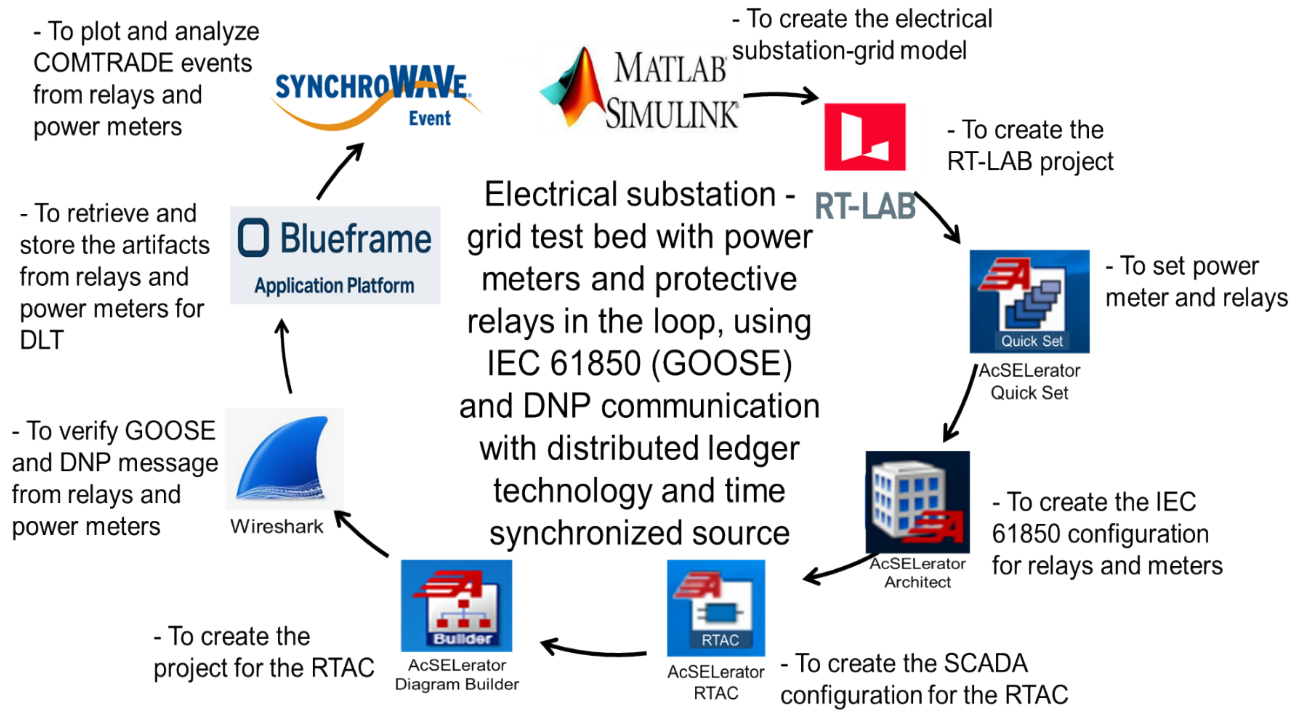


Figure 3. Software applications to build the electrical substation-grid test bed.

This electrical substation-grid test bed was implemented by using a real-time simulator with HIL based on previous published test beds [2, 3]. The MATLAB/Simulink software was used to create the electrical substation-grid test bed model. The RT-LAB software was used to create the RT-LAB project configuration and integrate the electrical substation-grid test bed model with the real-time simulator. Also, the RT-LAB software was used to run the power system simulation tests. The AcSELeRator Quickset software was used to set the SEL-451 protective relays [4] and SEL-734 and SEL-735 power meters [5, 6]. These devices were connected to the HMI computer to measure currents and voltages from SEL protective relays and power meters. The IEC 61850 protocol transmitted the GOOSE (Generic Object Oriented Substation Events) messages that were configured with the GOOSE Dataset of protective relays and power meters before being installed. The SEL-451 protective relays and SEL-735 power meters were set with CID (Configured IED Description) files to create the GOOSE messages [4, 5]. The AcSELeRator Architect software was used to create and download the IEC 61850 CID files for the SEL-451 protective relays and SEL-735 power meters. The SEL-734 power meters had DNP instead of the IEC 61850 (GOOSE) protocol [6]. The SEL-734 power meters were connected to a remote terminal unit or RTAC. The RTAC polled data from the power meters with DNP, and transmitted the measurements from the SEL-734 power meters. The AcSELeRator RTAC software was used to create the configuration for the SEL-3530-4 RTAC [7] and SEL-734 power meters. The AcSELeRator Diagram Builder software was downloaded to create the future SCADA architecture for the electrical substation-grid test bed. The

Wireshark software was used to collect and verify the GOOSE messages from the SEL-451 protective relays and SEL-735 power meters, and DNP messages from SEL-734 power meters. The Synchronwave software was used to plot and analyze the COMTRADE (Common Format for Transient Data Exchange) events from SEL-451 relays and SEL-734 and SEL-735 power meters after running the simulations. Table 1 shows the software applications used to build the electrical substation-grid test bed.

Table 1. Software applications used to build the electrical substation-grid test bed

No	Software	Applications
1	MATLAB/ Simulink	<ul style="list-style-type: none"> Create the electrical substation-grid model
2	RT LAB	<ul style="list-style-type: none"> Create the RT-LAB project configuration Run the simulations
3	AcSELeator Quickset	<ul style="list-style-type: none"> Set the SEL-451 protective relays with IEC 61850 Set the SEL-735 power meters with IEC 61850 Set the SEL-734 power meters with DNP Communicate with the SEL protective relays and power meters Use the HMI of SEL protective relays and power meters
4	AcSELeator Architect	<ul style="list-style-type: none"> Create the IEC 61850 CID files for the SEL-451 protective relays and SEL-735 power meters Download the IEC 61850 CID files into the SEL-451 protective relays and SEL-735 power meters
5	AcSELeator RTAC	<ul style="list-style-type: none"> Create the architecture for the SEL-3530-4 RTAC and SEL-734 power meters Communicate and download the configuration to the SEL-3530-4 RTAC Create the configuration for the SEL-3555 RTAC with SCADA^a
6	AcSELeator Diagram Builder	<ul style="list-style-type: none"> Create the SCADA project for the electrical substation-grid^a
7	Wireshark	<ul style="list-style-type: none"> Collect and verify the GOOSE messages from relays and power meters Collect and verify the DNP messages from SEL-734 power meters
8	Blueframe	<ul style="list-style-type: none"> Retrieve and store the artifacts from protective relays and power meters
9	Synchronwave	<ul style="list-style-type: none"> Plot and analyze the COMTRADE events from protective relays and power meters

^aFuture tasks

2.3 RT-LAB PROJECT FOR THE ELECTRICAL SUBSTATION-GRID TEST BED

The RT-LAB project implementation for the electrical substation-grid test bed included wiring protective relays and power meters with a real-time simulator. MATLAB/Simulink and RT-LAB software were used to create the RT-LAB project configuration. This RT-LAB project configuration was implemented in the host computer that deployed the RT-LAB project configuration in the target computer (real-time simulator) and ran the simulations with the HIL. This RT-LAB project configuration was created using two subsystems—one master block (SM_Master) with the simulated electrical substation-grid test bed circuit, and another block to perform the scope supervision (SC_Console). The SC_Console block checked the simulation tests. The phase currents and phase to neutral voltages from the SEL-451 protective relays and SEL-734 and SEL-735 power meters, and the breaker pole states of the electrical substation feeders, were collected during the simulation from the SC_Console block. Figure 4A and B show the SM_Master (electrical substation/grid circuit) and SC_Console (scope supervision) of the RT-LAB project configuration.

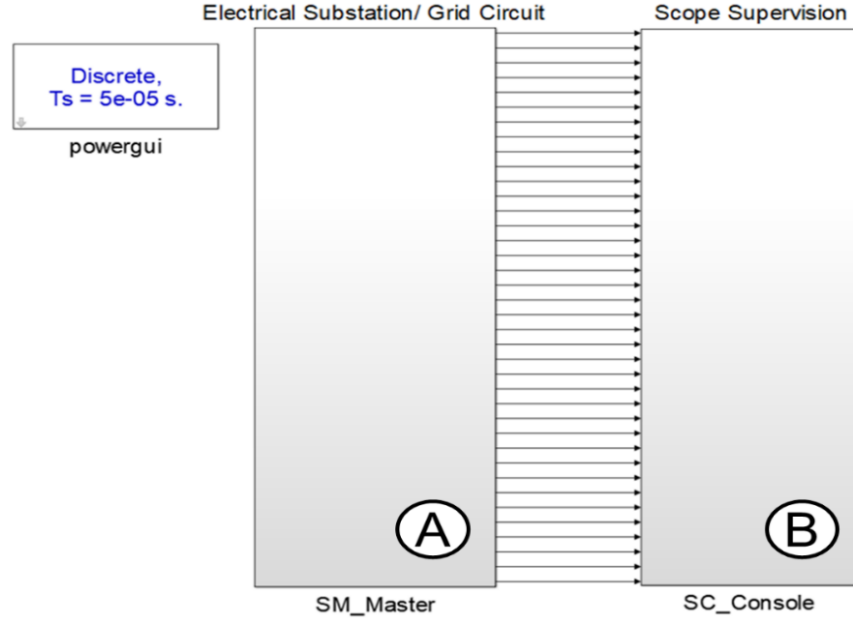


Figure 4. SM_Master (A) and SC_Console (B) subsystems.

Inside the SM_Master block (Figure 4A), the electrical substation-grid test bed circuit (Figure 5) was set. The electrical substation was implemented using a sectionalized bus configuration with two 34.5/12.47 kV PTs of 10 MVA connected in parallel. The electrical substation had two breaker feeders of 12.47 kV that were controlled by two SEL-451 protective relays-in-the-loop; therefore, the A, B, and C phase currents and phase to neutral voltages were collected from the breaker feeder locations. Each breaker feeder was connected to a radial power grid, with two 12.47 kV power lines connected to power loads. The protection devices of the power loads were medium-voltage (MV) Class T fuses (TCC [Time-Current Characteristic] 170-6-2) [8]. One power line had two power loads with 50 T fuses [8], and the other power line had two power loads with 100 T fuses [8]. The A, B, and C phase currents and phase to neutral voltages for the 50 and 100 T fuses [8] were measured with the SEL-734 and SEL-735 power meters, respectively, based on the one-line diagram of electrical substation-grid test bed in Figure 2. The electrical substation-grid test bed system is shown in Figure 5 and includes the utility source, electrical substation, power lines, and power load feeders. As shown in Figure 5A, the SEL-451 protective relays measured the A, B, and C phase currents and phase to neutral voltages from the breaker feeder locations, and breaker trip/close signals. As shown in Figure 5B, the SEL-734 and SEL-735 power meters measured the A, B, and C phase currents and phase to neutral voltages from the fuse feeders. The fault block (Figure 5D) set the single line-to-ground (SLG), line-to-line ground (LLG), line-to-line (LL), three line (3L), and three line-to-ground (3LG) electrical faults at any location of the electrical substation-grid. The fault signal circuit (Figure 5C) set the time to start the fault state at the fault block.

Sectionalized Bus Configuration - Electrical Substation-Grid Testbed
(Task 5 – DarkNet Project) Advanced Power System Protection Lab
Lab Space Manager: Emilio C. Piesciorovsky

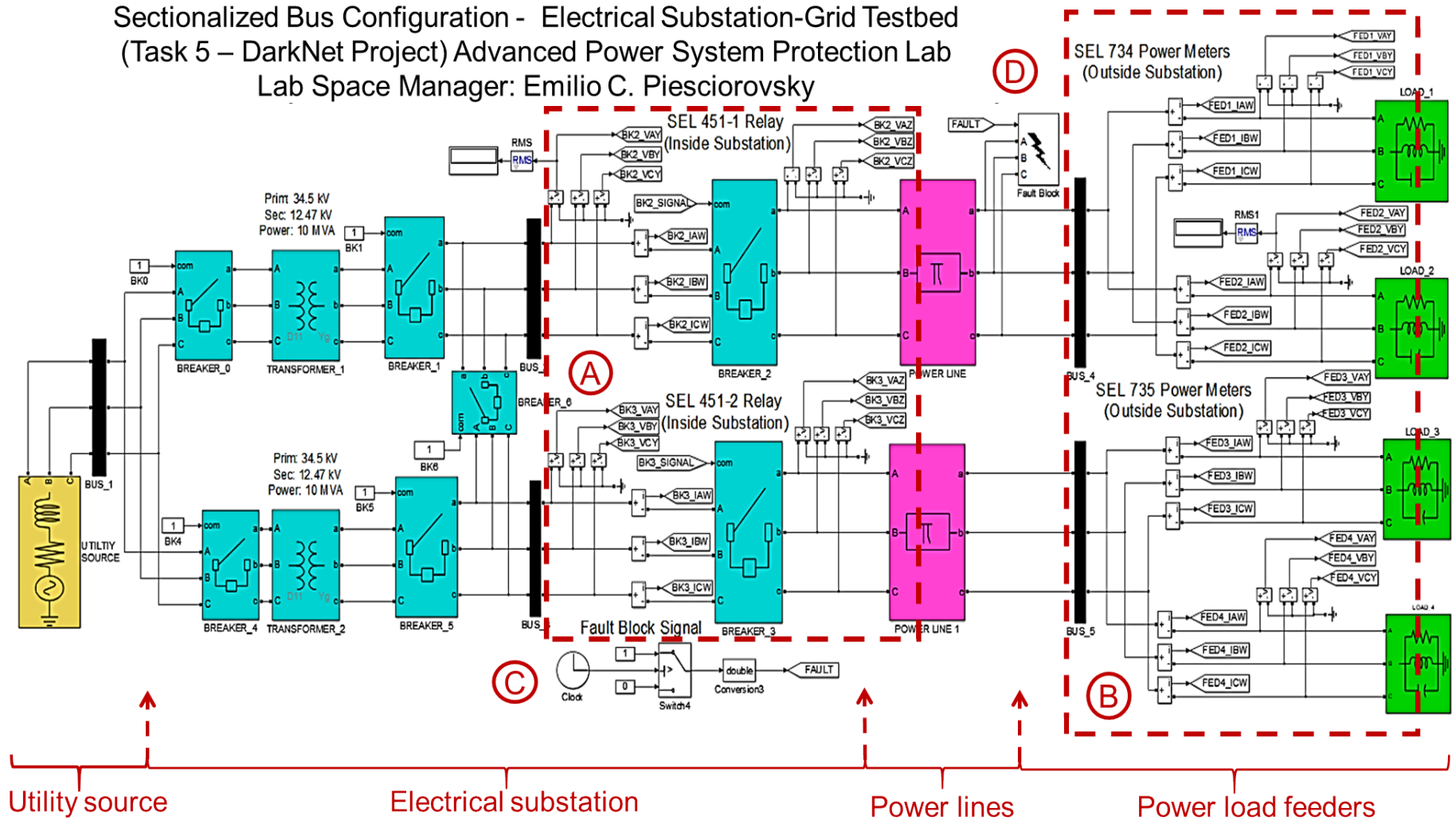


Figure 5. Electrical substation-grid test bed system.

The current interfaces of the SEL-451 protective relays are shown in Figure 6A and B, and the voltage interfaces are shown in Figure 6C and D. The A, B, and C phase primary currents and phase to neutral voltages from sensors on electrical substation breaker feeders (Figure 5A) were scaled into low-level voltage signals by the current (1 V/6,000 A) and voltage (1 V/9,000 V) gain blocks, respectively (Figure 6). Protective relays are typically connected to current transformers (CTs) and voltage transformers (VTs) that provide the scaled primary currents and voltages. The CTs and VTs are typically wired at the rear side's connectors of the protective relays. However, in this case, the low-level test interface (LLTI) located at the front side of the SEL-451 protective relay was used. The current and voltage scaling factors for the LLTI were collected from the SEL-451 protective relay manual [4]. The gains for the SEL-451 protective relays were equal to the inverse of the scaling factors times the measurement transformer ratios [9]. The current and voltage signals were limited by a saturation block of +3.3/-3.3 V to protect the LLTI of the SEL-451 protective relays, based on the manufacturer manual [4].

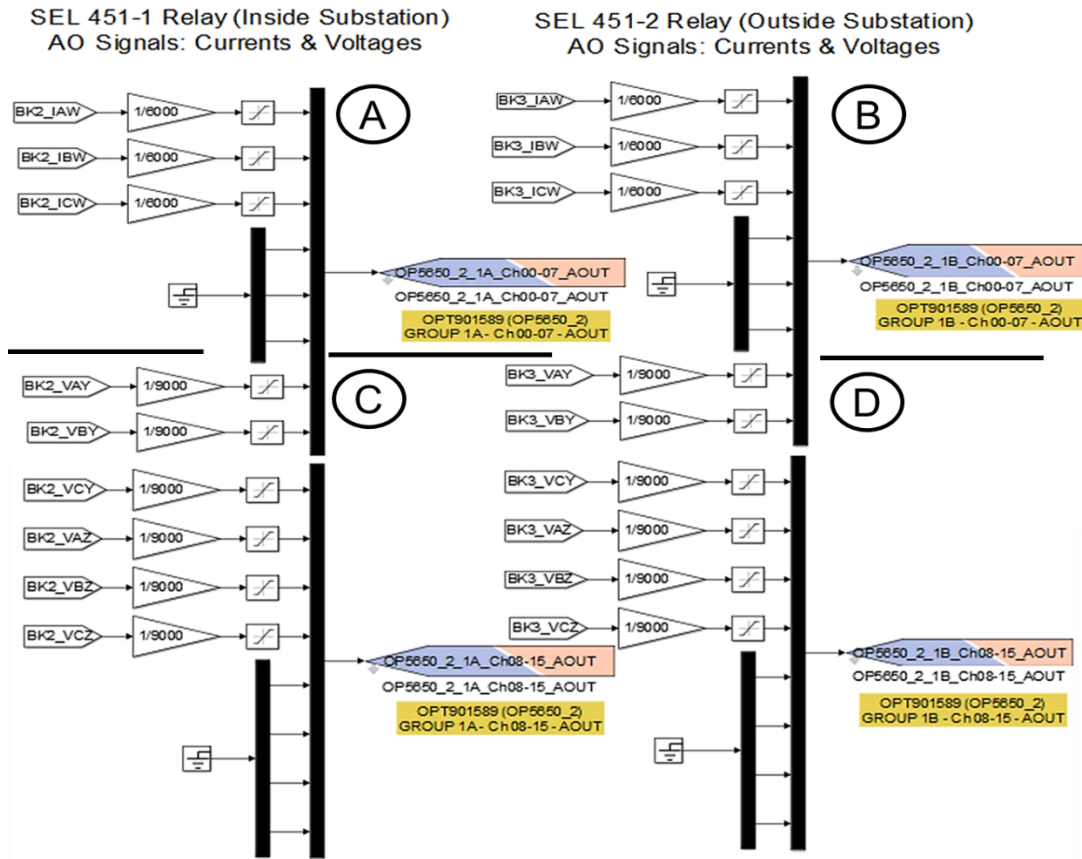


Figure 6. Current (A, B) and voltage (C, D) interfaces of SEL-451 relays.

The SEL-735 and SEL-734 power meter manuals [5, 6] do not provide information for the current and voltage scaling factors at the LLTI. Therefore, current and voltage amplifiers were connected between the real-time simulator and the SEL-734 and SEL-735 power meters. The current interfaces for the SEL-734 and SEL-735 power meters are shown in Figure 7A and B, and the voltage interfaces are shown in Figure 7C and D. The A, B, and C phase primary currents and phase to neutral primary voltages for the power loads (Figure 5B) were scaled with a 1 V/200 A and 1 V/9,000 V gain block, respectively (Figure 7). The power meters are typically connected to CTs and VTs that are wired at a device's rear side. Therefore, the current and voltage signals from the block gains were wired to current and voltage amplifiers, respectively, that were connected to the rear side of the SEL-734 and SEL-735 power meters.

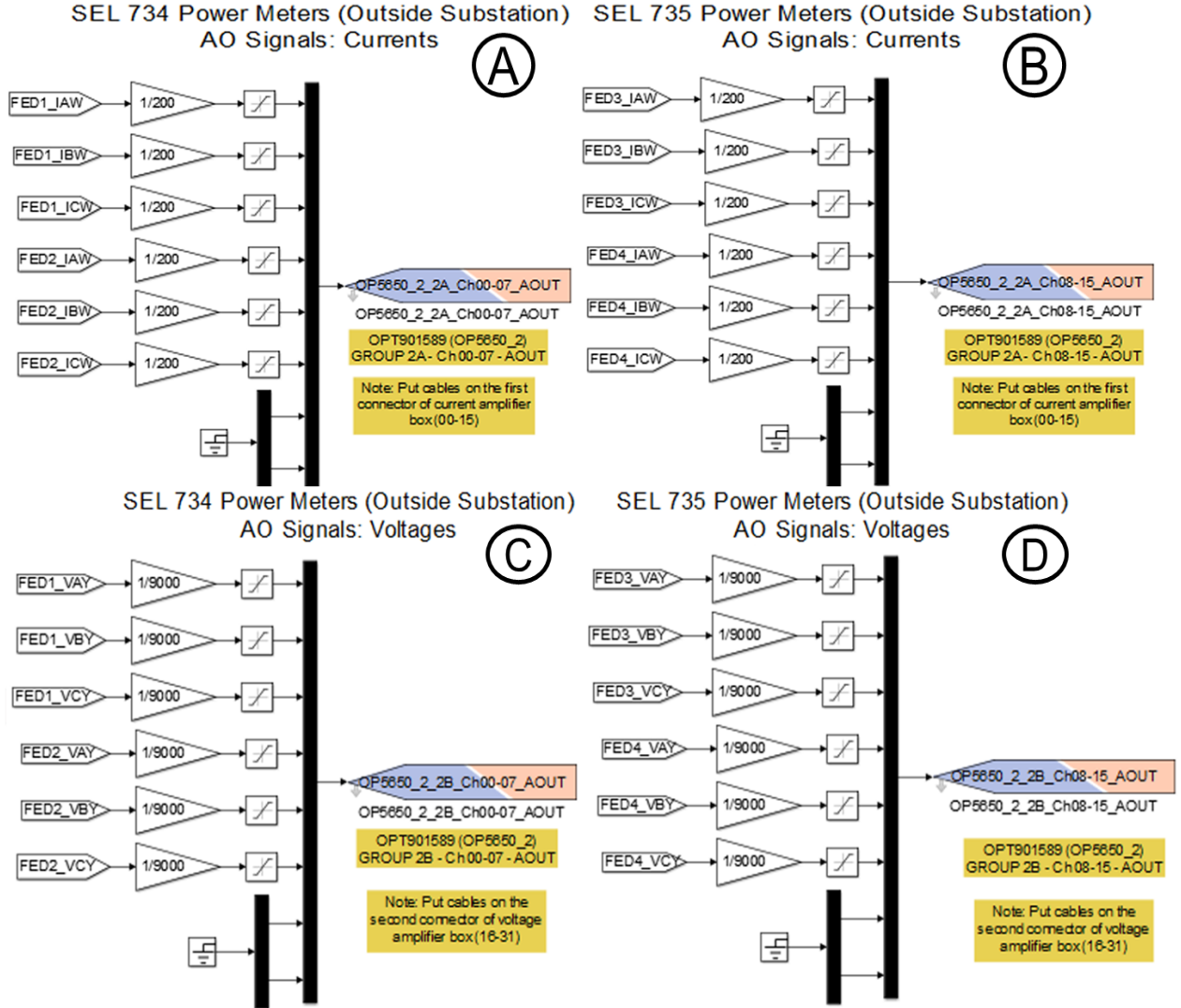


Figure 7. Current (A, B) and voltage (C, D) interfaces of SEL-734 and SEL-735 power meters.

The feeder breakers of the electrical substation (Figure 5A) were controlled by the SEL-451 protective relays. The breaker trip and close signals were generated by the SEL-451 protective relays. During the simulations, the breakers were closed at normal operations and tripped in electrical fault situations. Figure 8 shows the trip/close (Figure 8A) and pole state (Figure 8B) interfaces and trip/close signal circuits (Figure 8C, 8D) for the breakers of the SEL-451 protective relays. The trip and close signals were received from the SEL-451 protective relays in the loop by the trip/close interface (Figure 8A), and these signals were collected by the trip/close signal circuits (Figure 8C, D). For the SEL-451 protective relays, the trip (overcurrent pickup) and close signals were generated during the simulations of the SEL-451 relay control outputs. The circuit breaker models were commanded with one signal (close = 1, open = 0). In the trip/close signal circuits (Figure 8C, D), the trip and close signals were detected by a hit crossing block of 10 VDC for a trip signal of 14.3 VDC external source, and the J-K flip-flop blocks were placed to detect the trip and close signals received from the SEL-451 protective relays. In addition, the breaker pole states given by the trip and close signals were sent to the SEL-451 relay control inputs by the interface for circuit breaker pole states (Figure 8B) and using a 24 VDC external source to detect the three-phase circuit breaker pole states.

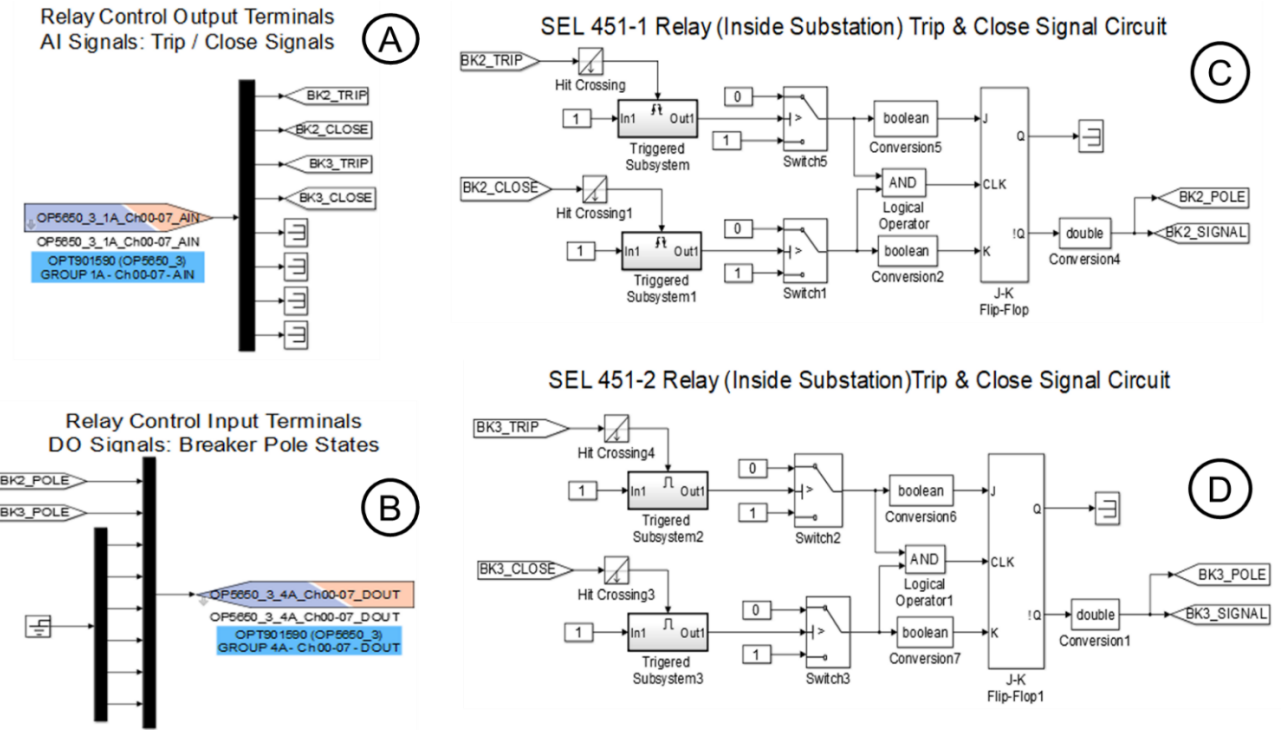


Figure 8. Trip/close (A) and pole state (B) interfaces and trip/close signal circuits (C, D) of breakers for the SEL-451 protective relays.

Inside the SM_Master block (Figure 4A), the data acquisition circuit (Figure 9) was set with the OpWrite File block that recorded the data from the SEL-451 protective relays and SEL-734 and SEL-735 power meters during the simulation. For the electrical substation breaker feeders provided by the SEL-451 protective relays in the loop, the A, B, and C phase primary currents and phase to neutral voltages, and breaker trip signals were collected (Figure 9A, B). For the power load feeders provided by the SEL-734 and SEL-735 power meters in the loop, the A, B, and C phase primary currents and phase to neutral voltages were collected (Figure 9C, D).

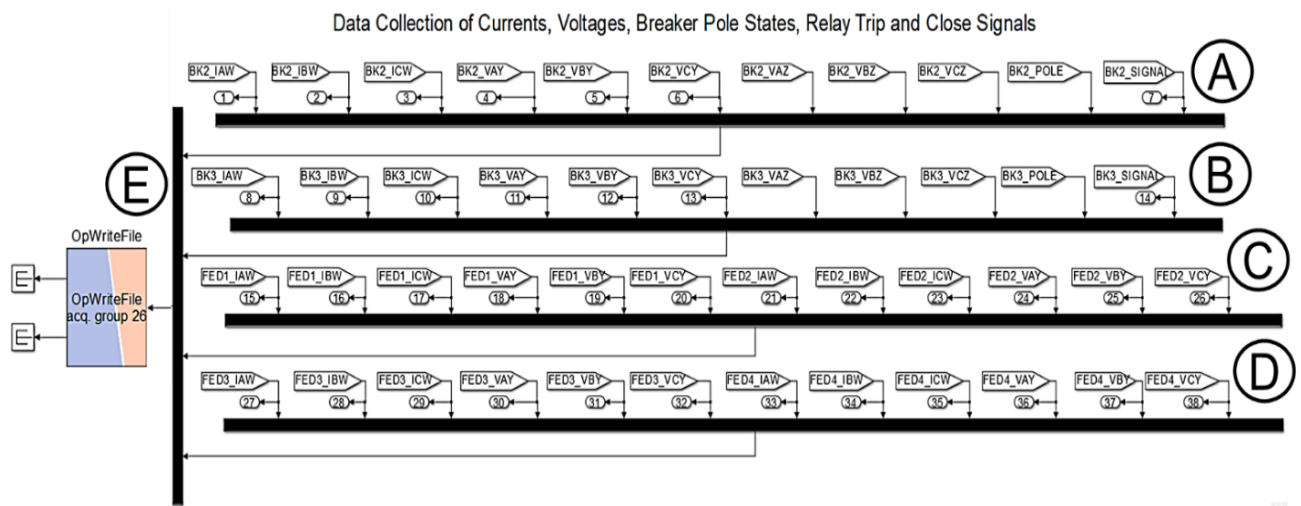


Figure 9. Data acquisition circuit to collect signals from inside (A, B) and outside (C, D) substation devices with OpWrite File block (E).

Inside the SC_console subsystem (Figure 4B), the OpComm block (Figure 10A) and scopes (Figure 10B–E) were set to supervise the simulations. The Opcomm block collected the signals simulated from the S_Master subsystem (Figure 4A). Then, the scopes were open during the simulations to supervise the experiments. The scopes for the electrical substation breaker feeders were provided by the SEL-451 protective relays in the loop that measured the A, B, and C phase primary currents and phase to neutral voltages, and breaker pole state signals (Figure 10B, C). The scopes for the power load feeders provided by the SEL-734 and SEL-735 power meters in the loop measured the A, B, and C phase primary currents and phase to neutral voltages (Figure 10D, E).

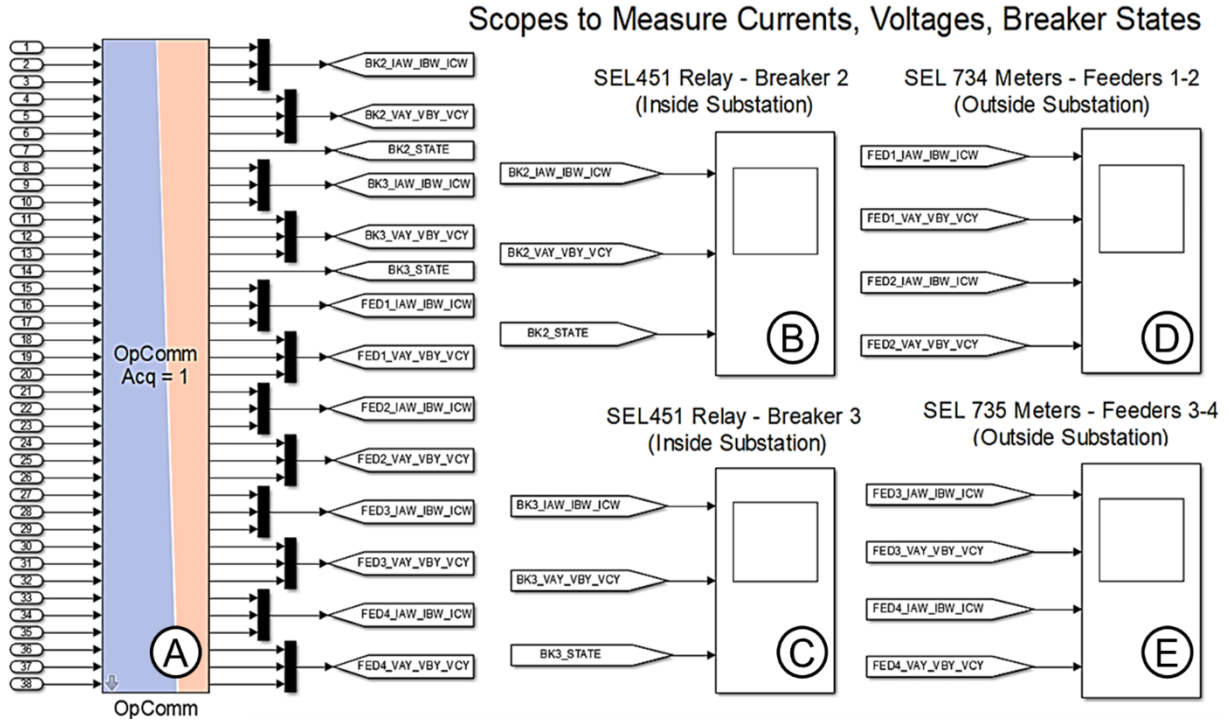


Figure 10. OpComm block (A) with scopes for inside (B, C) and outside (D, E) electrical substation devices.

Figure 11 shows the signals measured during the simulation of a SLG electrical fault located at the end of the power line (Figure 5D). Scope1 measured the signals from the SEL-451 protective relays that were connected to the faulted power line. Scope 4 measured the signals from the SEL-735 power meters that were wired at power load feeders of the non-faulted power line. Then, the signals for the SEL-451 relays and SEL-735 power meters could be supervised during the simulation. In this case, the A, B, and C phase primary currents (Figure 11A) and phase to neutral voltages (Figure 11B), and breaker pole state signals (Figure 11C) for the SEL-451 protective relays were measured at a faulted power line. In addition, the A, B, and C phase primary currents (Figure 11D-F) and phase to neutral voltages (Figure 11E-G) for the SEL-735 power meters were measured at a non-faulted power line.

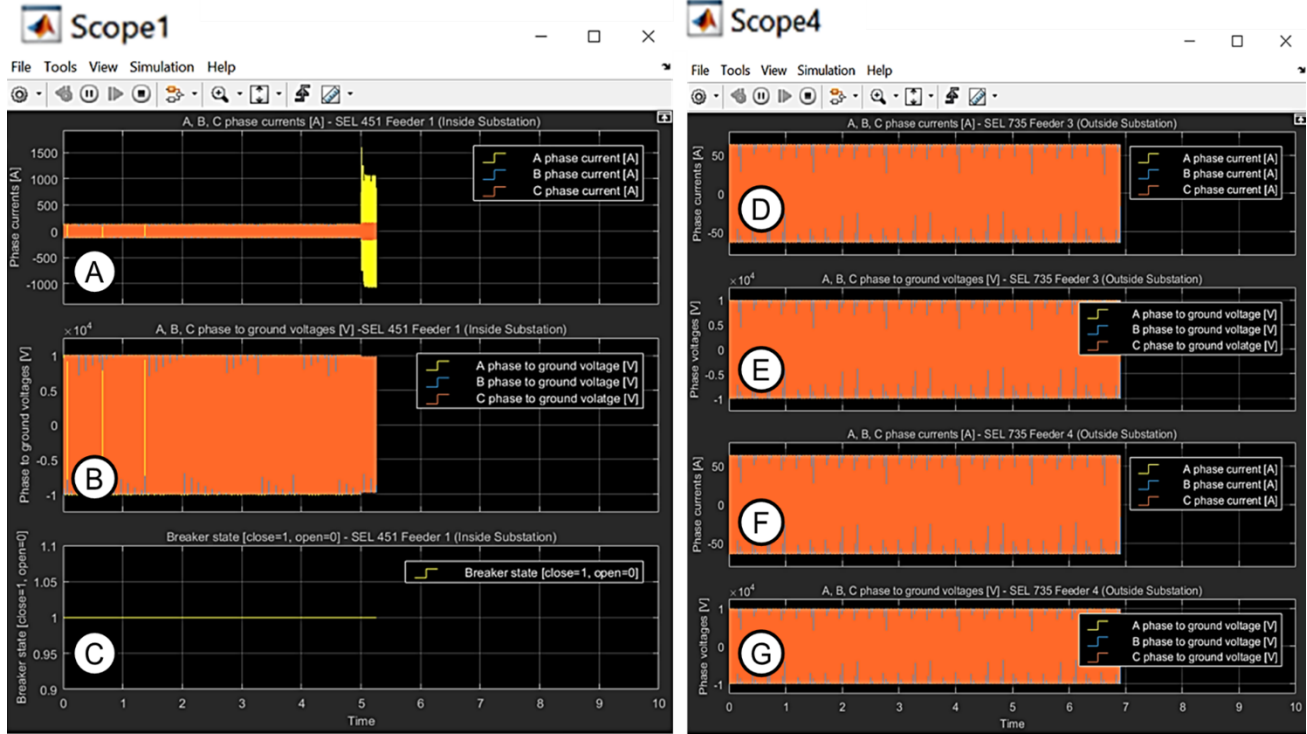


Figure 11. Scope for the SEL-451 protective relays (A–C) and SEL-735 power meters (D–G).

2.4 ELECTRICAL WIRING FOR INSIDE AND OUTSIDE SUBSTATION DEVICES

The electrical wiring diagrams for the electrical substation-grid test bed were based on connecting the analog and digital signals of protective relays inside the substation and power meters outside the substation. The two SEL-451 protective relays measured the phase currents and phase to neutral voltages from feeder breakers at the electrical substation. The SEL-451 relays were set with an inverse time overcurrent setting to protect the radial power lines, and the feeder breakers could trip or close from their SEL-451 protective relays. The SEL-734 and SEL-735 power meters measured the phase currents and phase to neutral voltages from the MV feeder fuses at power loads.

The analog signals for the SEL-451 protective relays were the A, B, and C phase currents and A, B, and C phase to neutral voltages that were collected from the feeder breaker locations. The phase currents and phase to neutral voltages were generated with the real-time simulator as low-voltage signals and connected to the LLTI at the front side of the SEL-451 protective relays. This was possible because the current and voltage scaling factors for the SEL-451 protective relays were provided by the manufacturer manual [4]. Figure 12 shows the wiring of analog signals for the SEL-451 protective relays. In the SEL-451 protective relays, CTs and VTs are typically connected on the rear side of the relays. However, in the real-time simulator with SEL-451 protective relays in the loop, the LLTI located on the front side of the SEL-451 relays (Figure 12B-III, C-IV) was used to feed the secondary currents and voltages from the feeder breakers located at the electrical substation. The LLTI analog signals of the SEL-451 protective relays were limited to a maximum peak voltage of 3.3 V based on the SEL-451 protective relay manufacturer manual [4]. The maximum peak voltage must be avoided to prevent damage to the LLTI for the SEL-451 protective relays. The LLTI of the SEL-451 protective relays was given by a 34 pin male connector (Figure 12A) and collected the A, B, and C phase currents and A, B, and C phase to neutral voltages from the feeder breakers at the electrical substation simulated with the real-time simulator (Figure 12E-I, E-II).

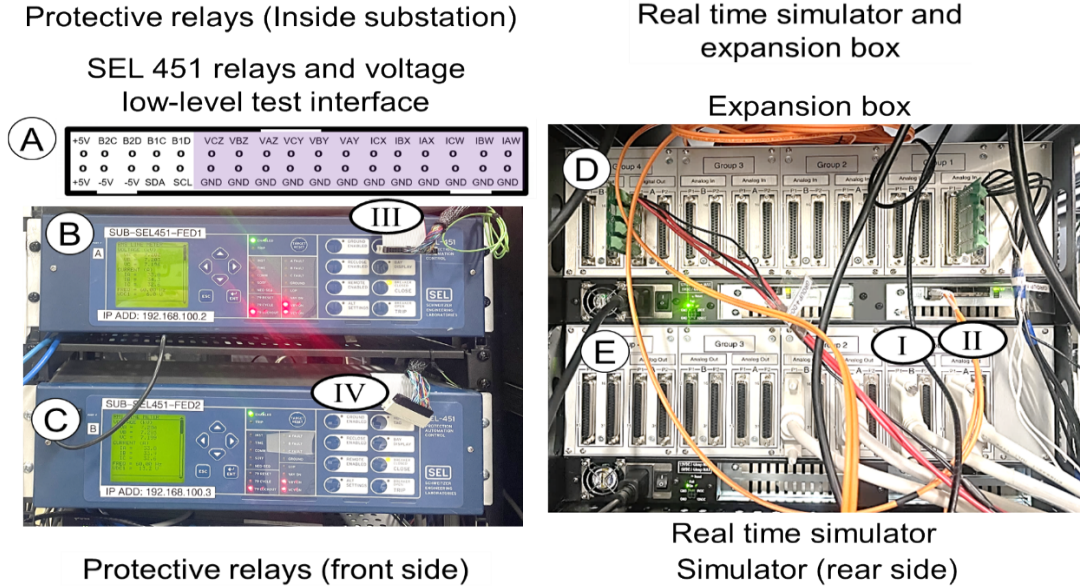


Figure 12. Wiring of analog signals for the SEL-451 relays.

The analog signals for the SEL-734 and SEL-735 power meters were the A, B, and C phase currents and A, B, and C phase to neutral voltages collected from the feeder fuse locations. The current and voltage scaling factors from the LLTI of the SEL-735 and SEL-734 power meters were not provided by their manuals [5, 6]. Therefore, current and voltage amplifiers were used to connect the analog signals from the real-time simulator to the SEL-734 and SEL-735 power meters. Figure 13 shows the wiring of analog signals for the SEL-734 and SEL-735 power meters. The phase currents and phase to neutral voltages were generated with the real-time simulator as low-voltage signals (Figure 13H-I, H-II). In this case, the low voltage signals were connected to current (Figure 13E-III) and voltage (Figure 13F-IV) amplifiers, and wires from the current and voltage amplifiers were connected to the current (Figure 13A-V, D-V) and voltage (Figure 13A-VI, D-VI) connectors on the rear side of the SEL-734 and SEL-735 power meters.

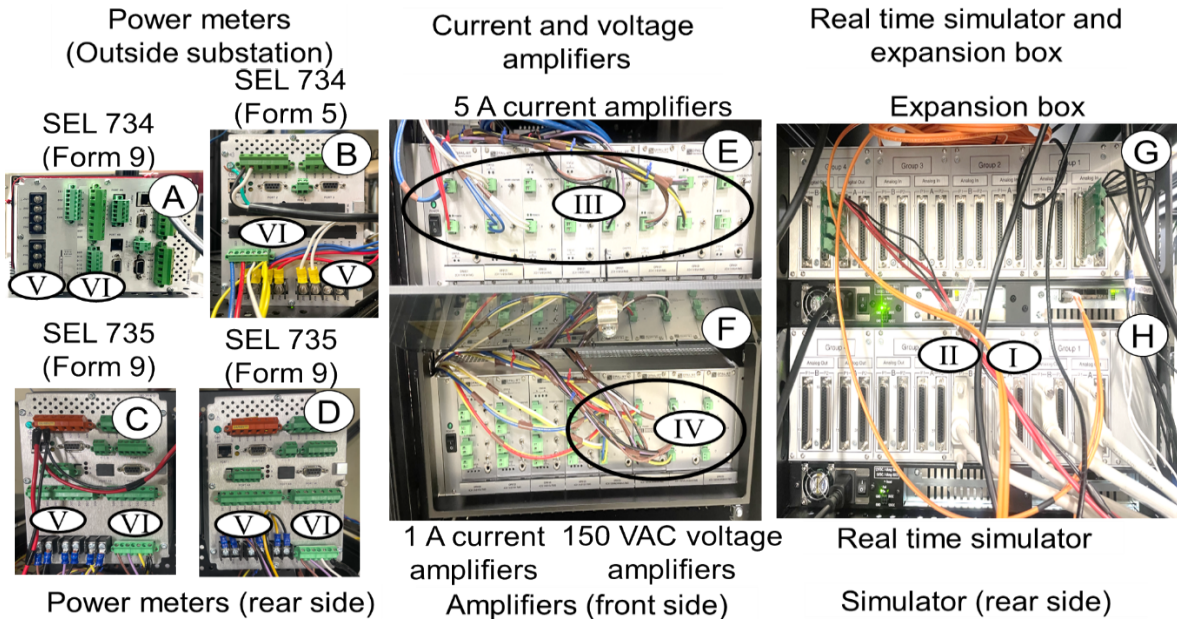


Figure 13. Wiring of analog signals for the SEL-734 and SEL-735 power meters.

One SEL-734 power meter used the Form 5 (2-Element, 3 Wire Delta) configuration (Figure 14), and the other one used the Form 9 (3-Element, 4 Wire Wye) configuration (Figure 15). The SEL-735 power meters used the Form 9 (3-Element, 4 Wire Wye) configuration (Figure 15). The Form 5 configuration was based on using two CTs and a Delta VT, whereas the Form 9 configuration was based on using three CTs and three VTs. The Form 5 configuration was based on measuring a balanced three-phase power system by using two CTs instead of three CTs. The current and voltage sensors in the MATLAB/Simulink model were set to measure the A, B, and C phase currents and A, B, and C phase to neutral voltages. Then, the Form 5 and 9 configurations were connected in the voltage and current amplifiers as shown in Figure 14 and Figure 15, respectively.

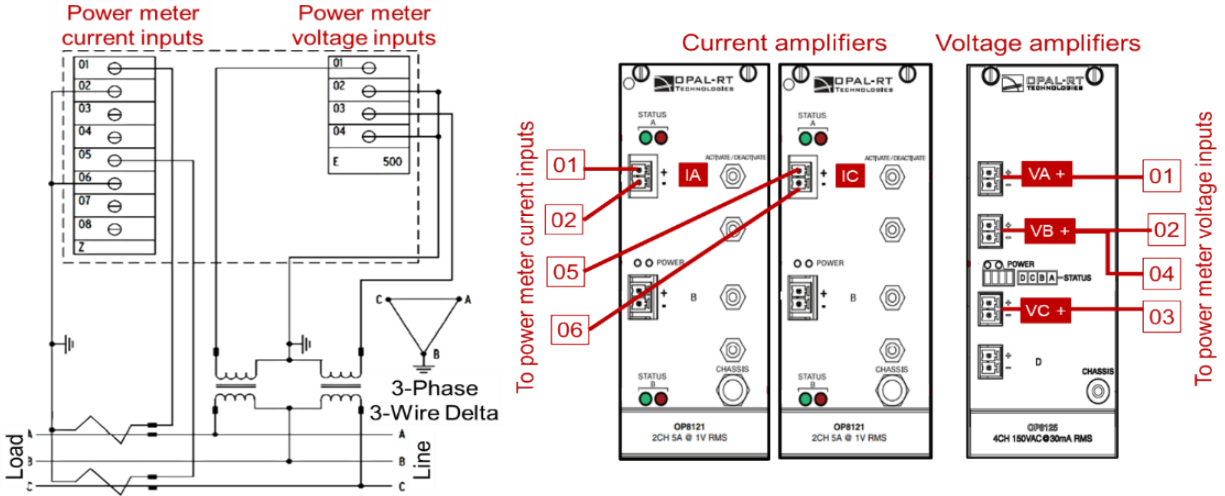


Figure 14. Form 5 (2-Element, 3 Wire Delta) configuration of power meter.

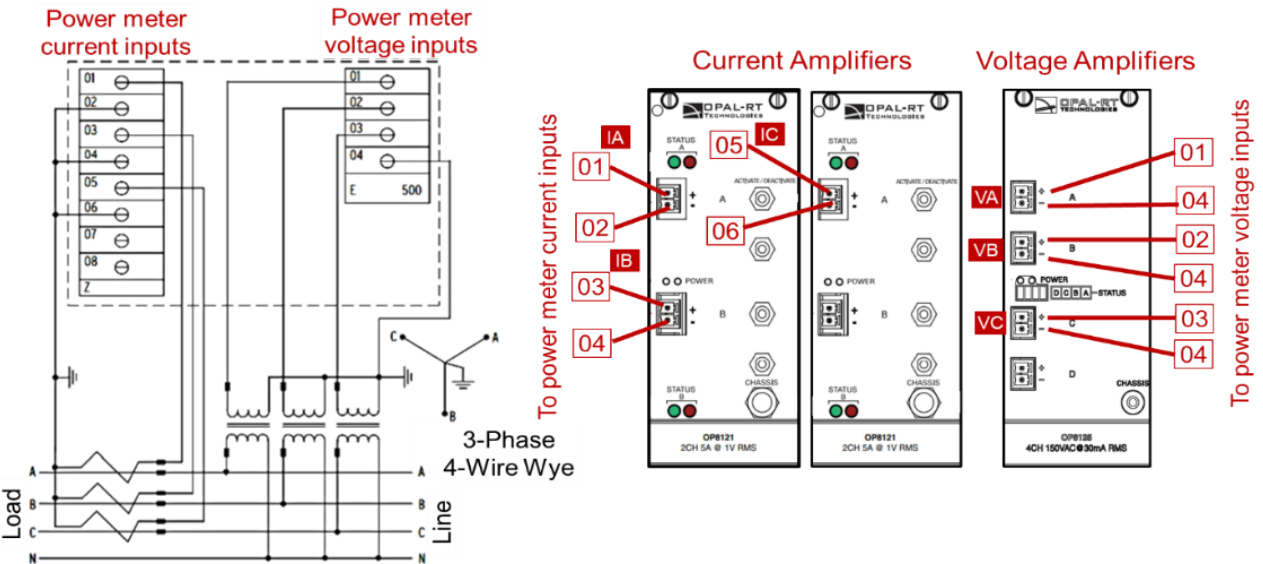


Figure 15. Form 9 (3-Element, 4 Wire Wye) configuration of power meter.

The SEL-734 and SEL-735 power meters were connected to power loads, and these power meters only measured the phase currents and voltages at fuse feeder locations. Because the SEL-734 and SEL-735 power meters did not control breakers, the digital signals were not connected to the SEL-734 and SEL-

735 power meters. The SEL-451 protective relays controlled the breakers at the electrical substation feeders, and the wiring of digital signals for the SEL-451 protective relays was set up (Figure 16).

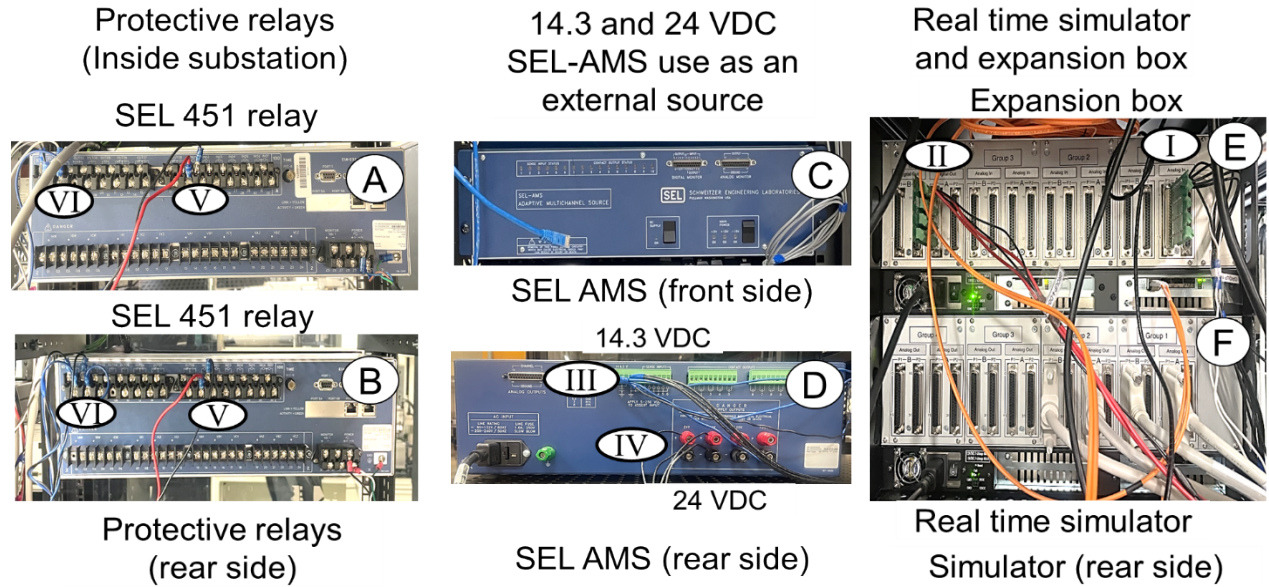


Figure 16. Wiring of digital signals for the SEL-451 protective relays.

As shown in Figure 16, the SEL-451 protective relays were connected to digital signals that represented the close and trip signals and breaker pole states. The trip and close signals were generated by the SEL-451 protective relays to operate the breakers. In addition, the trip signals were generated when an electrical fault happened based on the inverse time overcurrent protection scheme set on the SEL-451 protective relays. In this case, the digital inputs from the real-time simulator were wired with the SEL-451 relay control outputs that represented the close and trip signals of 14.3 VDC using an external source. In addition, the SEL-451 protective relays sensed the pole states of breakers. In this case, the digital outputs from the real-time simulator that represented the breaker pole states were wired to the control inputs of the SEL-451 relays to sense if the breakers were closed or open by measuring a voltage signal of 24 VDC using an external source. The 14.3 VDC measurements for the trip/close signals were collected from the SEL-Adaptive Multichannel Source external source (Figure 16D-III) and connected to the SEL-451 relay control outputs (Figure 16A-VI, B-VI). Then, the trip/close signals generated by the SEL-451 relays were sent to the real-time simulator (Figure 16E-I) that had the breakers for the electrical substation. The breaker pole states of the electrical substation from the real-time simulator (Figure 16E-II) were sensed with a 24 VDC from the SEL-Adaptive Multichannel Source external source (Figure 16D-IV) and connected to the SEL-451 relay control inputs (Figure 16A-V, B-V).

3. ELECTRICAL PROTECTION AND MEASUREMENT SYSTEM

In this section, the calculation and setting of the electrical protection and measurement system for the electrical substation-grid test bed are described. The inverse time overcurrent settings to coordinate the SEL-451 protective relays with the load fuses are calculated, verifying that the primary protection devices (load fuses) clear the electrical fault currents before the backup protection devices (overcurrent relays). Finally, the steps to set the protective relays and power meters for the electrical substation-grid test bed are presented.

3.1 CALCULATION OF INVERSE TIME OVERCURRENT SETTINGS

The electrical protection system of the substation and power grid was provided by two substation feeders that have two circuit breakers. Each substation feeder has a SEL-451 relay as a protective device. The circuit breakers were connected to power lines and two power loads, as shown in Figure 5. The protection devices of the power loads were fuses, and the currents and voltages of these fuses, were measured by the SEL-735 and SEL-734 power meters. Based on the electrical substation-grid test bed (Figure 5), the radial power system configuration with outside substation devices and maximum load currents is described in Table 2.

Table 2. Radial power system configuration with outside substation devices and maximum load currents

Power line	Load feeders	Power meter	Maximum load current ^a [A]	Type of MV fuse
Power line 1	1	SEL-734	35	50 T
	2	SEL-734	35	50 T
Power line 2	3	SEL-735	70	100 T
	4	SEL-735	70	100 T

^aMaximum load currents could be modified during the simulations by setting different power loads

The fuses for the power loads were selected based on calculating the maximum full loads by a power flow simulation and collecting the maximum full load currents as root mean square (RMS) values at the 50 and 100 T fuse locations in the electrical substation-grid circuit (Figure 2).

In the MV fuses, the minimum fuse rating should be at least 1.4 times the circuit's maximum load current [10]. The condition to select the fuses based on the maximum full load is represented by Eq. (1).

$$I_{fuse\ rating} \geq 1.4 \times I_{max\ full\ load} , \quad (1)$$

where $I_{fuse\ rating}$ is the fuse rating current in amperes, and $I_{max\ full\ load}$ is the maximum full load current in amperes.

The inverse time current (ITC) curves were used to calculate the protection schemes for the electrical substation-grid test bed. The fuse-relay overcurrent coordination between the 50 and 100 T fuses with the SEL-451 protective relays was calculated by setting the fuses and protective relays as primary and backup protections, respectively. The inverse time overcurrent settings of the SEL-451 relays were based on the U3 Very ITC curves [4] represented by Eq. (2).

$$T_R = TDS \times \left(0.0963 + \frac{3.88}{M^2 - 1} \right) \times 60 , \quad (2)$$

where T_R is the relay time in cycles, TDS is the time dial setting in seconds, and M is the multiple of pickup. The multiple of pickup is the ratio between the secondary input current and the relay's current pickup setting [11]. The secondary input current is the ratio between the primary input current and the CT ratio. Then, the multiple of pickup is given by Eq. (3).

$$M = \frac{I}{CTR \times I_p}, \quad (3)$$

where M is the multiple of pickup, I is the primary input current in amperes, CTR is the CT ratio, and I_p is the relay current pickup setting in amperes.

The ITC curve of relay was calculated by placing Eq. (3) in Eq. (4). The U3 Very ITC curve of relay is presented by Eq. (4).

$$T_R = TDS \times \left(K_1 + \frac{K_2}{(I/CTR/I_p)^{K_3} - 1} \right) \times 60, \quad (4)$$

where T_R is the calculated relay time in cycles, TDS is the time dial setting in seconds, I is the primary input current in amperes, CTR is the CT ratio, and I_p is the relay current pickup setting in amperes.

The clearing ITC curves for fuses were created by collecting data from the fuse manufacturer for the 50 and 100 T fuses (TCC 170-6-2) [12] and fitting the collected data with the US curves as a function of the primary current and selecting the F_0 – F_5 factors to match the manufacturer fuse curve with Eq. (5) to represent the clearing ITC curve of 7.2 kV fuses.

$$T_F = F_0 \times \left(F_1 + \frac{F_2}{(I/F_4/F_5)^{F_3} - 1} \right) \times 60, \quad (5)$$

where T_F is the calculated clearing time of 7.2 kV fuse in cycles, I is the primary input current in amperes, and F_0, F_1, F_2, F_3, F_4 , and F_5 are the curve constants for the fuses. Table 3 shows the calculated curve constants to fit the clearing ITC curves of 50 and 100 T fuses.

Table 3. Constants and factors of SEL-451 protective relays and 50/100 T fuses

Constants and factors	U3 curve (SEL-451) Eq. (4)	50 T fuse (SEL-734) Eq. (5)	100 T fuse (SEL-735) Eq. (5)
TDS	2	-	-
F_0	-	6	6
K_1	0.0963	-	-
F_1	-	0.002	0.002
K_2	3.88	-	-
F_2	-	3	3
K_3	2	-	-
F_3	-	2	2
CTR	80	-	-
F_4	-	70	140
I_p	5	-	-
F_5	-	1.6	1.6

The electrical fault analysis was conducted at the electrical substation-grid circuit (Figure 5), and the fault block was placed at the power load feeders. Using the MATLAB/Simulink software, the electrical fault currents were estimated at the electrical substation-grid test bed (Figure 5). The RMS current magnitudes from the A, B, and C phase breaker poles for the backup relay were collected. The SLG, LL, LLG, and 3L (or 3LG) electrical fault currents are described in Table 4. The maximum electrical fault current was 1,134 A for the 3L (or 3LG) electrical fault, and the minimum electrical fault current was 751 A for the SLG electrical fault. Because the power line radial configurations for the SEL-734 and SEL-735 power meter feeders were similar, electrical fault currents for both cases were the same.

Table 4. Electrical fault and pre-fault RMS current magnitudes for primary and backup protection devices

Test name (Fault location_ Fault type)	Fault type	Protective device	Fault state RMS current		
			Phase A (A)	Phase B (A)	Phase C (A)
SEL-734_AG-FAULT SEL-735-AG-FAULT	SLG	Primary device (fuse)	751	52	59
		Backup device (relay)	751	104	117
SEL-734_AB-FAULT SEL-735_AB-FAULT	LL	Primary device (fuse)	1,005	960	46
		Backup device (relay)	1,027	937	91
SEL-734_ABG-FAULT SEL-735_ABG-FAULT	LLG	Primary device (fuse)	1,080	957	58
		Backup device (relay)	1,080	957	115
SEL-734_ABC-FAULT (or SEL-734_ABCG-FAULT) SEL-735_ABC-FAULT (or SEL-735_ABC-FAULT)	3L or 3LG	Primary device (fuse)	1,134	1,134	1,134
		Backup device (relay)	1,134	1,134	1,134

The ITC curves of 50 and 100 T fuse-relay coordination are shown in Figure 17A and B, respectively. At maximum load currents on bus feeders, currents were not intersected by the relay and fuse ITC curves. However, at minimum and maximum electrical fault currents in the load feeders, currents were intersected by the relay ITC curves, evaluating the selectivity coordination between the primary (relay) and backup (fuse) protective devices.

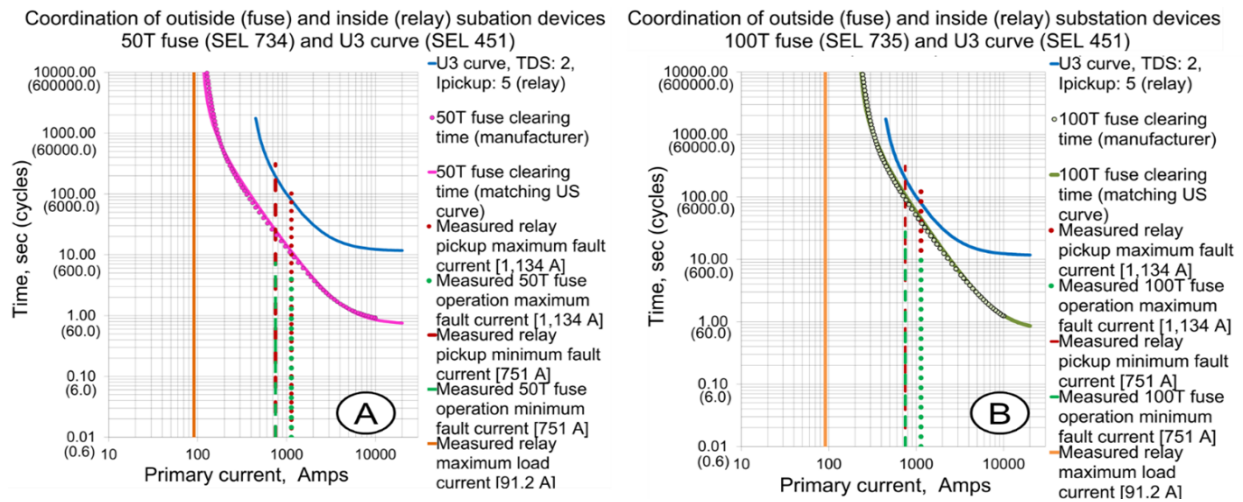


Figure 17. Inverse time overcurrent curve coordination of fuses and relays at SEL-734 (A) and SEL-735 (B) power meter locations.

For the primary and backup protective devices, the maximum interrupting current was the value at which the protection devices reached the minimum coordination time interval (CTI). Based on IEEE Std. 242-2001 [13], the minimum CTI for a fuse-relay is the relay's tolerance and setting error time (0.12 s = 7.2 cycles). In this study, the calculated minimum CTI for the fuse-relay protective device was 7.2 cycles. The calculated minimum CTIs between the fuse and relay protective devices for different electrical fault tests were estimated by Eq. (6).

$$CTI = (T_R - T_F), \quad (6)$$

where CTI is the calculated minimum CTI between backup and primary protective devices in cycles, T_R and T_F are the calculated times of the backup relay and feeder fuse at maximum electrical fault currents, respectively, in cycles.

The operation times of relays and fuses were calculated using Eqs. (4) and (5), respectively, and using the constants and factors of the SEL-451 protective relays and 50/100 T fuses. Then, the minimum CTIs for the 50 and 100 T fuses with SEL-451 relays were 66 and 22 cycles, respectively (Figure 18). The calculated CTIs between the backup SEL-451 protective relay and 50/100 T fuses for the SLG, LL, LLG, and 3L (or 3LG) electrical fault currents are shown in Figure 18.

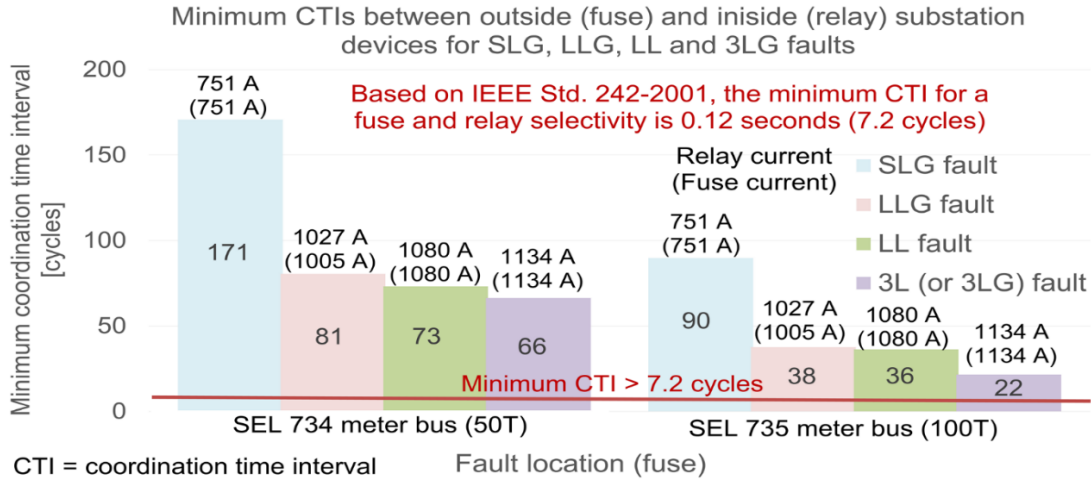


Figure 18. Minimum CTI between fuses and relays with electrical faults located at SEL-734 and SEL-735 power meter bus locations.

3.2 POWER PROTECTION AND METERING SYSTEM

In the electrical substation-grid test bed, the SEL-451 protective relays measured the phase currents and phase to neutral voltages and controlled the feeder breakers at the electrical substation. The SEL-735 and SEL-734 power meters were set at load feeder fuse locations to measure the phase currents and phase to neutral voltages for 50/100 T fuses. In addition, these power meters detected when fuses were blown by measuring the magnitude of phase currents.

3.3 PROTECTIVE RELAY SETTINGS

The SEL-451 protective relays were upgraded with IEC 61850 after receiving the new configuration files from the manufacturer because both relays had DNP instead of IEC 61850 protocol. The SEL-451 protective relays were set with the AcSELeRator Quickset software, serial cable, and laptop. The Meter and Terminal Identifiers, $CTRs$, and $PTRs$ set for the SEL-451 protective are shown in Table 5.

Table 5. Settings for the SEL-451 protective relays

Type of device	Meter identifier	Terminal identifier	CTR	PTR
SEL-451 relay	SUB_SEL451_FED1	SUBSTATION_FEEDER_1	80	60
SEL-451 relay	SUB_SEL451_FED2	SUBSTATION_FEEDER_2	80	60

Figure 19 shows the steps to set the General Global Settings for the SUB_SEL_451_FED1 protective relay. One breaker was selected because the current flows in one-direction for the radial power line feeder. The power system frequency and phase rotation were 60 Hz and ABC, respectively. The electrical fault conditions for the inverse (51) and instantaneous (50) overcurrent settings were selected to trip Breaker 1.

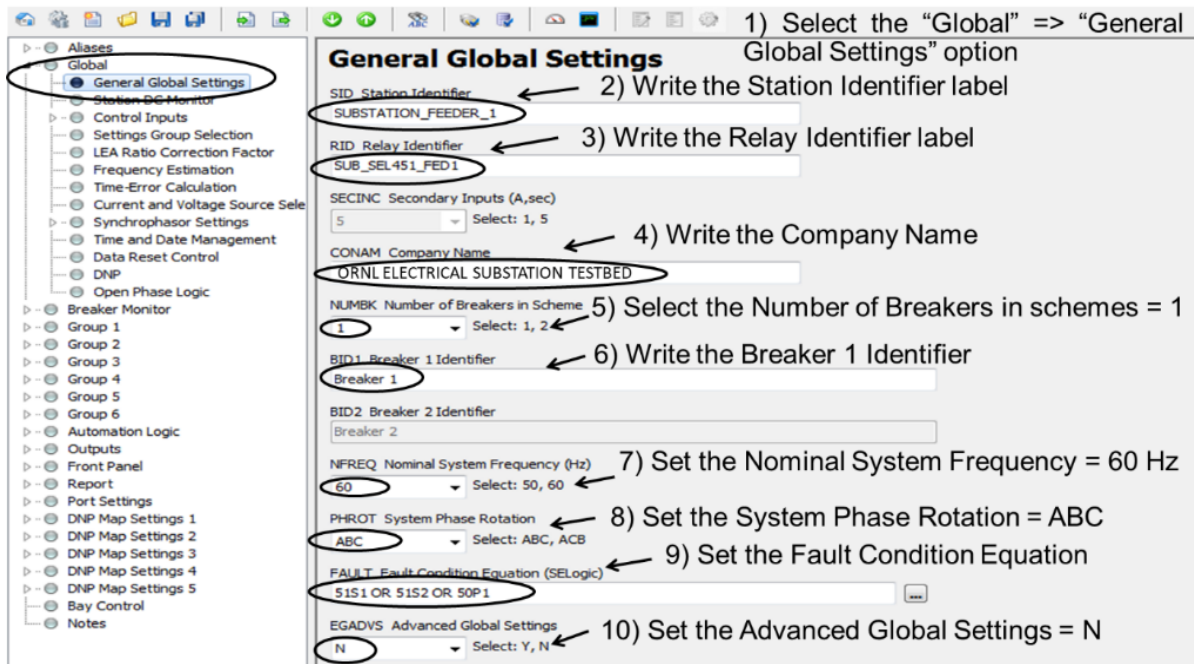


Figure 19. General Global Settings for the SUB_SEL451_FED1 protective relay.

Figure 20 shows the Breaker 1 settings for the SUB_SEL451_FED1 and SUB_SEL451_FED2 protective relays. From the Breaker Monitor menu, the Breaker 1 option was selected. Then, the Breaker 1 Monitoring setting was set to Y, the control input to sense the breaker pole state (52AA1) was set to IN101, and the default Breaker Monitor Trip and Close Equations were left as the default values given by the manufacturer.

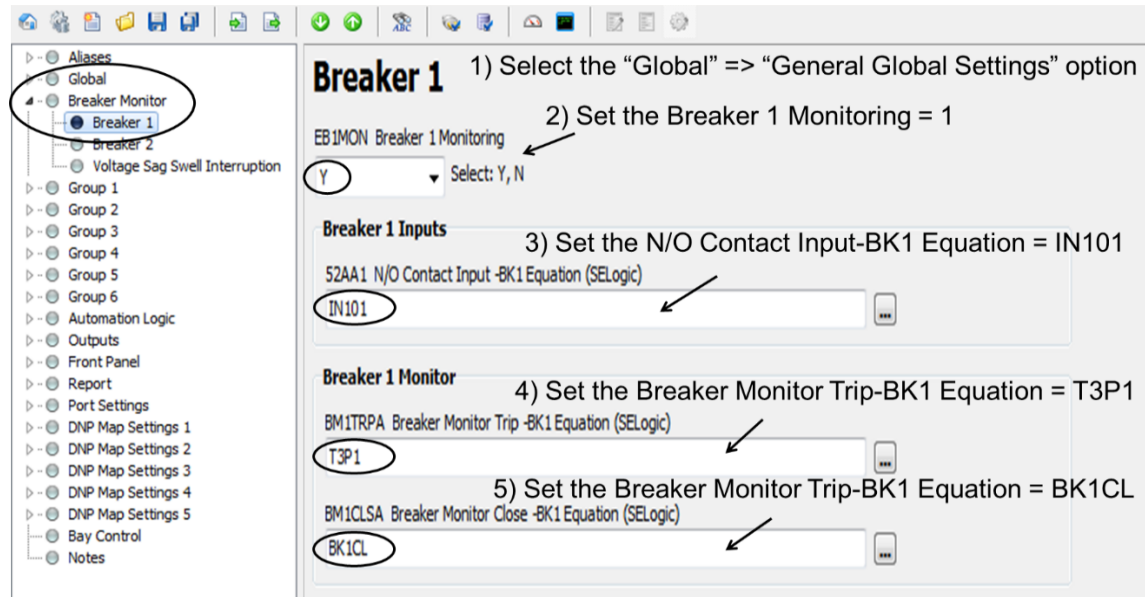


Figure 20. Breaker 1 settings for the SUB_SEL451_FED1 and SUB_SEL451_FED2 protective relays.

Figure 21 shows the Line Configuration settings for the SUB_SEL451_FED1 and SUB_SEL451_FED2 protective relays. From the Group 1 and Set 1 menu, the Line Configuration option was selected. Then, the current and potential transformer ratios were set to 80 and 60, respectively, to measure the primary phase currents and phase to neutral voltages from the secondary phase currents and phase to neutral voltages, which were collected at the electrical substation breaker feeders during the simulations.

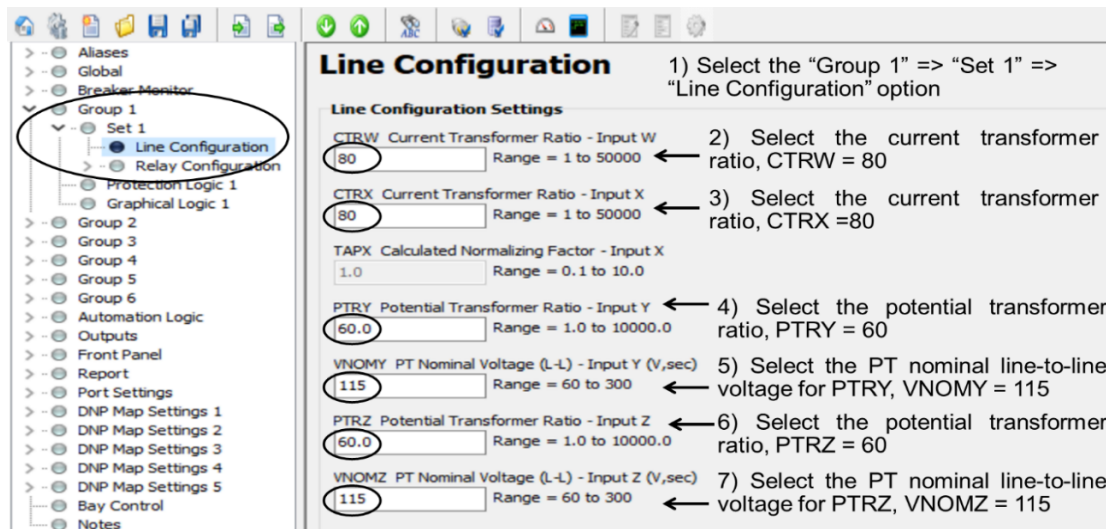


Figure 21. Line Configuration settings for the SUB_SEL451_FED1 and SUB_SEL451_FED2 protective relays.

Figure 22 shows the Relay Configuration Enables settings for the SUB_SEL451_FED1 and SUB_SEL451_FED2 protective relays. From the Group 1 and Set 1 menu, the Relay Configuration option was selected. Then, the Switch-Onto-Fault was set to Y because the protective relays were coordinated with the fuses on load feeders. The Selectable Inverse-Time Overcurrent Element was set to 1 by selecting 1 overcurrent element to set on the relay. In this case, the inverse time overcurrent setting of

the protective relays allowed them to work as backup protection devices for the 50 and 100 T fuses located on load feeders.

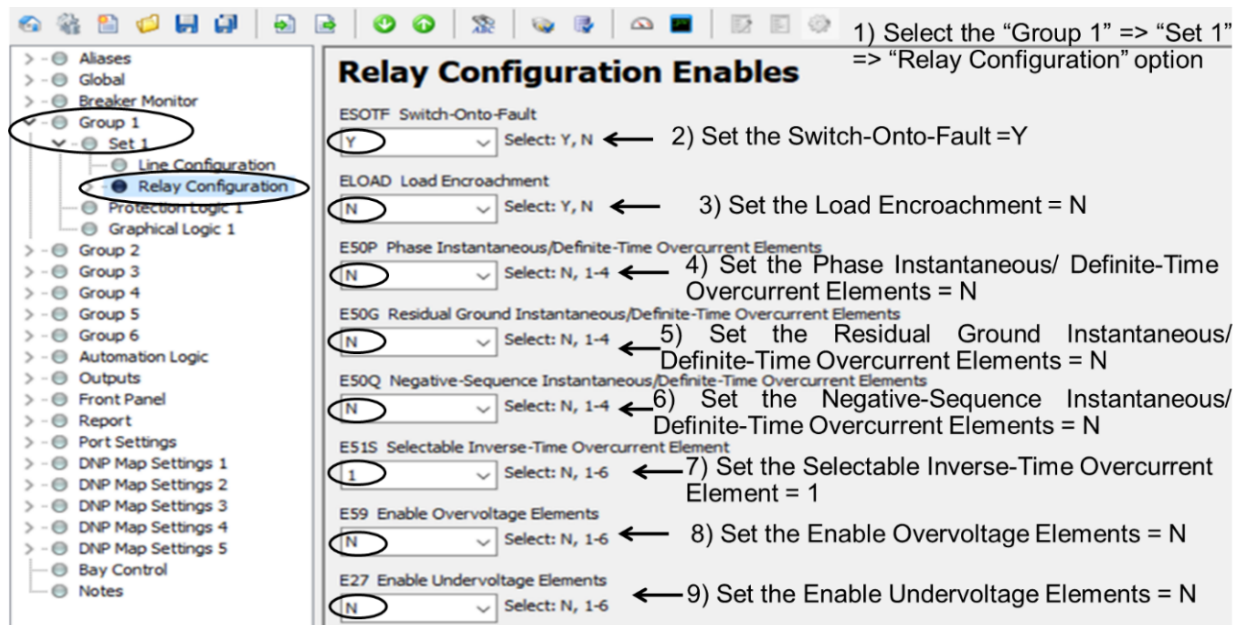


Figure 22. Relay Configuration Enables settings for the SUB_SEL451_FED1 and SUB_SEL451_FED2 protective relays.

Then, the enabled Time Overcurrent Element 1 option was set for the SUB_SEL_451_FED1 and SUB_SEL451_FED2 protective relays. As shown in Figure 23, the Group 1, Set 1, Line Configuration, and Relay Configuration menus were selected to set to the Time Overcurrent option. The 51S1 Operating Quantity to control time overcurrent element was the IMAXL (maximum line current). The settings of the inverse time overcurrent element were selected based on the selectivity coordination between the fuses and relays (Figure 17A, B). Based on that, the secondary overcurrent pickup, inverse time overcurrent curve, and inverse time dial settings were set in 5.00 A, U3 curve, and 2.00, respectively.

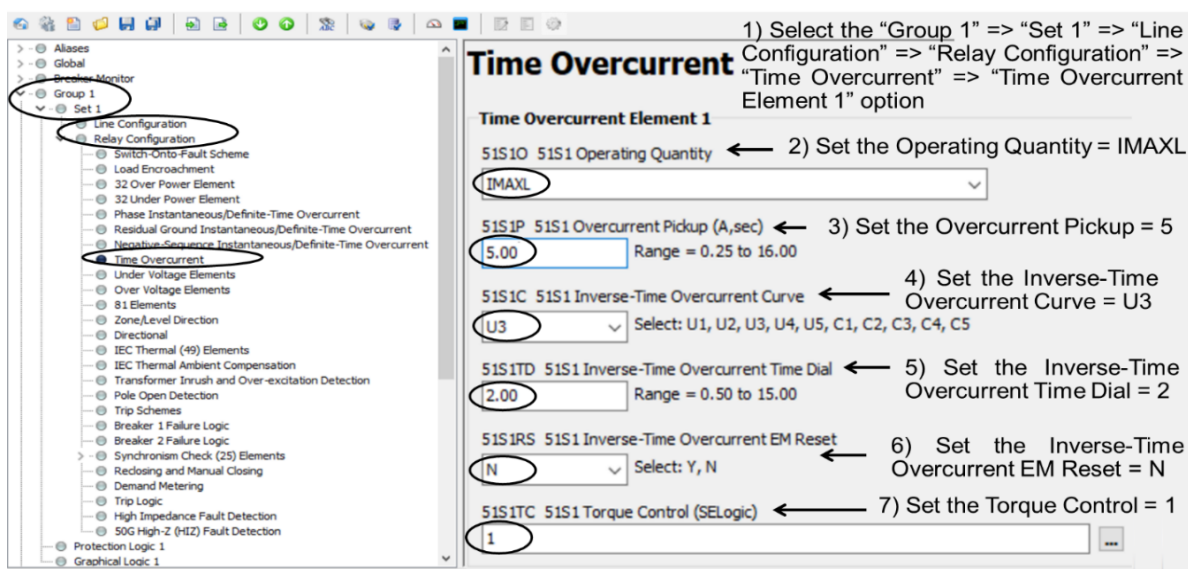


Figure 23. Time Overcurrent settings for the SUB_SEL451_FED1 and SUB_SEL451_FED2 protective relays.

Initially, the SEL-451 protective relays had DNP communication. Both protective relays were upgraded with the IEC 61850 protocol by downloading the new relay configuration submitted by the manufacturer. On the rear side of these SEL-451 protective relays, Ethernet Port 5C was set with IEC 61850 protocol. The protocols and IP addresses for the SEL-451 protective relays are described in Table 6.

Table 6. Protocols and IP address for the SEL-451 protective relays

Type of device	Meter identifier	Ethernet port	Protocol	Subnet mask (Ethernet IP address)
SEL-451 relay	SUB_SEL451_FED1	5C	IEC 61850	255.255.255.0 (192.168.100.2/24)
SEL-451 relay	SUB_SEL451_FED2	5C	IEC 61850	255.255.255.0 (192.168.100.3/24)

Figure 24 shows the Protocol Selection and Communications settings of the SUB_SEL451_FED1 and SUB_SEL451_FED2 protective relays. The communication settings of the SUB_SEL451_FED1 and SUB_SEL451_FED2 protective relays were placed by selecting the Port Setting menu and Port 5 option. Then, Enable Port was set to Y. The Maximum Access Level for Port 5 was set to default C, and the Enable Ethernet Firmware Upgrade was set to N.

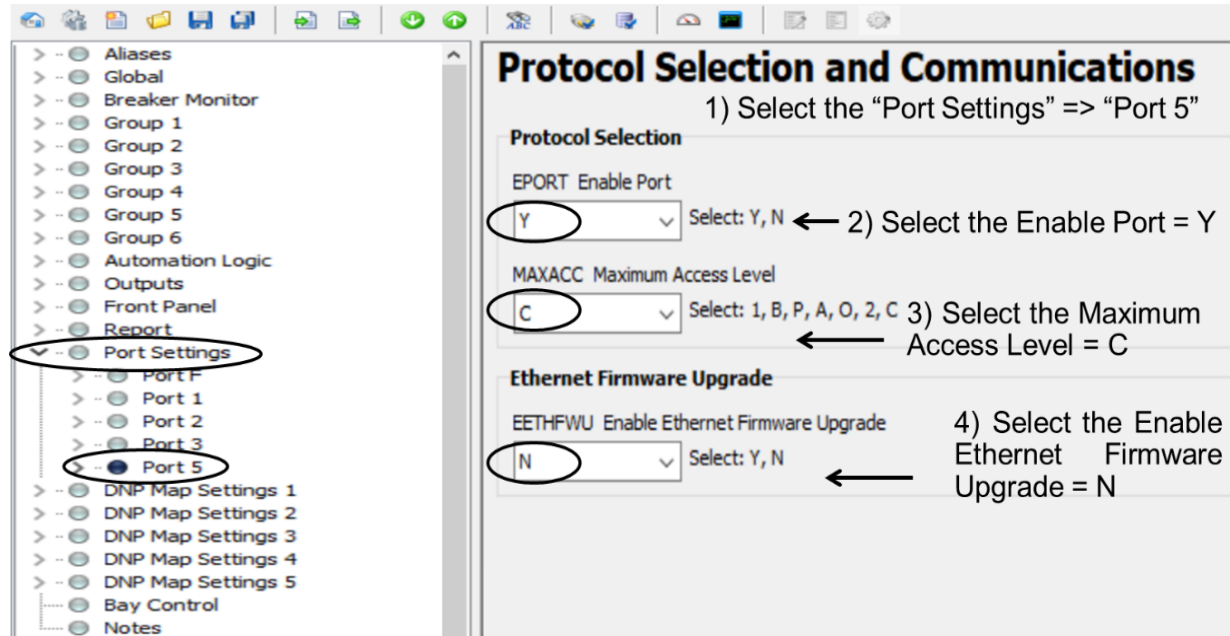


Figure 24. Protocol Selection and Communications settings for the SUB_SEL451_FED1 and SUB_SEL451_FED2 protective relays.

The IP Configuration settings for the SUB_SEL451_FED1 protective relay are shown in Figure 25. The Port Setting and Port 5 menus were selected to select the IP Configuration option. From Table 5, the IP address of the SUB_SEL451_FED1 device was set to 192.168.100.2/24, and port 5C was enabled. The other communication settings were left with the default values.

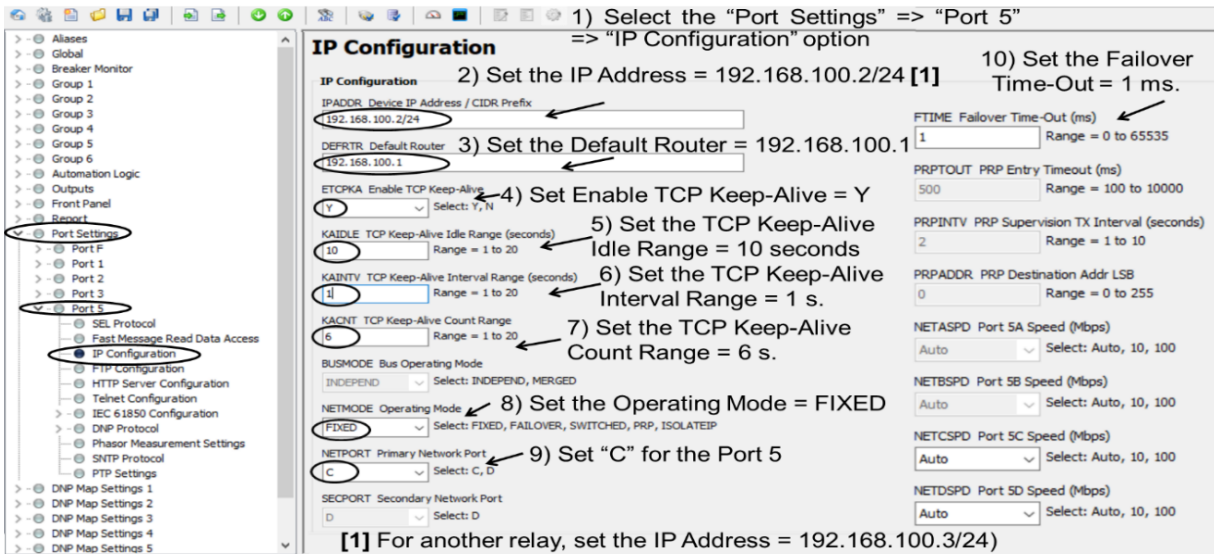


Figure 25. IP Configuration settings for the SUB_SEL451_FED1 protective relay.

Then, the Telnet Configuration, IEC 61850 Configuration, and IEC 61850 Mode/Behavior Configuration settings were selected (Figure 26A–C, respectively). The Port Settings and Port 5 menus were selected to set the Telnet Configuration and IEC 61850 Configuration options (Figure 26A, B).

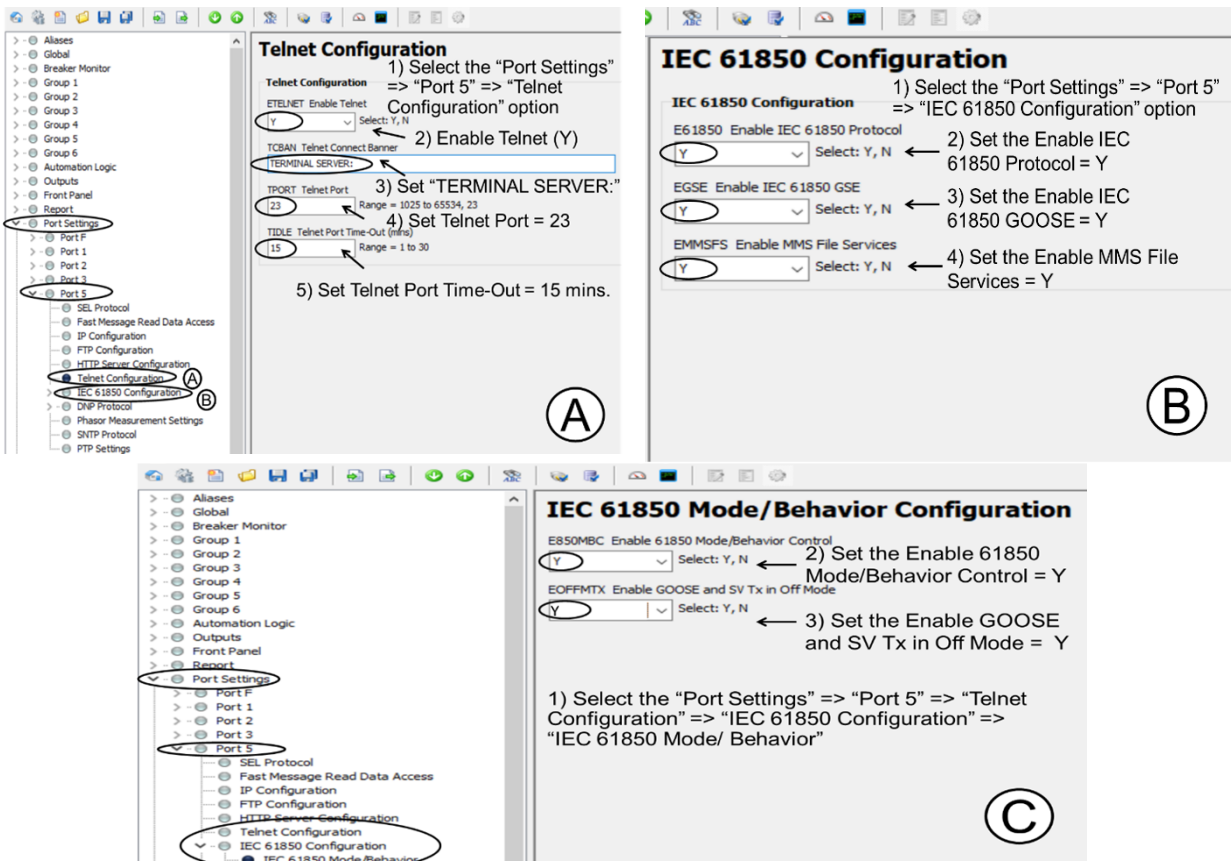


Figure 26. Telnet Configuration (A), IEC 61850 Configuration (B), and IEC 61850 Mode/Behavior Configuration (C) settings for the SUB_SEL451_FED1 and SUB_SEL451_FED2 protective relays.

In the Telnet Configuration, the Enable Telnet setting was set to Y to communicate the SEL-451 protective relays from a computer with the Network – Telnet option (using the AcSELeRator Quickset software), and the Telnet Port was set to 23. In the IEC 61850 Configuration, the Enable IEC 61850 Protocol and GOOSE messages were set to Y. The IEC 61850 Mode/Behavior Configuration settings were set to Y to enable the GOOSE messages for the SEL-451 relays.

3.4 POWER METER SETTINGS

The SEL-734 and SEL-735 power meters were installed to measure the phase currents, phase to neutral voltages, power system frequency, and power for load feeders at 50 and 100 T fuse locations. The objective was to collect these measurements and to determine whether the fuses were blown by measuring the phase currents. The SEL-734 and SEL-735 power meters were set with the AcSELeRator Quickset software, serial cable, and laptop. The Meter and Terminal Identifiers, *CTRs*, and *PTRs* were set in the General Settings and Identifier and Scaling options for the SEL-734 and SEL-735 power meters, respectively. In Table 7, one SEL-734 power meter was set to a horizontal configuration, and the other was set to a vertical panel configuration. The SEL-735 power meters were configured using vertical panel configurations. Table 7 shows the General Settings for the SEL-734 and SEL-735 power meters. Figure 27A and B show the General Settings and Identifier and Scaling Settings for the GRID_SEL_734_FED1 and GRID_SEL_735_FED1 power meters, respectively, based on Table 7. The *CTR* and *PTR* for the power meters were set to 225 and 449, respectively. The Voltage Scaling, Power and Demand Scaling, and Energy Scaling settings were left in KILO (default setting) to obtain the measurements on power meter displays for voltage (kV), demand (kW, kVAR, kVA), and energy (kWh, kVARh, kVAh).

Table 7. General Settings for the SEL-734 and SEL-735 power meters

Type of device	Meter identifier	Terminal identifier	<i>CTR</i>	<i>PTR</i>
SEL-734 meter ^H	GRID_SEL734_FED1	GRID_FEEDER_1	225	449
SEL-734 meter ^V	GRID_SEL734_FED2	GRID_FEEDER_2	225	449
SEL-735 meter ^V	GRID_SEL735_FED1	GRID_FEEDER_3	225	449
SEL-735 meter ^V	GRID_SEL735_FED2	GRID_FEEDER_4	225	449

H = horizontal, *V* = vertical

The SEL-734 power meters do not have the IEC 61850 protocol. Therefore, SEL-734 power meters were set with the DNP. Ethernet Port 1 for the SEL-734 power meters was set with the DNP, and Ethernet Port 1 for SEL-735 power meters was set with the IEC 61850 protocol. The protocols and IP address for the SEL-734 and SEL-735 power meters are described in Table 8.

Table 8. Protocols and IP address for the SEL-734 and SEL-735 power meters

Type of device	Meter identifier	Ethernet port	Protocol	Ethernet IP address (DNP IP address)
SEL-734 meter	GRID_SEL734_FED1	1	DNP	192.168.100.4 (192/168.100.5)
SEL-734 meter	GRID_SEL734_FED2	1	DNP	192.168.100.6 (192/168.100.7)
SEL-735 meter	GRID_SEL735_FED1	1	IEC 61850	192.168.100.8
SEL-735 meter	GRID_SEL735_FED2	1	IEC 61850	192.168.100.10

Group 1

- Set 1
 - General Settings**
 - Fault and Voltage Element Settings
 - Demand Metering Settings
 - Transformer/Line Losses Settings
 - Voltage Sag/Swell/Interruption Settings
 - KYZ Pulse Settings
 - Harmonic Trigger Settings
 - Gain Adjustment Settings
 - Analog Output Settings
- Logic 1
 - Graphical Logic 1
- Daylight Saving Time
- Time-Of-Use
- Global
- Report
- Front Panel
- Meter Energy Preload
- DNP Map Settings
- Port F
- Port 1
- Port 2
- Port 3

General Settings

Meter Identifier Labels

MID Meter Identifier (20 chars): GRID_SEL_734_FED1

TID Terminal Identifier (20 chars): GRID_FEEDER_1

Nominal Voltage

VBASE L-L Voltage Base: 120.00 Range = 20.00 to 300.00

Current and Potential Transformer Ratios

CTR Phase (IA,IB,IC) CT Ratio, CTR:1: 225.0000 Range = 1.0000 to 10000.0000

CTRN Neutral (IN) CT Ratio, CTRN:1: 225.0000 Range = 1.0000 to 10000.0000

PTR Phase (VA,VB,VC) PT Ratio, PTR:1: 449.0000 Range = 1.0000 to 10000

EITCI Enable ITC for Current: N Select: N, 1-6

EITCV Enable ITC for Voltage: N Select: N, 1-6

(A)

General

- Identifier and Scaling**
- Global

Metering

- Demand
- Loss Compensation
- Energy Preload
- Configurable Registers

Inputs/Outputs

- Events and Logging
- Daylight Saving Time
- Time-of-Use

SELogic

- Communication
- Front Panel
- Touchscreen

Identifier and Scaling Settings

Meter Identifier Labels

MID Meter Identifier (20 chars): GRID_SEL735_FED1

TID Terminal Identifier (20 chars): GRID_FEEDER_3

Current and Potential Transformer Ratios

CTR Phase (IA,IB,IC) CT Ratio, CTR:1: 225.0000 Range = 1.0000 to 10000.0000

PTR Phase (VA,VB,VC) PT Ratio, PTR:1: 449.0000 Range = 1.0000 to 10000.0000

Instrument Transformer Compensation

EITCI Enable ITC for Current: N Select: N, 1-6

EITCV Enable ITC for Voltage: N Select: N, 1-6

Analog Quantity Scaling Settings

VOLT_SCA Voltage Scaling: KILO Select: UNITY, KILO, MEGA

ENRG_SCA Energy Scaling: KILO Select: UNITY, KILO, MEGA

POWR_SCA Power and Demand Scaling: KILO Select: UNITY, KILO, MEGA

PRI_SCA Show Analog Quantities in Primary: Y Select: Y, N

(B)

Figure 27. General Settings for GRID_SEL_734_FED1 (A) and GRID_SEL_735_FED1 power meters.

The Ethernet Settings of the GRID_SEL_734_FED1 power meter are shown in Figure 28. From the Port 1 menu, the Ethernet Settings option was selected. Then, the Port Security Settings (Figure 28A) were set in the SEL-734 power meter. Ethernet Port 1 was enabled by setting the Enable Port to Y. The Enable Telnet setting was also set to Y to communicate and set the SEL-734 power meter from a computer with the AcSELeator Quickset software using the Network – Telnet communication option. The MODBUS communication was disabled by setting the Enable MobBus to N. The DNP communication was enabled by setting the DNP session to 1 in the Enable DNP Sessions (0-5) option. Figure 28B shows the Communication Settings values. The Telnet Port One was set to 23. The Subnet Mask was set to 255.255.255.0, and the IP address for Ethernet Port 1 was set to 192.168.100.4 for the GRID_SEL734_FED1, based on Table 8.

Ethernet Settings

Port Security Settings

EPORT Enable Port 1) Enable the port (Y)
Y Select: Y, N

ETELNET Enable Telnet 2) Enable Telnet (Y)
Y Select: Y, N

MAXACC Telnet SEL ASCII Maximum Access Level 3) Enable Access level 2
2 Select: 1, E, 2

EMODBUS Enable ModBus 4) No enable Modbus
N Select: Y, N

EDNP Enable DNP Sessions (0-5) 5) Enable DNP Session 1
1 Select: 0-5

Communications Settings

TPORT Telnet Port One
23 Range = 1025 to 65534, 23 6) Set Telnet port: 23

TIDLE Telnet Port One Idle Time (minutes)
15

DEFTRT Default Router (www[h].xxx[h].yyy[h].zzz[h])
192.168.100.1 Range = ASCII string with a maximum length of 19. 7) Set default router: 192.168.100.1

SUBNETM Subnet Mask (www[h].xxx[h].yyy[h].zzz[h])
255.255.255.0 Range = ASCII string with a maximum length of 19. 8) Set subnet mask 255.255.255.0

IPADDR IP Address (www[h].xxx[h].yyy[h].zzz[h])
192.168.100.4 Range = ASCII string with a maximum length of 19. 9) Set IP address: 192.168.100.4

Figure 28. Ethernet Settings of the GRID_SEL_734_FED1 power meter.

The SEL-734 power meters were set with DNP communication because the IEC 61850 protocol communication was not available on these power meters. The SEL-735 power meters were set with the IEC 61850 protocol. Figure 29 shows the Ethernet Settings of the GRID_SEL_735_FED1 power meter. From the Communication and Ports menus, the Port 1 (Ethernet) option was selected. Then, the Port Security Settings (Figure 29A) were set in the SEL-735 power meter. Ethernet Port 1 was enabled by setting the Enable Port to Y. The Enable Telnet setting was set to Y to communicate and set the SEL-735 power meter from a computer with the AcSElerator Quickset software using the Network – Telnet communication option. The MODBUS communication was disabled by setting the Enable ModBus to N, and the DNP communication was disabled by setting the DNP session to 0 in the Enable DNP Sessions (0-5) option. As shown in Figure 29B, the IEC 61850 protocol was enabled by setting the Enable IEC 61850 Protocol to 1, and the GOOSE messages was enabled by setting the Enable IEC 61850 GSE to Y. Then, DNP and PMU sessions were set to 0 because these protocols were disabled. Finally, the Communication Settings (Figure 29C) were set for the SEL-735 power meter. The Primary Telnet Port was set to 23. The Subnet Mask was set to 255.255.255.0, and the IP address for Ethernet Port 1 was set to 192.168.100.8 for the GRID_SEL735_FED1 power meter based on Table 8.

Ethernet Settings

Port Security Settings

EPORT Enable Port 1) Enable the port (Y)
Y Select: Y, N

ETELNET Enable Telnet 2) Enable Telnet (Y)
Y Select: Y, N

MAXACC Maximum Access Level 3) Enable Access level 2
2 Select: 1, E, 2

ETCPKA Enable TCP Keep-Alive 5) No enable TCP Keep-Alive
N Select: Y, N

EFTPSERV Enable FTP 6) Enable FTP (Y)
Y Select: Y, N

IEC 61850 Settings

E61850 Enable IEC 61850 Protocol 7) Enable IEC61850 (1)
1 Select: 0-6

EGSE Enable IEC 61850 GSE 8) Enable IEC61850 GOOSE(Y)
Y Select: Y, N

ESNT Enable SNTP 9) Set OFF
OFF Select: OFF, UNICAST, MANYCAST, BROADCAST

EDNP Enable DNP Sessions (0-5) 10) SET the DNP session (0)
0 Select: 0-5

EPMIP Enable PMU Sessions 11) No enable PMU sessions (0)
0 Select: 0-2

Communications Settings

TPORT Primary Telnet Port 12) Set Telnet port: 23
23 Range = 1025 to 65534, 23

IPADDR IP Address 13) Set IP address: 192.168.100.8
192.168.100.8 Range = ASCII string with a maximum length of 15.

SUBNETM Subnet Mask 14) Set subnet mask 255.255.255.0
255.255.255.0 Range = ASCII string with a maximum length of 15.

DEFTRT Default Router (Gateway) 15) Set default router: 192.168.100.1
192.168.100.1 Range = ASCII string with a maximum length of 15.

TIDLE Primary Telnet Port Timeout (minutes)
15 Range = 1 to 30, OFF

Figure 29. Ethernet Settings of the GRID_SEL_735_FED1 power meter.

4. TIME SYNCHRONIZATION SYSTEM

In this section, the time synchronization system is described by presenting the communication architecture and configuration for the inside and outside substation devices with the Ethernet switches and DLT devices. The time frame based on using the SEL-2488 Satellite-Synchronized Network Clock and the DarkNet timing sources are presented. The process to communicate and set the SEL-2488 Satellite-Synchronized Network Clock is described, and the synchronized time protocols for the inside and outside substation devices based on their available ports are described.

4.1 TIME FRAME SOURCES

The time synchronization system was based on using a primary and backup time source frame. The internal clock of the SEL-2488 Satellite-Synchronized Network Clock and DarkNet timing source were available on the time synchronization system. Figure 30 shows the time synchronization system. The DarkNet and SEL-2488 internal clock signals are the primary and backup time source frames, respectively. The internal clock timing source was implemented to synchronize the time stamps for the SEL-451 protective relays and SEL-734 and SEL-735 power meters, and the DLT devices (CISCO Ethernet switches). The SEL-2488 Satellite-Synchronized Network Clock had the Precision Time Protocol (PTP) and Inter-Range Instrumentation Group–Time Code Format B (IRIG-B) protocols. However, not all IEDs in the electrical substation could be set with PTP because an extra Ethernet port was necessary for this timing protocol. Therefore, the PTP was used for CISCO switches (Figure 30A) and HMI servers (control center and local substation), and the IRIG-B protocol was used for the SEL-451 protective relays (Figure 30B) and SEL-734 and SEL-735 power meters (Figure 30C).

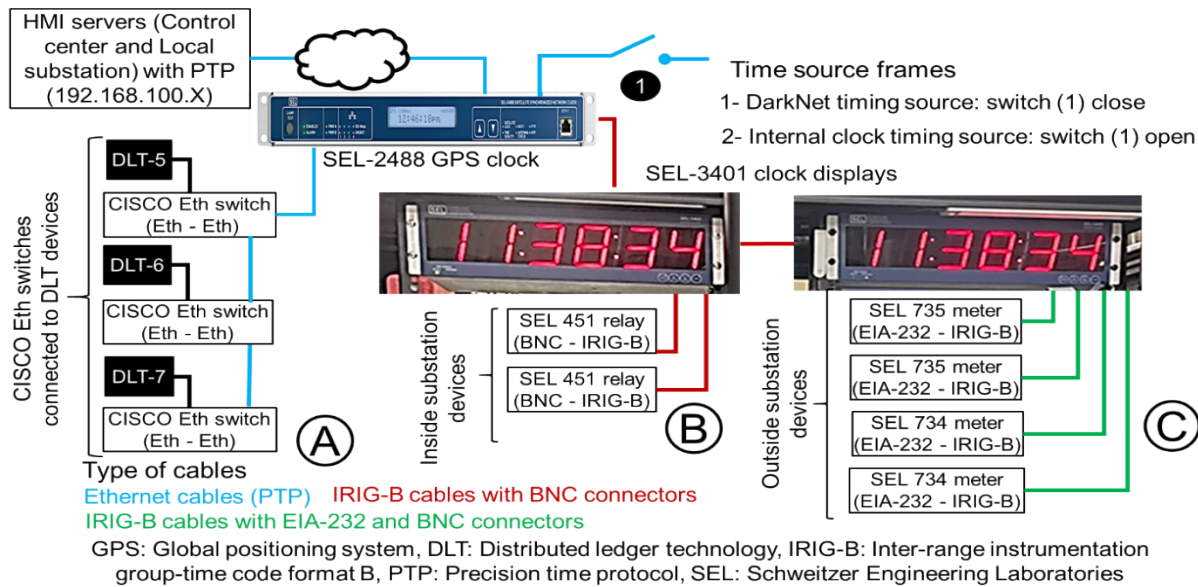


Figure 30. Time synchronization system for electrical substation-grid test bed.

UTC was implemented at the electrical substation-grid test bed because it was the easiest method to ensure that all devices are producing the same kind of time stamps. UTC has the advantage that if protective relays from different electrical substations are in different time zones, the protective relays at both sides of the transmission line will have the same time stamp, and relay events from both protective relays will have the same time reference, avoiding the local time where each protective relay could be located. The clock displays show the UTC time (Figure 31), but because the test bed is at the Grid

The Local Time Settings were selected from the System and Date/Time menus, and the Local Time Settings option was selected. Then, the Local Time-Zone Offset from UTC was set to -05:00 in hours: minutes, based on the Eastern UTC-05:00 zone. Figure 33 shows the Local Time Settings of the SEL-2488 Satellite-Synchronized Network Clock.

The screenshot shows the SEL-2488 configuration interface. On the left sidebar, the 'System' menu is expanded, and 'Date/Time' is selected. The main panel is titled 'Date/Time' and contains the 'Local Time Settings' tab. The 'Local Time Zone Offset from UTC' is set to '-05:00 (±HH:MM)'. The 'Daylight Saving Time Mode' is set to 'United States Daylight Saving Time'. The 'Start of Daylight Saving Time' section shows 'Start Time: 02:00 (HH:MM)', 'Start Month: March', 'Start Week: Second', and 'Start Day of Week: Sunday'. The 'End of Daylight Saving Time' section shows 'End Time: 02:00 (HH:MM)'. A map of the United States is displayed on the right, showing time zones: Pacific UTC-8, Mountain UTC-7, Central UTC-6, Eastern UTC-5, Hawaii-Alutian UTC-10, and Alaska UTC-9. The 'Submit' button is highlighted at the bottom. Annotations with arrows point to the 'Local Time Settings' tab, the 'Local Time Zone Offset from UTC' field, and the 'Submit' button.

1- Select the "System" => "Date/Time" => "Local Time Settings" option

2- Select the Local Time Zone Offset from UTC that corresponds to the Eastern Time (-05:00)

3- Select the "Submit" option

Figure 33. Local Time Settings of the SEL-2488 Satellite-Synchronized Network Clock.

As shown in Figure 34, the Manual Date/Time was set by selecting the System and Date/Time menus, and the Manual Date/Time option was selected. Then, the date YYYY/MM/DD and the time HH:MM:SS in the Manual Date and Manual Time options were set, respectively. The SEL-2488 Satellite-Synchronized Network Clock was set by an internal clock as a backup in case the primary time frame source from DarkNet was interrupted.

The screenshot shows the SEL-2488 configuration interface. On the left sidebar, the 'System' menu is expanded, and 'Date/Time' is selected. The main panel is titled 'Date/Time' and contains the 'Manual Date/Time' tab. The 'Manual Date' is set to '2021/11/15 (YYYY/MM/DD)' and the 'Manual Time' is set to '19:22:15 (HH:MM:SS)'. A 'New Major Alarm' banner is visible at the top right. A green banner indicates 'Settings successfully updated.' The 'Submit' button is highlighted at the bottom. Annotations with arrows point to the 'Manual Date/Time' tab, the 'Manual Date' field, the 'Manual Time' field, and the 'Submit' button.

1- Select the "System" => "Date/Time" => "Manual Date / Time" option

2- Put the actual date "YYYY/ MM / DD"

3- Put the actual time "HH: MM : SS", check the Eastern time on an internet clock and set the exact time.

Note: The SEL-2488 satellite synchronized network clock was set with the "Manual Date/ Time" option, in case other time frame sources were interrupted.

4- Select the "Submit" option

Figure 34. Manual Date/Time settings for the SEL-2488 Satellite-Synchronized Network Clock.

The General Network Settings were set by selecting the Network Management menu, and the IP Configuration option was selected. The process to set the IP Configuration Settings of the SEL-2488 Satellite-Synchronized Network Clock is shown in Figure 35. The SEL-2488 Satellite-Synchronized Network Clock was enabled for the ETH (Ethernet) ports. The ETH port F, located at the front side of the SEL-2488 Satellite-Synchronized Network Clock, was left with the default IP address, and it was used as an alternative to set this device from the front side. The other Ethernet ports located at the rear side of the SEL-2488 Satellite-Synchronized Network Clock were set as possible alternatives to be used with the Network Time Protocol (NTP) to connect servers, computers, and other devices that set their time through NTP.

Port	Enabled	Alias	IP Address	HTTPS	Captive Port	NTP Server	SNMP
ETH F	<input checked="" type="checkbox"/>		192.168.1.2 /24	<input checked="" type="checkbox"/>	<input checked="" type="checkbox"/>	<input type="checkbox"/>	<input type="checkbox"/>
ETH 1	<input checked="" type="checkbox"/>		192.168.100.21 /24	<input checked="" type="checkbox"/>	<input type="checkbox"/>	<input checked="" type="checkbox"/>	<input type="checkbox"/>
ETH 2	<input checked="" type="checkbox"/>		10.0.0.22 /24	<input checked="" type="checkbox"/>	<input type="checkbox"/>	<input checked="" type="checkbox"/>	<input type="checkbox"/>
ETH 3	<input checked="" type="checkbox"/>		192.168.102.23 /24	<input type="checkbox"/>	<input type="checkbox"/>	<input checked="" type="checkbox"/>	<input type="checkbox"/>
ETH 4	<input checked="" type="checkbox"/>		192.168.103.24 /24	<input type="checkbox"/>	<input type="checkbox"/>	<input checked="" type="checkbox"/>	<input type="checkbox"/>

Figure 35. IP Configuration settings for the SEL-2488 Satellite-Synchronized Network Clock.

Finally, the Front Panel setting of the SEL-2488 Satellite-Synchronized Network Clock was set by selecting the System menu, and the Front Panel option was selected. The steps to set the Front Panel settings for the SEL-2488 Satellite-Synchronized Network Clock are shown in Figure 36. In the SEL-2488 Satellite-Synchronized Network Clock, the Date Display Format and Time Display Format were set to Month/Day/Year and UTC options, respectively, and the settings for the Timeout were enabled and set by the default settings.

Settings successfully updated.

1- Select the "System" => "Front Panel" option

Date Display Format:

- ☐ None
- ☒ Month / Day / Year
- ☐ Day / Month / Year
- ☐ Year / Month / Day
- ☐ Day of Year

Time Display Format:

- ☐ 12 hour local time
- ☐ 24 hour local time
- ☒ UTC

☒ Enable Timeout

Timeout: * 15 (Minutes)

Contrast: * 4

3- Select the "Submit" option

Figure 36. Front Panel settings for the SEL-2488 Satellite-Synchronized Network Clock.

4.3 SYNCHRONIZED TIME PROTOCOLS

Time synchronization is an essential tool to study electrical fault and disturbance events at power systems. The SEL-2488 Satellite-Synchronized Network Clock has eight BNC ports, which can be configured for demodulated IRIG-B. The demodulated IRIG-B provides time output for protection applications, synchronizing relays, phasor measurement units, and other devices to within ± 40 ns average accuracy to UTC [14]. The SEL-2488 Satellite-Synchronized Network Clock has four Ethernet ports that can use the NTP to distribute time to devices on the substation local-area network, such as servers, computers, and other devices that set their time through the NTP or Simple NTP. In addition, the Ethernet ports of the SEL-2488 Satellite-Synchronized Network Clock can support hardware time stamping to set the PTP defined by IEEE 1588-2019 [15].

The SEL-2488 Satellite-Synchronized Network Clock was used for synchronizing and timing the DLT devices, servers (or computers), SEL-734 and SEL-735 power meters, and SEL-451 protective relays. Although the DLT devices used the PTP, the SEL-734 and SEL-735 power meters and SEL-451 protective relays do not have available the PTP, so the IRIG-B protocol was used for those devices. Fortunately, the SEL-2488 Satellite-Synchronized Network Clock had Ethernet and IRIG-B outputs that provided PTP and IRIG-B communication. It is a typical that both protocols could be available in electrical substations because not all devices have PTP Ethernet ports. In addition, the SEL-734 and SEL-735 power meters were provided with IRIG-B ports instead of PTP Ethernet ports [5, 6]. The SEL-451 protective relays could have the option of PTP Ethernet ports, but this option was only available for the SEL-451 relays with the ETH Port A on the rear side [4]. The SEL-451 protective relays for the breaker feeders at the electrical substation had only the ETH Port C and D available on the rear side.

5. COMMUNICATION SYSTEM

In this section, the communication system for the electrical substation-grid test bed is presented. The protocols for the inside and outside substation devices of the electrical substation-grid test bed are described, based on using the IEC 61850 (GOOSE message) and DNP communication. The process to set the IEC 61850 map for the SEL-451 relays and SEL-735 power meters is described. Also, the steps to set the DNP map for the SEL-734 power meters with the configuration of the SEL-3530-4 RTAC is presented. Finally, the steps to communicate from a computer with the inside and outside substation devices using the Telnet communication is defined to access all devices of the electrical substation-grid test bed.

5.1 IEC 61850 VS. DNP COMMUNICATION

The communication systems used by electrical utility companies include both the DNP and IEC 61850 protocol. The DNP is most widely used by US electrical utility companies, but the IEC 61850 standard is gaining recognition as a benchmark for local communication protocols. IEC 61850 has been widely adopted around the world, and many companies currently using DNP are also choosing to adopt cross-functionality for both the DNP and IEC 61850 [16]. The DNP focuses on the transportation of simple data in a lightweight manner for the purpose of remote communication. The IEC 61850 mainly focuses on communication among assets, such as protective relays, power meters, and local HMI/SCADA systems, inside a local facility. Another major difference is that the IEC 61850 protocol focuses on the context of data. The DNP focuses on data and largely passes contextualization off for engineers to address. IEC 61850 integrates context into the system by mapping data to logical nodes with predefined, contextual names. This ensures that context is never lost in the shuffle of compiling data [16]. In the electrical substation-grid test bed, the communication system was based on using both protocols. The IEC 61850 protocol with GOOSE messages was used for the SEL-451 protective relays and SEL-735 power meters, and the DNP communication was used for the SEL-734 power meters.

5.2 SETTING OF THE IEC 61850 MAP FOR DEVICES

The communication system was based on using IEC 61850 protocol with GOOSE messages for the SEL-451 relays and SEL-735 power meters. The CID files were used to create the CID project files to configure IEC 61850 devices [17]. The SEL-451 protective relays and SEL-735 power meters were set with CID files to set the IEC 61850 communication with GOOSE messages. The CID project files for the devices with IEC 61850 were created, completed, and submitted to the SEL-451 relays and SEL-735 power meters by using the AcSElerator Architect software [4, 5]. The steps to create the CID project file are shown in Figure 37. The AcSElerator Architect software was downloaded and opened. Then, the File menu and New option were selected, and the project was saved as “TASK_5” on the desktop computer. This project file was used to add the CID files for the SEL-451 relays and SEL-735 power meters to work with GOOSE messages (IEC 61850).

1) Download the AcSElerator Architect software in a laptop.

2) Open the AcSElerator Architect software

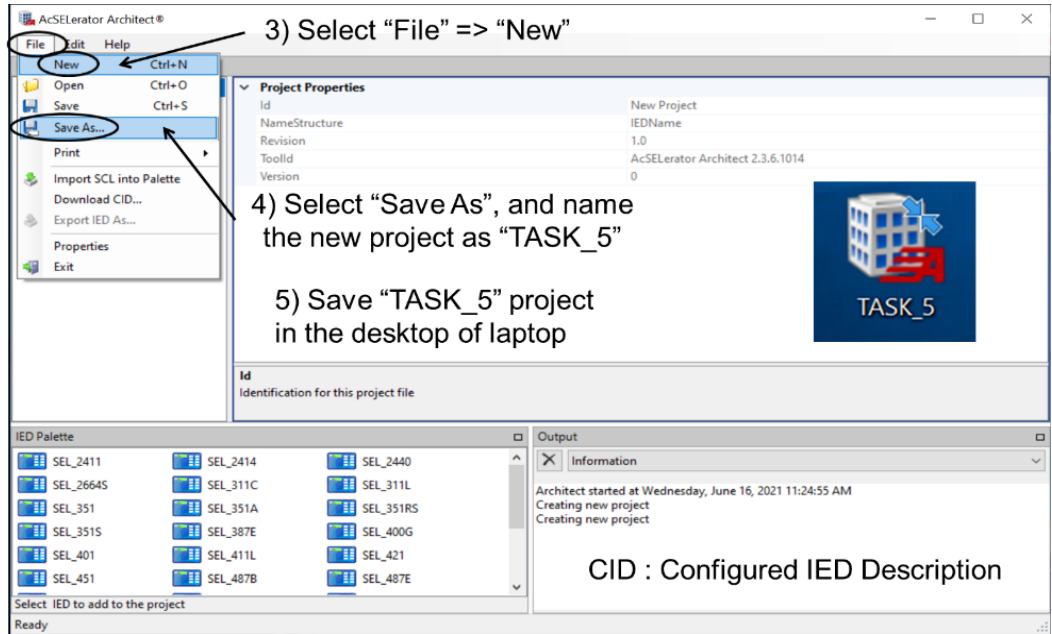


Figure 37. The created CID project file.

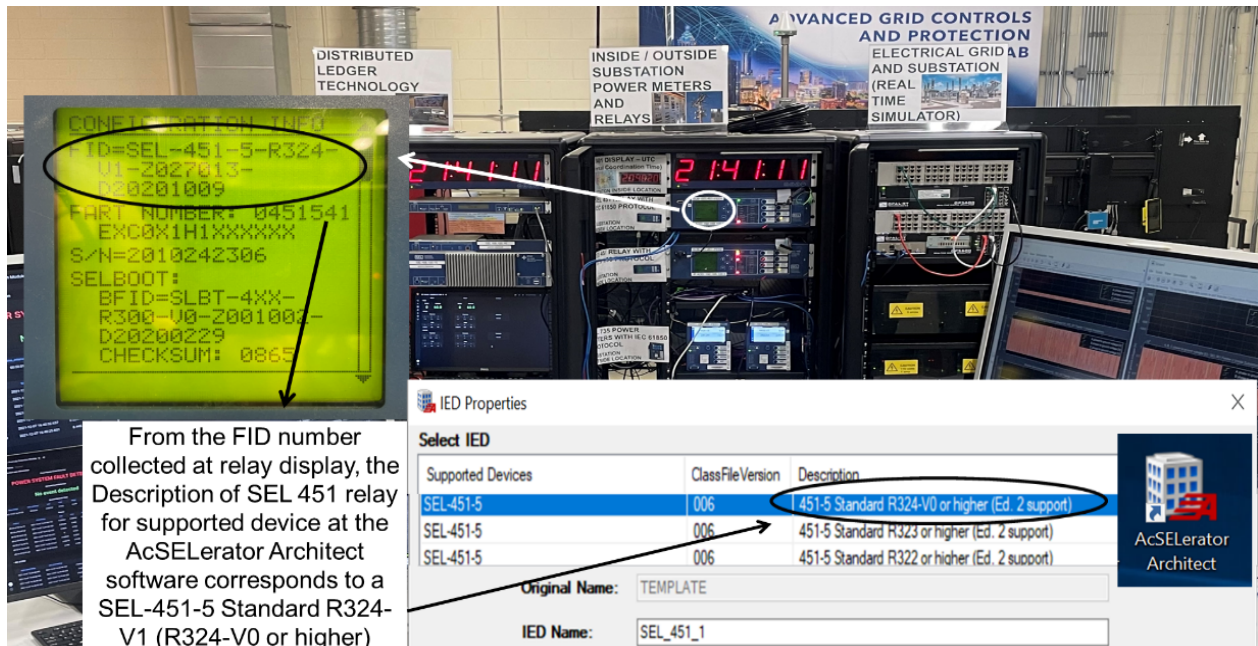


Figure 38. Firmware Identifier number of the SEL-451 protective relay.

Once the TASK_5 project file was saved in the desktop computer, the Firmware Identifier number (SEL-451-5-R324-V1-Z027013-D20201009) of the SEL-451 protective relay was collected from the device display at the test bed location (Figure 38). Then, the TASK_5 file was opened from the desktop computer by the AcSElerator Architect software, and the SEL_451 device was selected from the IED Palette (Figure 39A). The selected supported device for the AcSElerator Architect software was given by the 415-5 Standard R324-V0 or higher description because the Firmware Identifier number collected from the SEL-451 relay was **SEL-451-5-R324-V1-Z027013-D20201009**, which corresponds to a SEL-451-5 device and R324-V1 version. The selected IED was named "SEL_451_1," and the device was added to

the TASK_5 folder by selecting OK (Figure 39A). The SEL451_1 device file was saved in the TASK_5 folder by selecting the Enable control of IEC 61850 Mode/Behavior and Direct control with enhanced security options (Figure 39B).

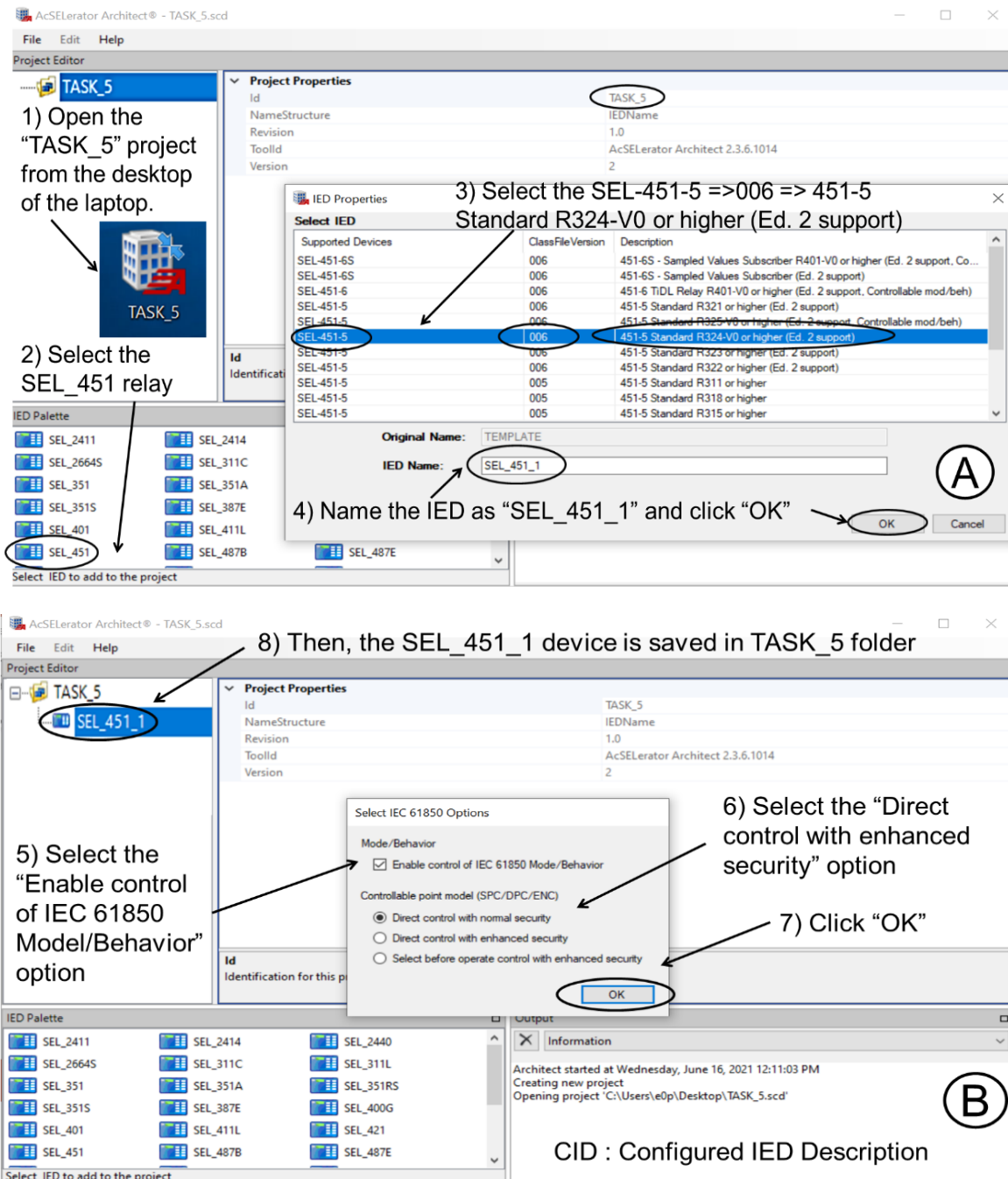


Figure 39. Steps to select the IED.

The SEL_451_1 device was opened, and the Properties tab was selected to add the IED Properties (Figure 40). For Ethernet Port 5C of the SUB_SEL451_FED1 device, the IP Address was set to 192.168.100.2, the Subnet Mask was set to 255.255.255.0, and the Gateway was set to 192.168.100.1. To set the Properties for the SUB_SEL451_FED2 device, the IP Address was set to 192.168.100.3 (Table 6).

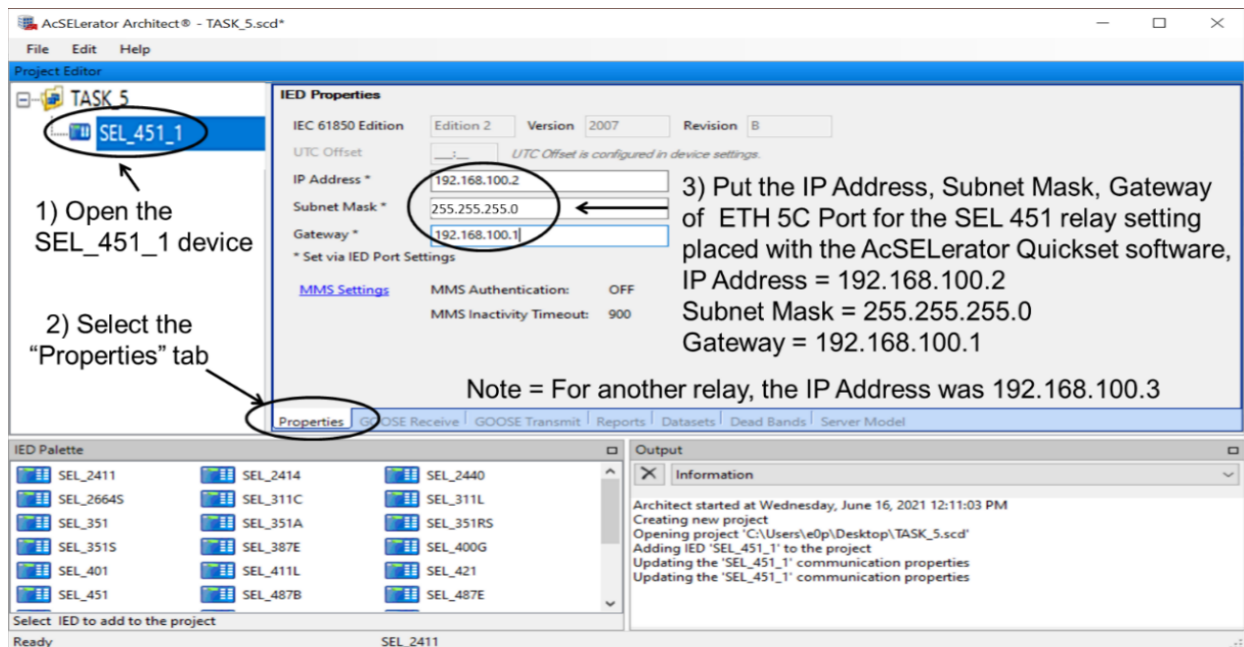


Figure 40. Steps to set the IED Properties.

Figure 41 shows the steps to set the GOOSE Transmit message of the IED (SEL_451_1). The GOOSE Transmit tab was selected and right-clicked to add a New message line. The New Message was named "NewGOOSEMessage." The Description was defined as Metered Values, the Goose ID was set as SEL_451_1, and the CFG.LLN0.BRDSet01 Dataset was selected.

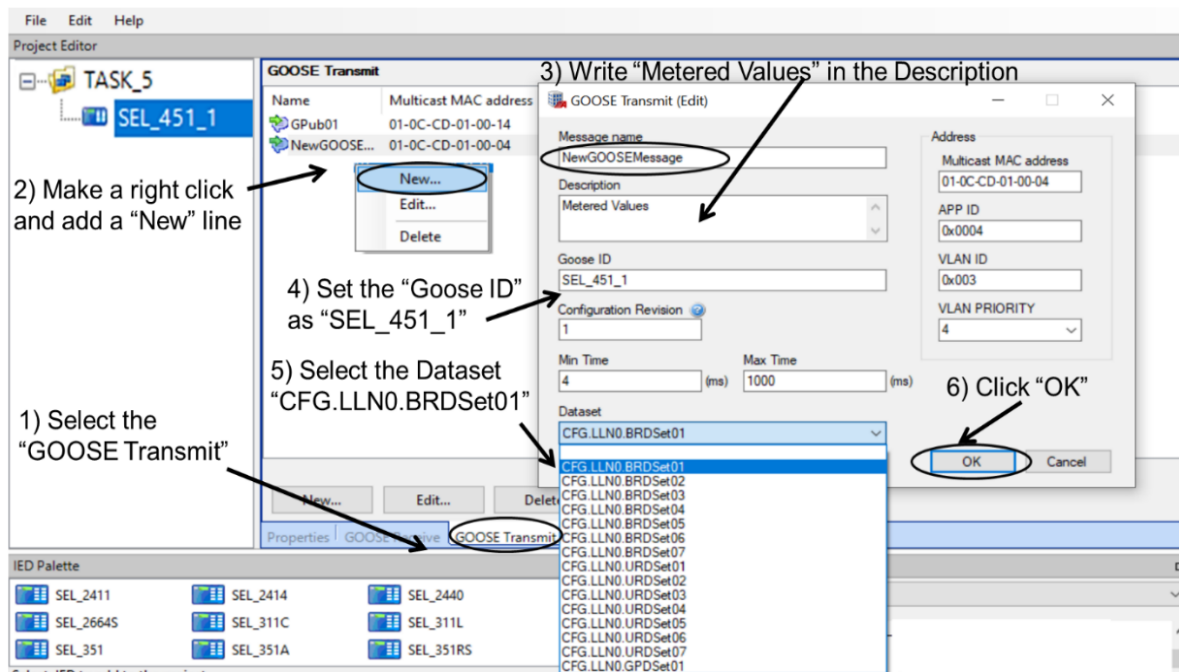


Figure 41. Steps to set the GOOSE Transmit (Metered Values) message of the IED.

Figure 42 shows the steps to set the Dataset (Metered Values) for the IED (SEL_451_1). The Datasets tab was selected. Then, the configurable CFG.LLN0.BRDSet01 Dataset for Metered Values was opened. To

edit the Dataset, the MX (Measurands) option from the FC (Function Constraint) was selected in the IED Data Items (Figure 42A). Then, all items from this Dataset were deleted to add the new ones. As shown in Figure 42B, from the MX (Measurands), the magnitude of Breaker 1 10-cycle average fundamental A phase current was selected at the A2 => phsA => InstCVal => mag.f path, and the angle of Breaker 1 10-cycle average fundamental A phase current was selected at the A2 => phsA => InstCVal => ang.f path. To set those elements at the Dataset, each element was selected and dragged from the left to the right column. When all desired Metered Values were selected for the Dataset, OK was selected (Figure 42B).

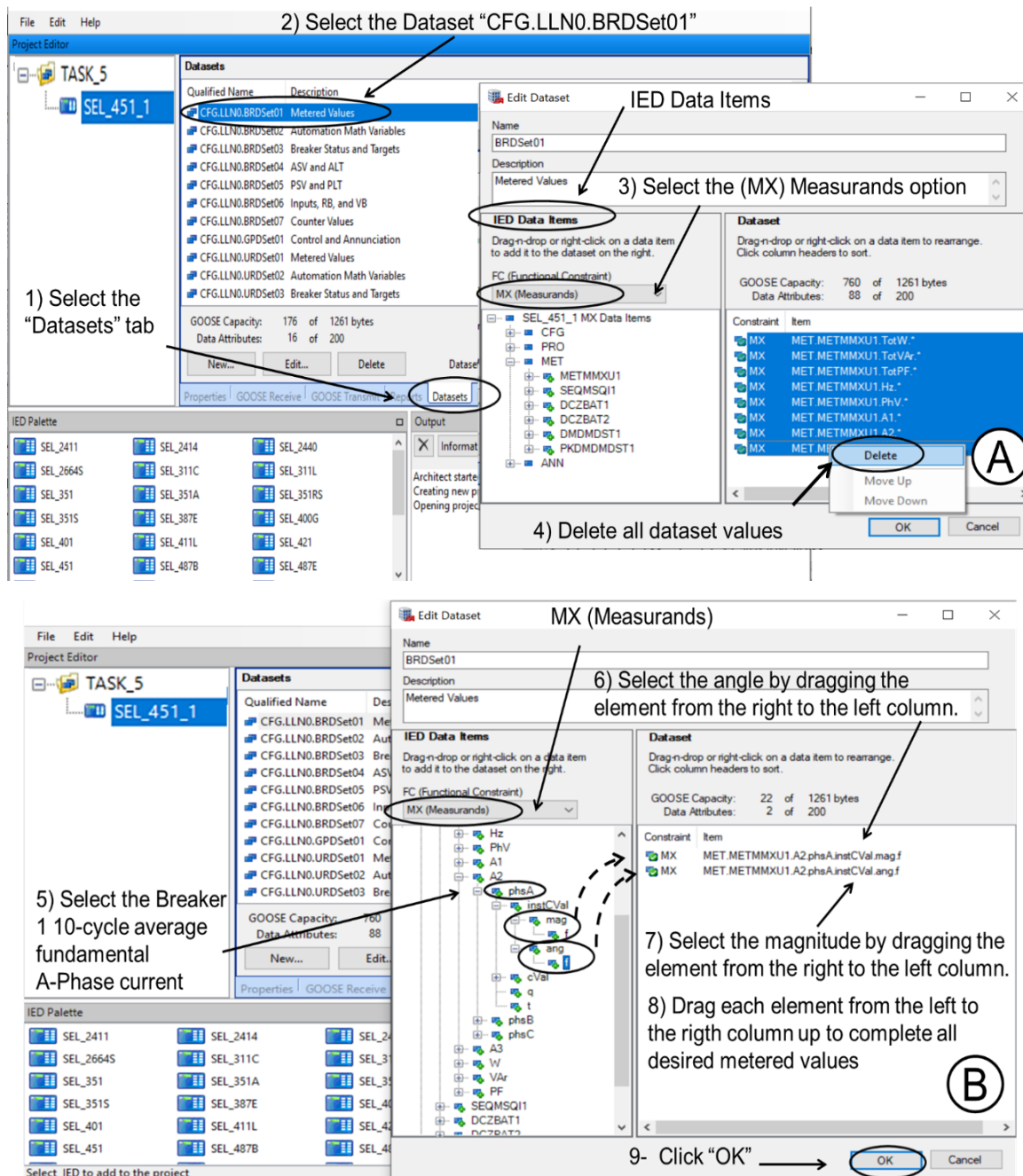


Figure 42. Steps to set the Dataset (Metered Values) of the IED.

As shown in Figure 43, once the Dataset was configured with all elements that correspond to the desired measured values to be transmitted by the SEL_451_1 device (SUB_SEL451_1), the CID file of the IED (SEL_451_1) was submitted by connecting the computer to Ethernet Port 5C of the SUB_SEL451_1 device. The steps to submit the CID file to the SUB_SEL451_1 device are shown in Figure 43. From the TASK_5 project, the Properties tab was selected, and the IP address of Ethernet Port 5C for the SUB_SEL451_1 device was set. Then, the SEL_451_1 was selected and right-clicked to select the Send CID option. The FTP Address, User Name, and Password were completed, and Next was selected to submit the CID file to the SUB_SEL451_1 device. The User Names for the SEL-451 protective relays and SEL-735 power meters were 2AC and FTPUSER, respectively.

The password for both IEDs (SEL-451 protective relay and SEL-735 power meter) was TAIL.

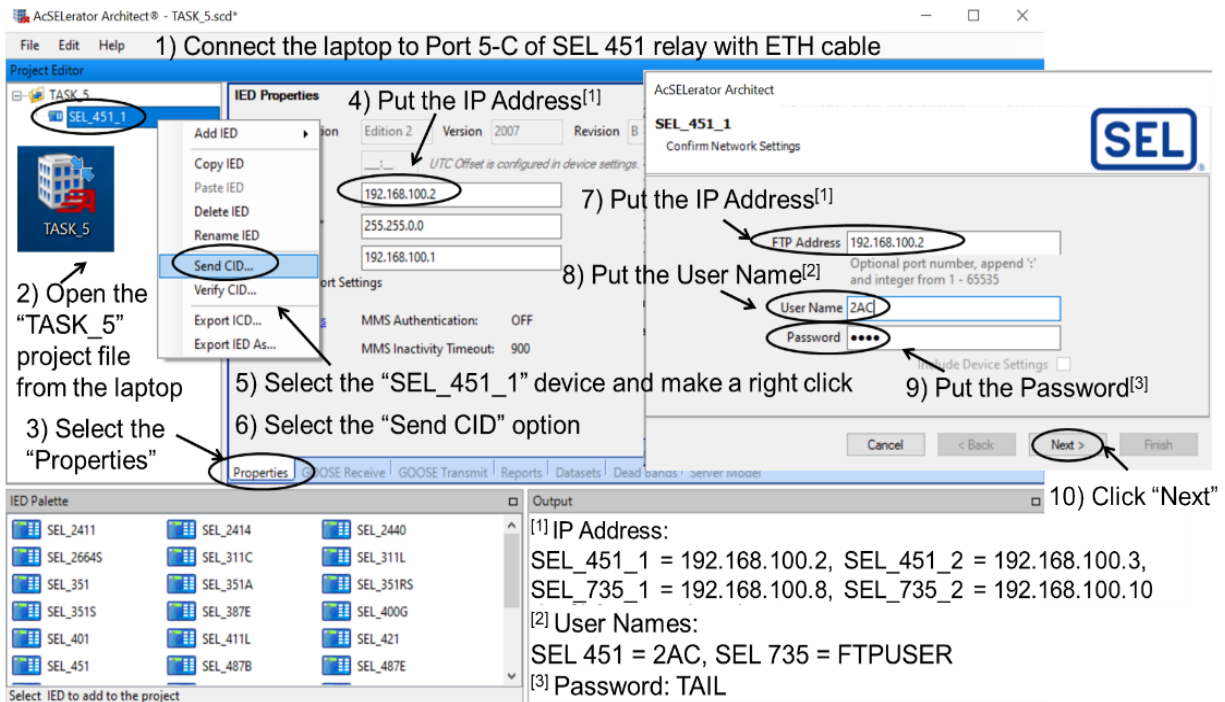


Figure 43. Steps to submit the CID file to the IED.

5.3 IEC 61850 MAPS FOR THE SEL-451 RELAYS AND SEL-735 POWER METERS

The IEC 61850 maps for the SEL-451 relays and SEL-735 power meters were collected from the Datasets of the CID files for each IED. The map of SEL-451 relays had 18 elements, and the map of SEL-735 power meters had 17 elements. The CID datasets of the SEL-451 protective relays and SEL-735 power meters are shown in Figure 44A and B, respectively. As shown in Figure 44A, the CID dataset for the SEL-451 protective relays was provided by the A, B, and C phase current magnitudes (01-03-05) and angles (02-04-06), the power system frequency (07), the A, B, and C phase to neutral voltage magnitudes (08-10-12) and angles (09-11-13), the three-phase total reactive (14) and real (15) power, the three-phase displacement power factor (16), the date-time (17), and the breaker pole state (18). As shown in Figure 44B, the CID dataset for the SEL-735 power meters was provided by the A, B, and C phase current magnitudes (01-03-05) and angles (02-04-06), the A, B, and C phase to neutral voltage magnitudes (07-09-11) and angles (08-10-12), the power system frequency (13), the three-phase total reactive (14) and real (15) power, the three-phase displacement power factor (16), and the date-time (17).

Constraint	Item		Constraint	Item	
MX	MET.METMMXU1.A2.phsA.instCVal.mag.f (01)	<div>(A)</div>	MX	MET.FUNDMMXU1.A.phsA.instCVal.mag.f (01)	<div>(B)</div>
MX	MET.METMMXU1.A2.phsA.instCVal.ang.f (02)		MX	MET.FUNDMMXU1.A.phsA.instCVal.ang.f (02)	
MX	MET.METMMXU1.A2.phsB.instCVal.mag.f (03)		MX	MET.FUNDMMXU1.A.phsB.instCVal.mag.f (03)	
MX	MET.METMMXU1.A2.phsB.instCVal.ang.f (04)		MX	MET.FUNDMMXU1.A.phsB.instCVal.ang.f (04)	
MX	MET.METMMXU1.A2.phsC.instCVal.mag.f (05)		MX	MET.FUNDMMXU1.A.phsC.instCVal.mag.f (05)	
MX	MET.METMMXU1.A2.phsC.instCVal.ang.f (06)		MX	MET.FUNDMMXU1.A.phsC.instCVal.ang.f (06)	
MX	MET.METMMXU1.Hz.instMag.f (07)		MX	MET.FUNDMMXU1.PhV.phsA.instCVal.mag.f (07)	
MX	MET.METMMXU1.PhV.phsA.instCVal.mag.f (08)		MX	MET.FUNDMMXU1.PhV.phsA.instCVal.ang.f (08)	
MX	MET.METMMXU1.PhV.phsA.instCVal.ang.f (09)		MX	MET.FUNDMMXU1.PhV.phsB.instCVal.mag.f (09)	
MX	MET.METMMXU1.PhV.phsB.instCVal.mag.f (10)		MX	MET.FUNDMMXU1.PhV.phsB.instCVal.ang.f (10)	
MX	MET.METMMXU1.PhV.phsB.instCVal.ang.f (11)		MX	MET.FUNDMMXU1.PhV.phsC.instCVal.mag.f (11)	
MX	MET.METMMXU1.PhV.phsC.instCVal.mag.f (12)		MX	MET.FUNDMMXU1.PhV.phsC.instCVal.ang.f (12)	
MX	MET.METMMXU1.PhV.phsC.instCVal.ang.f (13)		MX	MET.FUNDMMXU1.Hz.instMag.f (13)	
MX	MET.METMMXU1.TotVAr.instMag.f (14)		MX	MET.FUNDMMXU1.TotVAr.instMag.f (14)	
MX	MET.METMMXU1.TotW.instMag.f (15)		MX	MET.FUNDMMXU1.TotW.instMag.f (15)	
MX	MET.METMMXU1.TotPF.instMag.f (16)		MX	MET.FUNDMMXU1.TotPF.instMag.f (16)	
MX	MET.METMMXU1.Hz.t (17)		MX	MET.FUNDMMXU1.Hz.t (17)	
ST	PRO.BK1XCBR1.Pos.stVal (18)				

Figure 44. CID datasets of SEL-451 protective relays (A) and SEL-735 power meters (B).

Table 9 shows the logical node, attribute, and description of the Metered Values for the SEL-451 relays and SEL-735 power meters (IEC 61850 protocol). The Logical Node, Attribute, Data Source, and Description were collected from the instruction manuals of the SEL-451 protective relays [4] and SEL-735 power meters [5] provided by the manufacturer.

Table 9. Logical Node, Attribute, Data Source, and Description values for the SEL-451 protective relays and SEL-735 power meters (IEC 61850)

CID dataset values		SEL-451 protective relays [4] and SEL-735 power meter [5] IEC 61850 communication data from instruction manuals			
Device	Value #	Logical Node	Attribute	Data Source	Description
SEL-451 relays (Figure 44A)	01	METMMXU1	A2.phsA.instCVal.mag.f	B1IAFM	Breaker 1 10-cycle average fundamental A phase current (magnitude)
	02	METMMXU1	A2.phsA.instCVal.ang.f	B1IAFA	Breaker 1 10-cycle average fundamental A phase current (angle)
	03	METMMXU1	A2.phsB.instCVal.mag.f	B1IBFM	Breaker 1 10-cycle average fundamental B phase current (magnitude)
	04	METMMXU1	A2.phsB.instCVal.ang.f	B1IBFA	Breaker 1 10-cycle average fundamental B phase current (angle)
	05	METMMXU1	A2.phsC.instCVal.mag.f	B1ICFM	Breaker 1 10-cycle average fundamental C phase current (magnitude)
	06	METMMXU1	A2.phsC.instCVal.ang.f	B1ICFA	Breaker 1 10-cycle average fundamental C phase current (angle)
	07	METMMXU1	Hz.instMag.f	FREQ	Measured system frequency
	08	METMMXU1	PhV.phsA.instCVal.mag.f	VAFM	10-cycle average fundamental A phase voltage (magnitude)
	09	METMMXU1	PhV.phsA.instCVal.ang.f	VAFA	10-cycle average fundamental A phase voltage (angle)
	10	METMMXU1	PhV.phsB.instCVal.mag.f	VBFM	10-cycle average fundamental B phase voltage (magnitude)
	11	METMMXU1	PhV.phsB.instCVal.ang.f	VBFA	10-cycle average fundamental B phase voltage (angle)
	12	METMMXU1	PhV.phsC.instCVal.mag.f	VCFM	10-cycle average fundamental C phase voltage (magnitude)
	13	METMMXU1	PhV.phsC.instCVal.ang.f	VCFA	10-cycle average fundamental C phase voltage (angle)
	14	METMMXU1	TotVAr.instMag.f	3Q_F	Fundamental reactive three-phase power
	15	METMMXU1	TotW.instMag.f	3P_F	Fundamental real three-phase power
	16	METMMXU1	TotPF.instMag.f	3DPF	Three-phase displacement power factor
	17	METMMXU1	Hz.t	—	Time stamp from measured system frequency ^a
	18	BKR1CSWI1	Pos.stVal	52ACL1?1:2 ^a	Circuit breaker 1, Pole A closed/open
SEL-735 power meters (Figure 44B)	01	FUNDMMXU1	A.phsA.cVal.mag.f	IA_FUND	I_a current magnitude in amperes, updated rate of 10/12 cycles
	02	FUNDMMXU1	A.phsA.cVal.ang.f	IA_ANG	I_a current angle in degrees, updated rate of 10/12 cycles
	03	FUNDMMXU1	A.phsB.cVal.mag.f	IB_FUND	I_b current magnitude in amperes, updated rate of 10/12 cycles
	04	FUNDMMXU1	A.phsB.cVal.ang.f	IB_ANG	I_b current angle in degrees, updated rate of 10/12 cycles
	05	FUNDMMXU1	A.phsC.cVal.mag.f	IC_FUND	I_c current magnitude in amperes, updated rate of 10/12 cycles
	06	FUNDMMXU1	A.phsC.cVal.ang.f	IC_ANG	I_c current angle in degrees, updated rate of 10/12 cycles
	07	FUNDMMXU1	PhV.phsA.cVal.mag.f	VA_FUND	V_{an} voltage magnitude in kilovolts, updated rate of 10/12 cycles
	08	FUNDMMXU1	PhV.phsA.cVal.ang.f	VA_ANG	V_{an} voltage angle in degrees, updated rate of 10/12 cycles
	09	FUNDMMXU1	PhV.phsB.cVal.mag.f	VB_FUND	V_{bn} voltage magnitude in kilovolts, updated rate of 10/12 cycles
	10	FUNDMMXU1	PhV.phsB.cVal.ang.f	VB_ANG	V_{bn} voltage angle in degrees, updated rate of 10/12 cycles
	11	FUNDMMXU1	PhV.phsC.cVal.mag.f	VC_FUND	V_{cn} voltage magnitude in kilovolts, updated rate of 10/12 cycles
	12	FUNDMMXU1	PhV.phsC.cVal.ang.f	VC_ANG	V_{cn} voltage angle in degrees, updated rate of 10/12 cycles
	13	FUNDMMXU1	Hz.Mag.f (Hz.instMag.f)	FREQ	Measured system frequency in hertz
	14	FUNDMMXU1	TotVAr.Mag.f (TotVAr.instMag.f)	Q3_FUND	Fundamental reactive three-phase power in kilovolt amps reactive, updated rate of 10/12 cycles
	15	FUNDMMXU1	TotW.Mag.f (TotW.instMag.f)	W3_FUND	Fundamental real three-phase power in watts, updated rate of 10/12 cycles
	16	FUNDMMXU1	TotPF.Mag.f (TotPF.instMag.f)	PFD3	Three-phase displacement power factor
	17	FUNDMMXU1	Hz.t	—	Time stamp from measured system frequency ^a

^aThe time stamp was collected from the frequency values for the SEL-451 relays and SEL-735 power meters

5.4 SETTING OF DNP MAP FOR THE SEL-734 POWER METERS

The DNP map for the SEL-734 devices located at the load feeders with 50 T fuses (Figure 2) was set by using the AcSElerator Quickset software and connecting the power meter device with a computer (using a serial cable). The computer communicated with the SEL-734 power meter, and the setting data of the device were read. Then, the DNP Map Settings menu and Map 1 option were selected to set the DNP Map Settings (Figure 45). As shown in Figure 45A, the DNP Analog Input Map was completed by selecting and opening the DNP-AI_MAP. The DNP points from the superior window were moving to the inferior window by selecting the green arrow up to complete all desired analog input DNP points to be transmitted with the SEL-734 power meters. The Selected DNP Points were arranged by the Name, User Map Index-Device Index. These analog input DNP points (User Map Index-Device Index) were the A, B, and C phase current magnitudes (0-0, 2-2, 4-4) and angles (1-1, 3-3, 5-5), A, B, and C phase voltage magnitudes (6-36, 8-38, 10-40) and angles (7-37, 9-39, 11-41), power system frequency (12-104), three-phase real power (13-87), three-phase reactive power (14-95) and three-phase power factor (15-99). As shown in Figure 45B, the analog output DNP points were set on the DNP-AO_MAP. These analog output DNP points (User Map Index-Device Index) were the Days (0-49), Hours (1-48), Milliseconds (2-46), Minutes (3-47), Months (4-50), and Years (5-51).

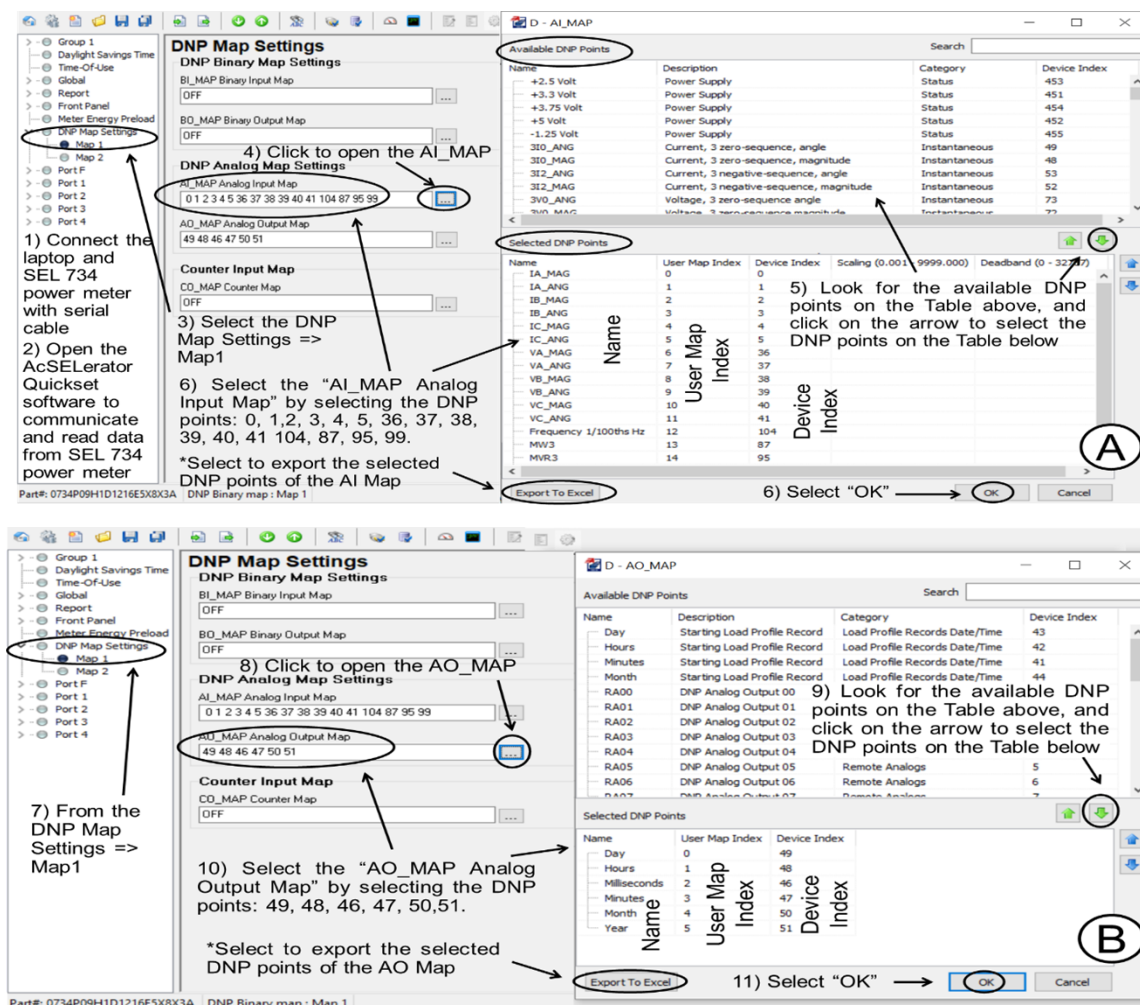


Figure 45. Steps to set the DNP map of SEL-734 power meters.

The DNP maps for the analog inputs and outputs of the SEL-734 power meters were exported from the power meters once the devices were set with the AcSELeRator Quickset software. Figure 45A and B show the Export To Excel tab. This option allowed the DNP maps for analog inputs and outputs to be saved as Excel files. These DNP map Excel files were used to set the RTACs with the SEL-734 power meters. Table 10 shows an exported DNP map for analog inputs and outputs of the SEL-734 power meters.

Table 10. Exported DNP map for analog inputs and outputs of SEL-734 power meters

DNP map signal	Name	User Map Index	Device Index
Analog input map	IA_MAG	0	0
	IA_ANG	1	1
	IB_MAG	2	2
	IB_ANG	3	3
	IC_MAG	4	4
	IC_ANG	5	5
	VAB_MAG	6	42
	VAB_ANG	7	43
	VBC_MAG	8	44
	VBC_ANG	9	45
	VCA_MAG	10	46
	VCA_ANG	11	47
	Frequency 1/100ths Hz	12	104
	MW3	13	87
	MVR3	14	95
	PF3	15	99
Analog output map	Days	0	49
	Hours	1	48
	Milliseconds	2	46
	Minutes	3	47
	Months	4	50
	Years	5	51

5.5 RTAC FOR THE SEL-734 POWER METERS

The SEL-734 power meters were connected to an RTAC to poll the DNP map points and collect the data measured by the SEL-734 power meters. To implement this, an RTAC was installed with the SEL-734 power meters at the electrical substation-grid test bed. The configuration of the SEL-3530-4 RTAC was set with a URL given for a web server (<https://172.29.131.1>) and connected to a computer to the USB port of the RTAC (front side). Once the web server was reached, the RTAC configuration Username and Password were set, and the Firmware version of the RTAC was collected from the Dashboard menu (Figure 46).

Dashboard

Device Information

Host Name:	SEL-3530-4-0030A71F2A87
Device Name:	
Device Location:	
Device Description:	
Allowed Web Connections:	20
Web Session Timeout (Min):	5
HMI Read-Only Mode Timeout (Min):	5
Enable HMI Read-Only Mode:	<input type="checkbox"/>
Tie Alarm LED to OUT101:	<input checked="" type="checkbox"/>
Firmware Version:	SEL-3530-4-R144-V3-Z000013-D20190508
Firmware Checksum:	4d88630328132b2b9c133eb10146a44d
Project ID:	
Serial Number:	1192400285
Part Number:	35304BA0X1211X0XXXXXX
Config:	00000000
Dev Code:	73
Power Source Scale (0.5 - 1.5):	1
Default Home Page:	Dashboard

System Statistics

Main Task Usage:	0%
Automation Task Usage:	0%
Memory Usage (RAM):	124976 KB
Memory Available (RAM):	649184 KB
Storage Usage:	130764 KB
Storage Available:	1770360 KB
Number of Users Logged In:	1
Current Project:	Factory Default
Modified Time of Project:	
Power Source Voltage:	-33.1809266

POST Summary

DDR2 SDRAM OK:	TRUE
Primary Flash OK:	TRUE
Secondary Flash OK:	TRUE
Serial Controller OK:	TRUE
USB B OK:	TRUE
Eth 01 OK:	TRUE
Eth 02 OK:	TRUE
Irig Controller OK:	TRUE
Contact IO Controller OK:	TRUE
Mainboard Controller OK:	TRUE

1) Connect the front side's USB port of SEL 3530-4 to an online laptop
2) Connect with the web server "https://172.29.131.1"
3) Put the RTAC configuration Username and password
4) Collect the Firmware version of SEL-3540-4 RTAC

Figure 46. Steps to find the Firmware version of the SEL-3530-4 RTAC.

The new project for the RTAC was created by using the AcSELeRator RTAC software and connecting the SEL-3530-4 RTAC with a computer at the USB port of the RTAC (front side). The steps to log in with the RTAC Database (Figure 47A) and create a new RTAC project (Figure 47B) are shown. The AcSELeRator RTAC software was opened. As shown in Figure 47A, the New Project option was selected, and the RTAC Username (admin) and Password (TAIL) were set by default to log in. As shown in Figure 47B, the RTAC type (SEL-3530) and Firmware Version (R144) were selected from the device Firmware version (SEL-3530-4-R144-V3-Z000013-D20190508) collected from Figure 46. The RTAC/Axion was applicable for the SEL-3530-4 RTAC type. The project name (Project1) for the RTAC was written, and Create was selected.

SEL AcSELeRator RTAC

1) Select the "New Project" option

2) Complete the User name: admin Password: TAIL

3) Click "Login"

4) Complete the "RTAC Type" and "RTAC Firmware Version"

Note: The RTAC/Axion is applicable for the SEL-3530-4 RTAC type

5) Put the "Project Name"

6) Click "Create"

Figure 47. Steps to log in with RTAC Database (A) and create a new RTAC project (B).

As shown in Figure 48A, the SEL-734 power meter was inserted in the new project. The Insert label was selected, and the SEL-700 Series => 734=> DNP Protocol path was selected. Then, as shown in

Figure 48B, the Device, Protocol, and Communication Type window was completed by placing the device name (SEL_734_1), selecting the connection type (Client-Ethernet), and selecting the Insert label to add the new device (SEL_734_1_DNP). The Insert label for the other device (SEL_734_2_DNP) was set by similar steps.

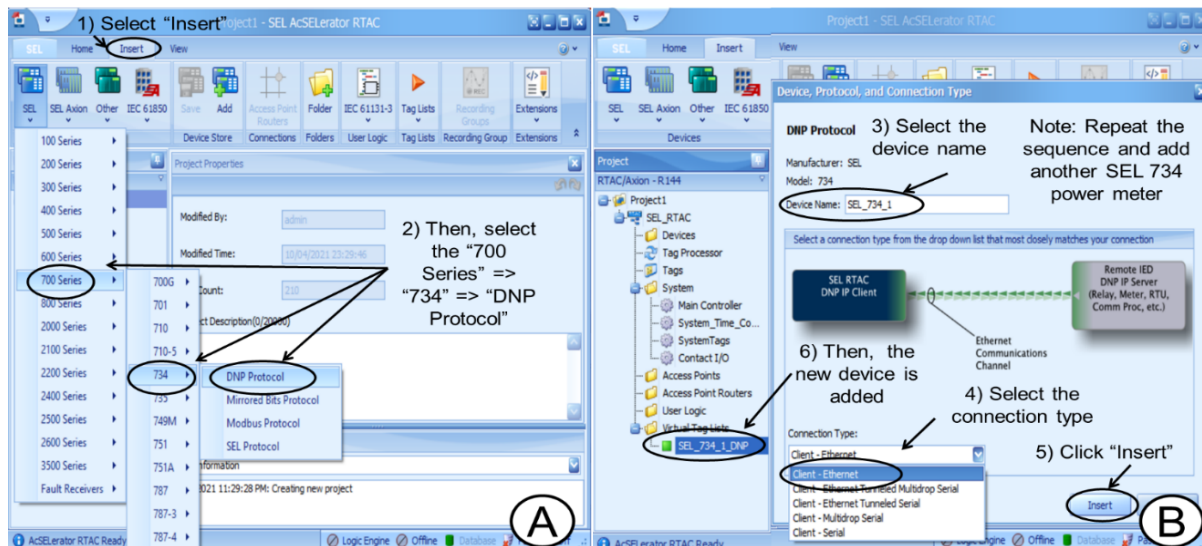


Figure 48. Steps to insert an SEL-734 device (A) and connection type (B).

As shown in Figure 49A, the SEL_734_1_DNP device label was selected, and the Settings options were completed. The Communications and DNP options in Figure 49A were completed by using the DNP Protocol and Ethernet Settings values that were set at Port 1 of the GRID_SEL734_FED1 power meter with the AcSELeRator Quickset (Figure 49B) software. The underlined letters (Figure 49A) were used to set the non-underlined letters (Figure 49B). The Settings for the other device (SEL_734_2_DNP) were set by similar steps.

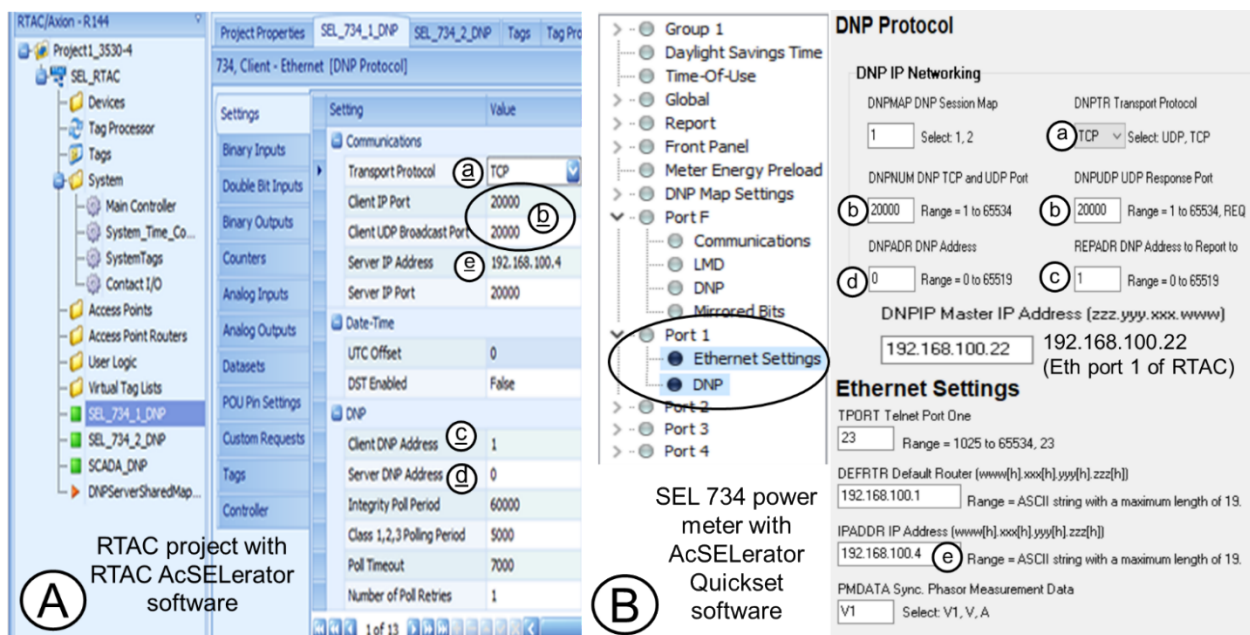


Figure 49. SEL-734 Settings based on RTAC AcSELeRator (A) and AcSELeRator Quickset (B) software.

The analog inputs for each device were added in the RTAC project. Figure 50 shows the steps to add analog inputs for the SEL_734_1_DNP device. As shown in Figure 50A, the SEL_734_1_DNP device was selected, and the Analog Inputs option was completed by adding 16 points using the “+” symbol. Once the 16 points for the analog inputs were added, the DNP points were renamed by using the exported DNP map for analog inputs of the SEL-734 power meter that are shown in Table 10 (Figure 50B). Then, all DNP points from the Enable column were set to True. The analog inputs added for the other device (SEL_734_2_DNP) were set by similar steps.

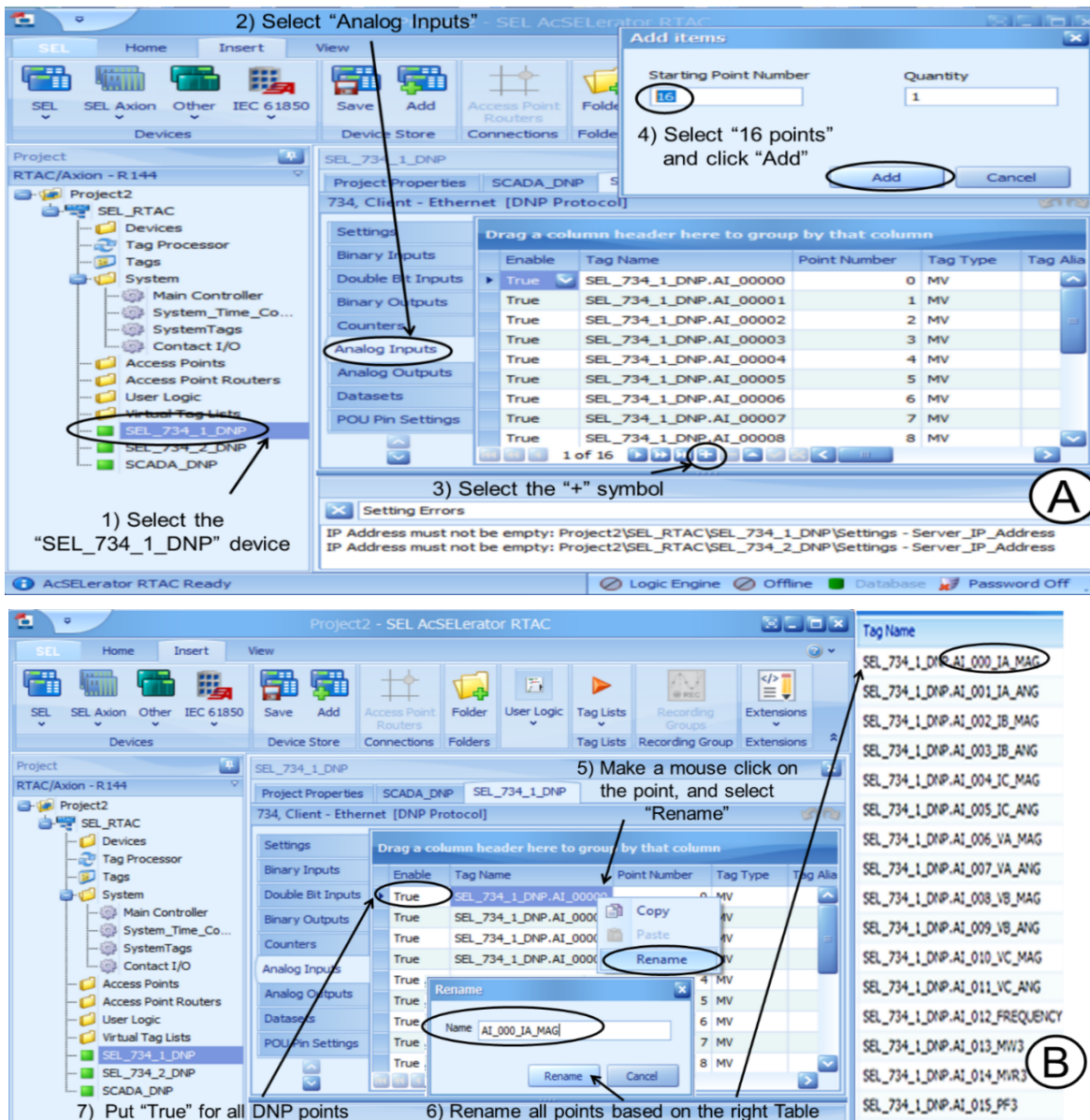


Figure 50. Steps to add analog inputs for the SEL-734 device at RTAC project.

Once the DNP points for the SEL738_DNP_1 and SEL738_DNP_2 devices were set, the SCADA_DNP device was inserted and selected. Figure 51 shows the steps to set the SCADA device at the RTAC project. The Settings menu was selected, and the Communications, Date-Time, and DNP options were set. The Map Name for the DNP option was set as the DNPServerShared.. to set the Map Name for the Tag Processor in the next step.

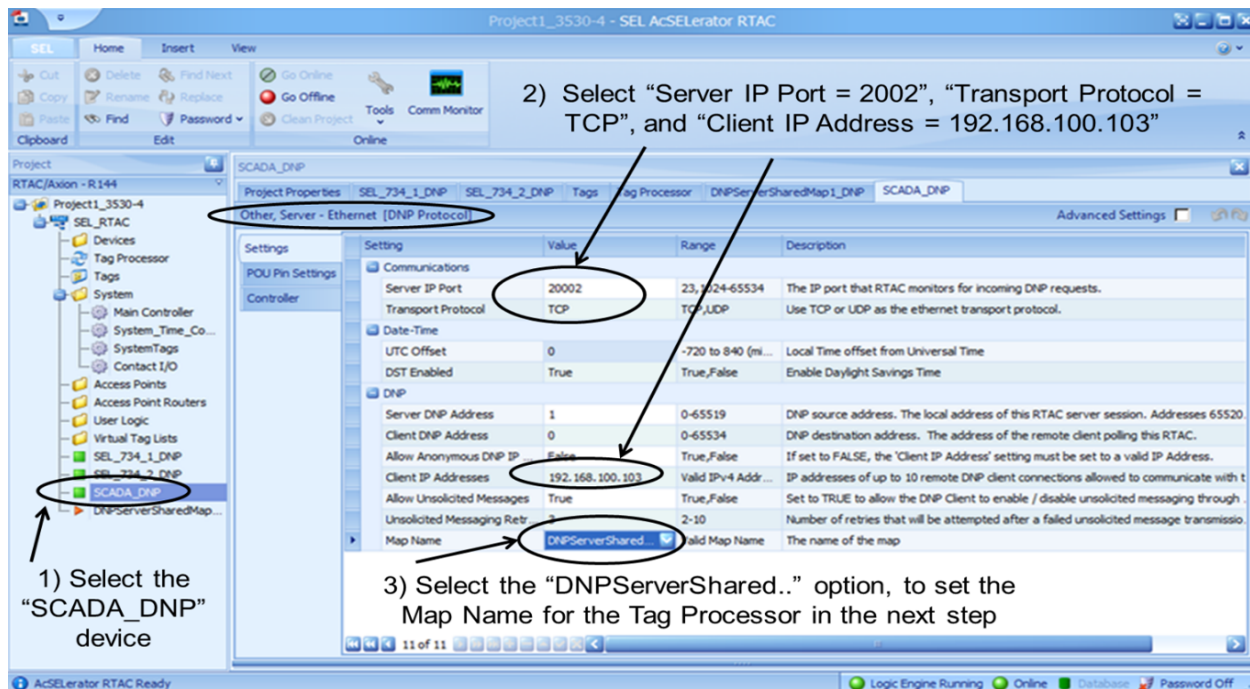
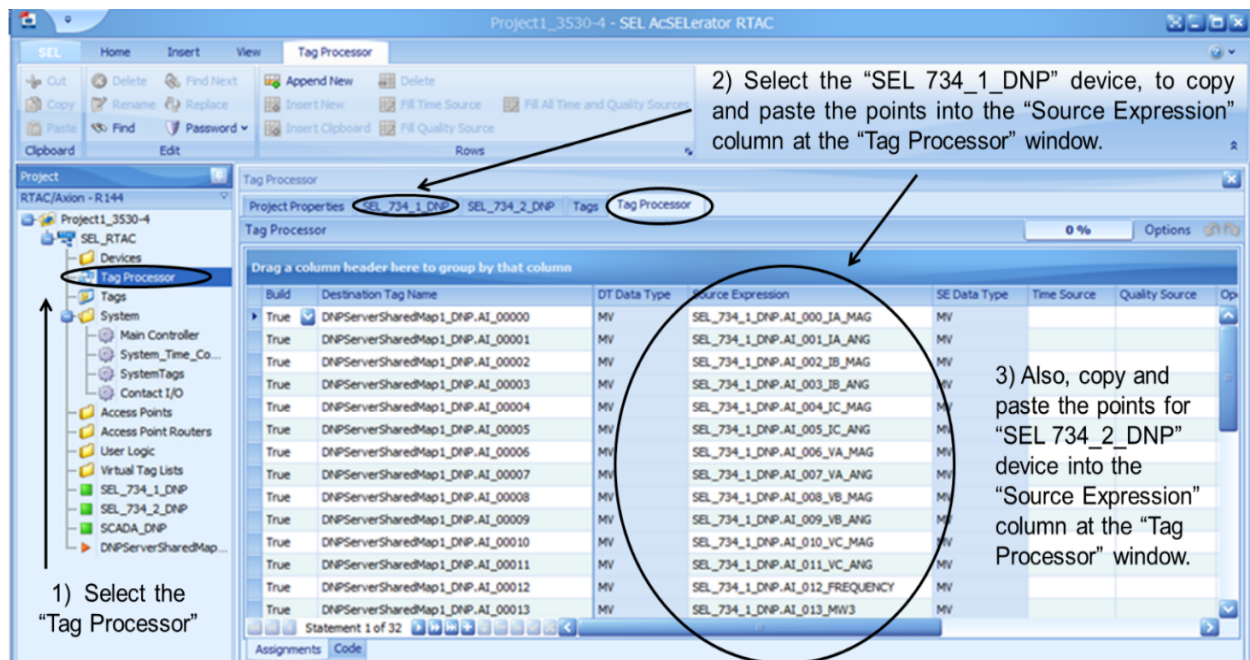


Figure 51. Steps to set the SCADA device at the RTAC project.

As shown in Figure 52, the Tag Processor was selected, and the DNP points for the Source Expression column were completed by copying and pasting the DNP points for the analog inputs of the SEL_734_1_DNP and SEL_734_2_DNP devices. The "Ctrl + C" and "Ctrl + V" commands were used to copy and paste, respectively, the DNP points for the analog inputs of the SEL_734_1_DNP and SEL_734_2_DNP devices into the Source Expression column.



Ctrl + C = To copy the tags of Devices into the Tag Processor, Ctrl + V = To paste the tags of Devices into the Tag Processor

Figure 52. Steps to set analog inputs of SEL-734 power meters in the Tag Processor.

Once the new project was created and saved at the SEL-3530-4 RTAC, the sent and received messages from the SEL_734_1_DNP and SEL_734_2_DNP devices could be counted from the RTAC by using the AcSELeRator RTAC software. Figure 53 shows the steps to observe the counted messages received and sent from the SEL_734_2_DNP device. The Go Online option was selected, and the Username and Password were filled out to log in through the SEL-3530-4 RTAC. Then, the SEL_734_2 device was selected, the Controller option was selected, and the device traffic was counted for sending and receiving messages of the SEL_734_2 device.

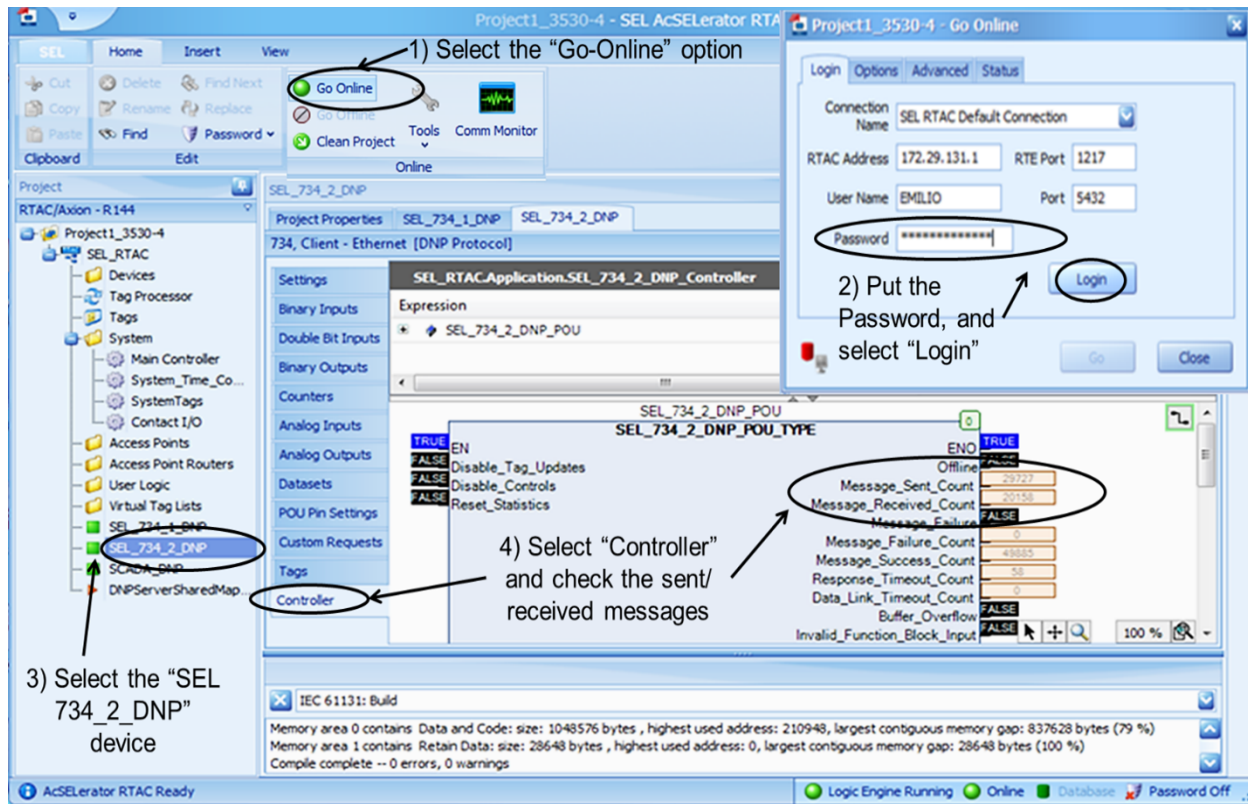


Figure 53. Steps to observe the device traffic with the controller.

5.6 TELNET NETWORK COMMUNICATION

In the electrical substation-grid test bed, the SEL-451 protective relays and SEL-734 and SEL-735 power meters were installed and set. These devices were used to collect events and change settings in simulation tests. The protective relays and power meters were installed at a communication system based on a Telnet Network that allowed the communication, setting, and data collection from an HMI computer with the AcSELeRator Quickset software. The steps to communicate with the inside and outside substation devices with the Telnet Network option are shown in Figure 54. The HMI computer was connected with an Ethernet cable to the communication system. Then, the AcSELeRator Quickset software was opened, and the Communication option was selected. The Network option was selected at the Active Connection Type. The Network label was selected, and the Host IP Address and Port Number (Telnet) were set as shown in Figure 54A. The Telnet port for all devices was set to 23. In the File Transfer Option section, the Telnet option was selected, the Level One (OTTER) and Two (TAIL) Passwords were written, and OK was selected to communicate with the device.

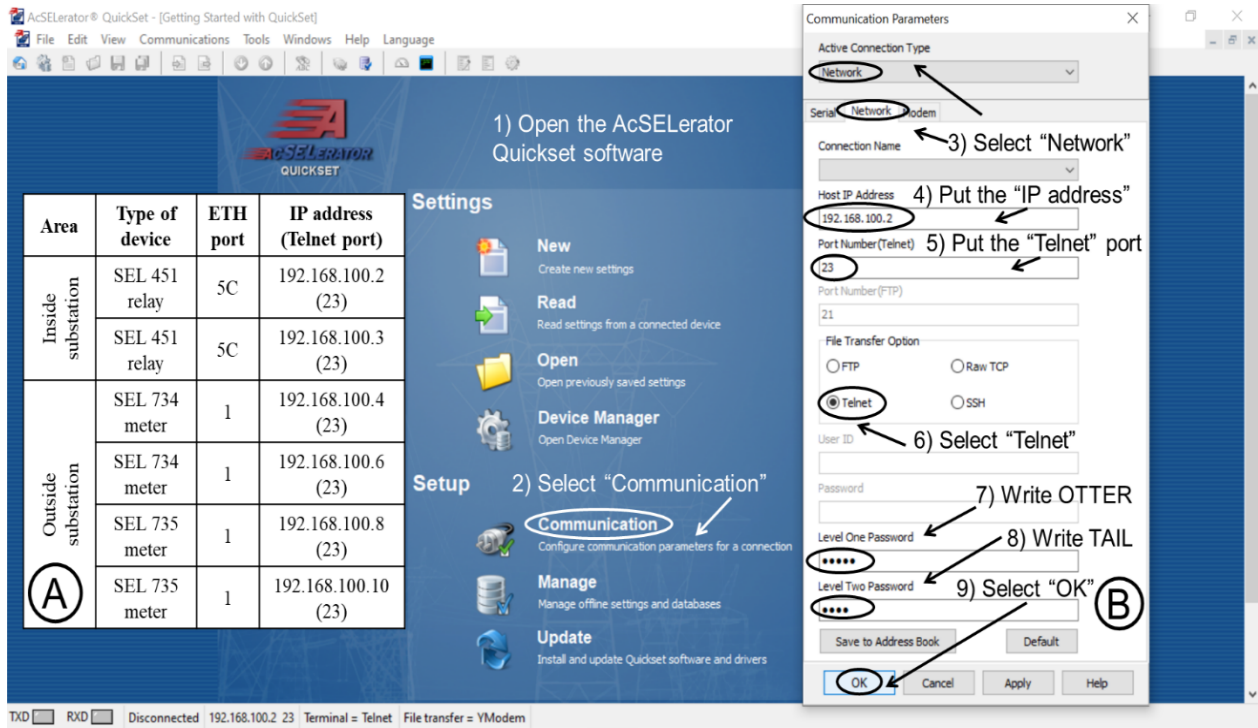


Figure 54. IP address (A) and steps (B) for Telnet Network communication.

6. DLT SYSTEM

In this section, the DLT system for the electrical substation-grid test bed is introduced and described. The DLT equipment and diagrams of the DLT system are presented, providing a summary of all DLT devices installed at the electrical substation-grid test bed, and presenting the overview of the DLT network.

6.1 DLT INTRODUCTION

The DLT includes platforms that maintain a consistent, shared ledger across a network of nodes. One form of ledger data structure is blockchains, which use cryptographic hashes to link blocks of data to form an immutable sequence [18]. This technology was used in the test bed for the protection of measurement data and configuration artifacts by storing them in the ledger.

One of the main challenges for this use case is that storing all the raw data produced by substation devices in the ledger would be impractical because of the size of the blockchain constantly growing as a result of immutability [19], and the limited storage capacity of DLT nodes if they maintain full copies of the ledger. Therefore, the data are collected and then hashed using the SHA256 hash function, which allows for arbitrary windows of data to be reduced to a 32-byte hash value that can be stored in the ledger. When the state of raw data—which is kept in an off-chain data store—must be verified, the hash of the data is recalculated and then compared with the hash value stored in the ledger. Thus, the ledger provides data integrity for the raw test bed data.

Hyperledger Fabric (HLF) was chosen as the DLT platform for the test bed. Considerations for the desired platform included having authentication and authorization built-in (i.e., a permissioned platform), capable of handling generic data (i.e., not focused on finance use cases), and being actively developed, maintained, and used. HLF is one of the most popular and active blockchain-based DLT platforms [20] with these features. The main software components of HLF are peers and orderers. Peers maintain copies of the ledger and evaluating transactions [21], and orderers order the transactions into consistent blocks and use the Raft consensus algorithm [22]. Smart contracts handle transaction logic, such as querying and sending data [23].

The Attestation Framework is a modular framework designed to use the DLT for attestation of device state. A storage module puts the raw data and configuration artifacts into an off-chain database while sending hash values and related metadata to the ledger. Other modules are responsible for calculating statistics from the device measurement data and network and using the data to detect anomalous events. When an event occurs, the framework performs an attestation check by comparing hashed baseline data in the ledger with current data.

6.2 DLT EQUIPMENT AND DIAGRAM

The HLF DLT runs on three different computers in the test bed. The primary role of these computers is to function as nodes in the DLT network (i.e., DLT node) by running HLF software components. These nodes maintain a full copy of the ledger and are involved in the evaluation and execution of transactions. Additionally, these computers run software for the off-chain database, monitor and collect metrics, and execute the Attestation Framework. One node was designated as the master node, responsible for management of the HLF network and running the off-chain software modules.

In the initial design of the architecture for this system, IEDs were considered as a possible platform for running the DLT software in the substation environment. However, these devices are typically designed to only run proprietary software. To address this, general purpose computers were instead use for this role. The main requirements established for the DLT computer hardware included a rugged design that

would enable stable operation within a substation environment and network interface support for PTP hardware timestamping. Hardware specifications were approximately based on those found in substation automation controllers such as the SEL-3530-4 RTAC, which range from early Intel i7s with 8GB of random-access memory (RAM) [24] to Intel Xeon processors with 16 GB of RAM [25]. Based on these criteria, the first devices selected were OnLogic industrial computers with Intel Core i7-6600U 2-core CPUs, 16 GB RAM, 128 GB of storage, and an Intel network interface controller with support for PTP hardware timestamping. These were later upgraded to OnLogic industrial computers with AMD Ryzen 9 3950X 16-core CPUs, 32 GB RAM, and 128 GB of storage. Although the upgrade was primarily for the purpose of benchmarking DLT platform performance characteristics, it also benefited running the additional software components needed for the Attestation Framework.

Each DLT node computer has two Ethernet network interfaces. One interface on each computer was configured for the DLT network (10.0.0.x), which allowed each node to communicate as part of the HLF network. The first DLT computer, designated as the master node, also had its second network interface configured for the SEL-735 power meters and SEL-451 protective relays network (192.168.100.x). This allowed it to receive IEC 61850 GOOSE and sampled values (SV) packets, hash the packet data, and send the hash as a transaction to the ledger.

The DLT nodes were connected to three Cisco IE3400 switches, which are rugged switches designed for power utility substations and support the PTP protocol [26]. Each DLT node was connected on its 10.0.0.x interface to a switch, and there was a trunk connection between each switch. The SEL-2488 Satellite-Synchronized Network Clock device provided PTP using the default UDP profile to the 192.168.100.x network on one of its Ethernet interfaces and to the 10.0.0.x network on another. The *linuxptp* package was used as the PTP client on each DLT node to synchronize the system clock with the PTP hardware clock of the network interface [27]. The master DLT node was configured to receive PTP on its 10.0.0.x interface, which provided the lowest latency timing owing to the PTP-supported Cisco switch. Figure 55 shows the overview diagram of the DLT network. Table 11 provides a summary of the DLT devices.

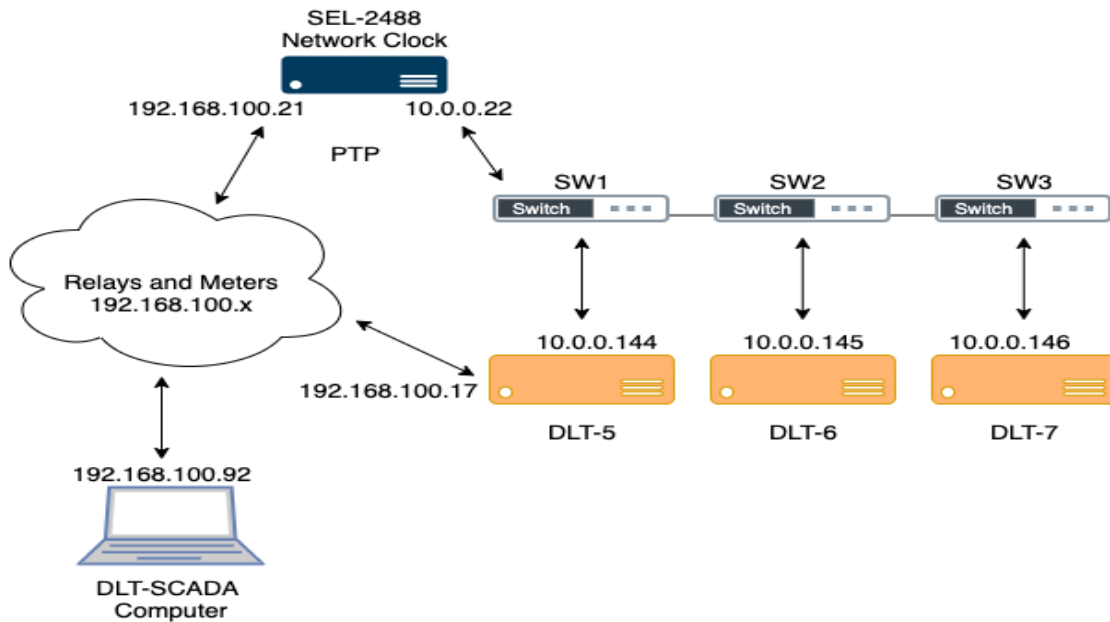


Figure 55. Overview of the DLT network.

Table 11. Summary of DLT devices

Name	Model	Operating system	Ethernet IP address
DLT-5 (master node)	OnLogic MC850-40	Ubuntu 20.04	10.0.0.144/192.168.100.17
DLT-6	OnLogic MC850-40	Ubuntu 20.04	10.0.0.145
DLT-7	OnLogic MC850-40	Ubuntu 20.04	10.0.0.146
SW1	Cisco IE3400	Cisco IOS	10.0.0.141 (management)
SW2	Cisco IE3400	Cisco IOS	10.0.0.142 (management)
SW3	Cisco IE3400	Cisco IOS	10.0.0.143 (management)
DLT-SCADA	MacBook Pro	MacOS 11.6	192.168.100.92

7. TEST BED ARCHITECTURE AND WORKSTATIONS

In this section, the test bed architecture, servers, and workstations of the electrical substation-grid test bed are described. The IP address and function of inside and outside substation devices and main communication devices at the control center are presented. Then, the workstations and servers integrated at the electrical substation-grid test bed are described, such as the host computer, DLT-SCADA computer, traffic network computer, control center and local HMI computers, virtual machine (VM), Blueframe computer, DLT master node, and EmSense high-speed SV emulator device.

7.1 TEST BED ARCHITECTURE

Many US electrical utility companies are adopting a layer-based security model in which each level builds more security into the network to protect critical resources and applications [28]. The architecture of the electrical substation-grid test bed has five layers (Figure 56). The Physical layer (Level 1) includes the power lines, breakers, PTs, feeder loads, and other power system elements that were simulated with the real-time simulator. The Protection and metering layer (Level 2) contains the HIL given by the protective relays and power meters. The Automation layer (Level 3) contains the remote terminal units. The Access layer (Level 4) contains the Ethernet switches and gateways. The Control layer (Level 5) contains the SCADA, HMI, and synchronized time system with DLT devices.

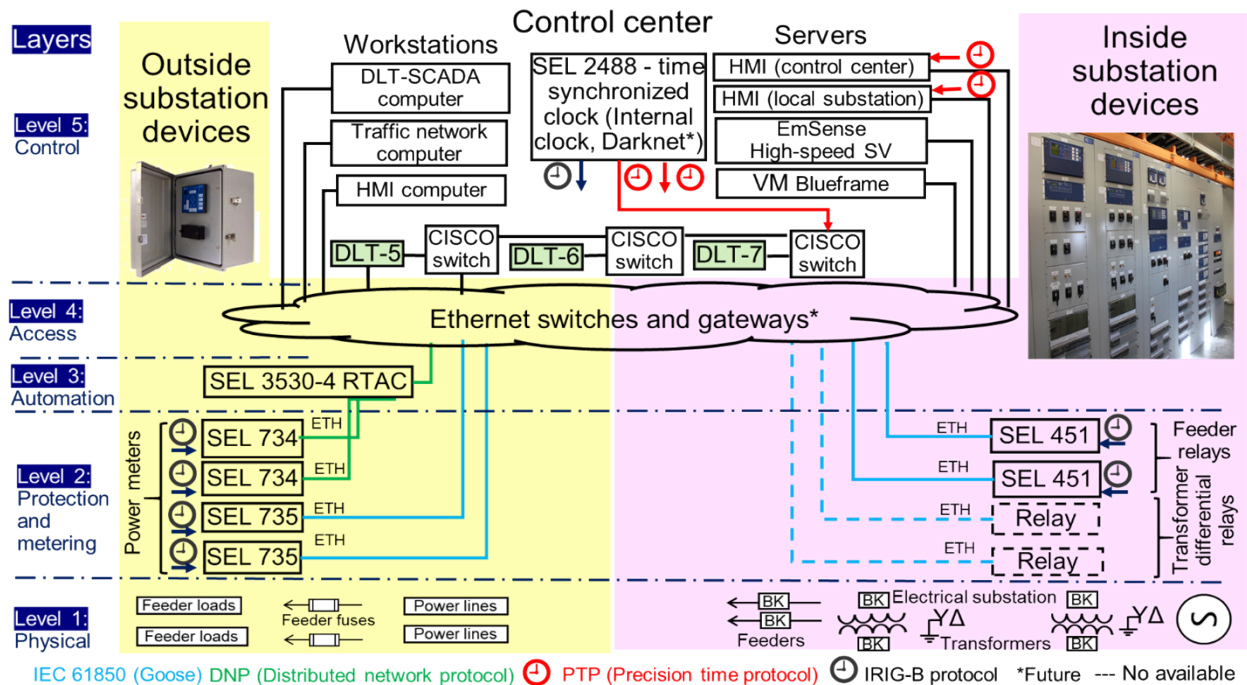


Figure 56. Architecture of the electrical substation-grid test bed with protective relays and power meters using DLT devices to study future cyber events.

In this architecture, the workstations are the DLT-SCADA, traffic network, and HMI computers. The host computer is not shown in Figure 56 because it was connected to a real-time simulator that simulated the power system elements of the Physical layer, which were wired to inside and outside substation devices in the Protection and metering layer. In addition, the architecture of the electrical substation-grid test bed contains the control center HMI, local substation HMI, and the EmSense high-speed SV and VM Blueframe servers.

The synchronized time protocols used in this architecture were based on the PTP and IRIG-B signals. The PTP communication was implemented at the DLT system through the Ethernet network, and the IRIG-B communication was implemented at the power meters and feeder relays. The SEL-451 relays and SEL-735 power meters transmitted IEC 61850 messages, and the SEL-734 power meters transmitted DNP messages. Both device messages are used frequently at electrical substations. In Table 12 and Table 13, the IP addresses of the devices at the electrical substation-grid test bed in Figure 56 are given. Table 12 provides the IP addresses and functions of the inside and outside substation devices. Table 13 provides the IP addresses and functions of the main devices at the control center.

Table 12. IP address and function of inside and outside substation devices

Location	IP address	Telnet ports	Type of device	Device identifier	Protocols	ETH Port	Function
Inside substation devices	192.168.100.2	23	SEL-451 relay	SUB_SEL451_FED1	IEC 61850	5C	Measurement of currents, voltages, power, frequency and pole states at substation breaker feeders
	192.168.100.3	23	SEL-451 relay	SUB_SEL451_FED2	IEC 61850	5C	Measurement of currents, voltages, power, frequency and pole states at substation breaker feeders
Outside substation devices	192.168.100.8	23	SEL-735 meter	SUB_SEL735_FED1	IEC 61850	1	Measurement of currents, voltages, power and frequency at load feeder 1 with 100 T fuses
	192.168.100.10	23	SEL-735 meter	SUB_SEL735_FED2	IEC 61850	1	Measurement of currents, voltages, power, and frequency at load feeder 2 with 100 T fuses
	192.168.100.4	23	SEL-734 meter	SUB_SEL734_FED1	DNP	1	Measurement of currents, voltages, power and frequency at load feeder 1 with 50 T fuses
	192.168.100.6	23	SEL-734 meter	SUB_SEL734_FED2	DNP	1	Measurement of currents, voltages, power, and frequency at load feeder 2 with 50 T fuses
	192.168.100.22	—	SEL-3530-4 RTAC	—	DNP	1	Poll for DNP points at SEL-734 power meters

Table 13. IP address and function of main devices at the control center

Location	Area	IP address	Type of device	Function
Control center	Timing and synchronization clock	192.168.100.21	SEL-2488 ETH1	Set time frame to SEL devices network
		10.0.0.22	SEL-2488 ETH2	Set time frame on DarkNet network
	Ethernet switches for the DLT devices	10.0.0.141	Cisco IE3400	Ethernet switch 1 for the DLT-5
		10.0.0.142	Cisco IE3400	Ethernet switch 2 for the DLT-6
		10.0.0.143	Cisco IE3400	Ethernet switch 3 for the DLT-7
	DLT devices	10.0.0.144	OnLogic MC850-40	DLT device DLT-5
		10.0.0.145	OnLogic MC850-40	DLT device DLT-6
		10.0.0.146	OnLogic MC850-40	DLT device DLT-7

7.2 TEST BED WORKSTATIONS AND SERVERS

For the DarkNet project, relevant data must be collected and recorded, especially during the simulations. These data can be used for later analysis. Because the devices (e.g., protective relays, power meters) that produce the data are synchronized with the master clock, the time stamps associated with the data are correlated. Several computers are used in this collection of data. The electrical substation-grid test bed used six computers that were located at desks and on racks. The four computer workstations set on the desk are shown in Figure 57, and they are the host computer (F), HMI computer (G), traffic network computer (H), and DLT-SACADA computer (I). In addition, the control center HMI, local substation HMI, VM Blueframe, and EmSense high-speed SV servers/computers were located in the test bed.

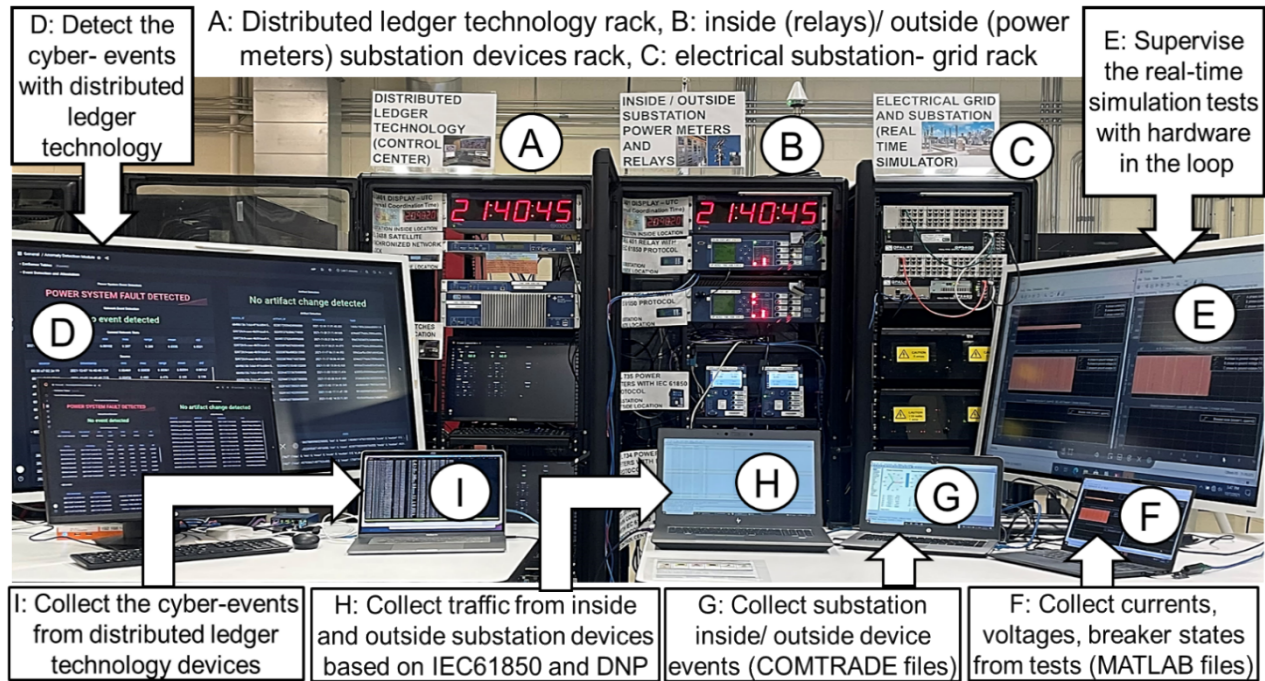


Figure 57. Electrical substation-grid test bed and workstations.

7.2.1 Host computer

The host computer was connected to the target computer (i.e., real-time simulator) and was allowed to edit, set, build, load, and run the RT-LAB project that performed the simulation test at the electrical substation-grid test bed. The host computer could set the test duration time, define the type of electrical faults (such as SLG, LL, LLG, and 3L [or 3LG]), measure the phase primary currents and phase to neutral primary voltages at protective relay/power meter locations during the tests, and measure the breaker pole state of the substation feeder breakers. The measured phase primary currents, phase to neutral primary voltages, and breaker pole states were also visualized during the tests to supervise the real-time simulations. The phase primary currents, phase to neutral primary voltages, and breaker pole states could be recorded at the end of each simulation test as MATLAB files to compare the simulation results with the events of the protective relays and power meters.

7.2.2 HMI computer

The HMI computer was connected to the protective relays and power meters of the electrical substation-grid test bed. This computer communicated with each device by using the Telnet Network option with the AcSElerator Quickset software. The HMI measured the data from each protective relay and/or power meter. The HMI computer could be used to change the settings of the power meters and protective relays at the electrical substation-grid test bed. The computer could be used to collect the protective relay and power meter events at the end of the simulation tests from the device's COMTRADE and CEV (Compressed Event) files.

7.2.3 DLT-SCADA computer

The DLT-SCADA computer was used to access the computers running the DLT software components. Each of the three DLT computers was configured with a Secure Shell server to allow remote shell access. Other protocols used for remote access included Secure Copy Protocol and Secure File Transfer Protocol for file transfers and HTTP for accessing web-based dashboards. Tools such as *pyinfra* [29] for configuration management were used from the DLT-SCADA computer to automate the deployment and configuration of software on the DLT nodes.

The shell scripts were created to automate tasks such as operating the HLF network and the Attestation Framework modules. For the HLF network, these tasks included starting up and shutting down the HLF network, generating keys and certificates and securely distributing them to the other DLT nodes, deploying the chaincode, and cleaning up the ledger state. The Attestation Framework primarily consisted of Python modules that were run using a terminal multiplexer tool, *tmux* [30], to more easily start and stop modules and observe their output. Each module was run inside a window within a *tmux* session, which could continue running even when the Secure Shell connection was closed. In addition to remote shell and file system access, the DLT-SCADA computer was used to create and view web-based dashboards using a Grafana [31] server running on the master node DLT computer (i.e., DLT-5). The Attestation Framework dashboard provided statistics and the status of anomaly events using data from the off-chain database. Another dashboard provided an overview of the HLF network state using metrics provided by the HLF containers and collected by Prometheus [32]. Figure 58 shows the IEC 61850 data displayed by one of the Attestation Framework modules.


```
dlt-5@dlt-5: ~  
{"magFreqHz":60,"magVoltagePhaseA":0,"angVoltagePhaseA":0,"magVoltagePhaseB":0,"angVoltagePhaseB":0,"magVoltagePhaseC":0,"angVoltagePhaseC":0,"magTotVar":1.6072738162620226e-07,"magTotW":8.2243595898034982e-06,"magTotPF":0.99980908632278442,"HzT":0,"breakerPosA":0}}  
{"gocbRef":"SUB_SEL451_FED1CFG/LLN0$G0$SUB_SEL451_FED1","datSet":"SUB_SEL451_FED1CFG/LLN0$8RDSet01","goID":"SUB_SEL451_FED1","appID":4,"srcMac":"00:30:A7:02:2E:19","dstMac":"01:0C:CD:01:00:04","stNum":6769243,"sqNum":0,"t":1638306304325,"allData":{"magCurrentPhaseA":0,"angCurrentPhaseA":0,"magCurrentPhaseB":0,"angCurrentPhaseB":0,"magCurrentPhaseC":0,"angCurrentPhaseC":0,"magFreqHz":60,"magVoltagePhaseA":0,"angVoltagePhaseA":0,"magVoltagePhaseB":0,"angVoltagePhaseB":0,"magVoltagePhaseC":0,"angVoltagePhaseC":0,"magTotVar":-1.0162025319004897e-06,"magTotW":9.3271974037634209e-06,"magTotPF":0.99411731958389282,"HzT":0,"breakerPosA":0}}  
{"gocbRef":"SUB_SEL451_FED2CFG/LLN0$G0$SUB_SEL451_FED2","datSet":"SUB_SEL451_FED2CFG/LLN0$8RDSet01","goID":"SUB_SEL451_FED2","appID":6,"srcMac":"00:30:A7:02:07:BF","dstMac":"01:0C:CD:01:00:06","stNum":6774069,"sqNum":0,"t":1638306304666,"allData":{"magCurrentPhaseA":0,"angCurrentPhaseA":0,"magCurrentPhaseB":0,"angCurrentPhaseB":0,"magCurrentPhaseC":0,"angCurrentPhaseC":0,"magFreqHz":60,"magVoltagePhaseA":0,"angVoltagePhaseA":0,"magVoltagePhaseB":0,"angVoltagePhaseB":0,"magVoltagePhaseC":0,"angVoltagePhaseC":0,"magTotVar":2.8343831104393757e-07,"magTotW":8.2623919297475368e-06,"magTotPF":0.99941211938858032,"HzT":0,"breakerPosA":0}}  
{"gocbRef":"SUB_SEL451_FED1CFG/LLN0$G0$SUB_SEL451_FED1","datSet":"SUB_SEL451_FED1CFG/LLN0$8RDSet01","goID":"SUB_SEL451_FED1","appID":4,"srcMac":"00:30:A7:02:2E:19","dstMac":"01:0C:CD:01:00:04","stNum":6769244,"sqNum":0,"t":1638306304828,"allData":{"magCurrentPhaseA":0,"angCurrentPhaseA":0,"magCurrentPhaseB":0,"angCurrentPhaseB":0,"magCurrentPhaseC":0,"angCurrentPhaseC":0,"magFreqHz":60,"magVoltagePhaseA":0,"angVoltagePhaseA":0,"magVoltagePhaseB":0,"angVoltagePhaseB":0,"magVoltagePhaseC":0,"angVoltagePhaseC":0,"magTotVar":-6.379177079907946e-07,"magTotW":9.0278526840847917e-06,"magTotPF":0.9975128173828125,"HzT":0,"breakerPosA":0}}  
{"gocbRef":"SUB_SEL451_FED2CFG/LLN0$G0$SUB_SEL451_FED2","datSet":"SUB_SEL451_FED2CFG/LLN0$8RDSet01","goID":"SUB_SEL451_FED2","appID":6,"srcMac":"00:30:A7:02:07:BF","dstMac":"01:0C:CD:01:00:06","stNum":6774070,"sqNum":0,"t":1638306305160,"allData":{"magCurrentPhaseA":0,"angCurrentPhaseA":0,"magCurrentPhaseB":0,"angCurrentPhaseB":0,"magCurrentPhaseC":0,"angCurrentPhaseC":0,"magFreqHz":60,"magVoltagePhaseA":0,"angVoltagePhaseA":0,"magVoltagePhaseB":0,"angVoltagePhaseB":0,"magVoltagePhaseC":0,"angVoltagePhaseC":0,"magTotVar":1.74123314877761e-07,"magTotW":8.1788357420009561e-06,"magTotPF":0.99977350234985352,"HzT":0,"breakerPosA":0}}  
{"gocbRef":"SUB_SEL451_FED1CFG/LLN0$G0$SUB_SEL451_FED1","datSet":"SUB_SEL451_FED1CFG/LLN0$8RDSet01","goID":"SUB_SEL451_FED1","appID":4,"srcMac":"00:30:A7:02:2E:19","dstMac":"01:0C:CD:01:00:04","stNum":6769245,"sqNum":0,"t":1638306305328,"allData":{"magCurrentPhaseA":0,"angCurrentPhaseA":0,"magCurrentPhaseB":0,"angCurrentPhaseB":0,"magCurrentPhaseC":0,"angCurrentPhaseC":0,"magFreqHz":60,"magVoltagePhaseA":0,"angVoltagePhaseA":0,"magVoltagePhaseB":0,"angVoltagePhaseB":0,"magVoltagePhaseC":0,"angVoltagePhaseC":0,"magTotVar":-9.2412994945334503e-07,"magTotW":9.212915754962489e-06,"magTotPF":0.99500691890716553,"HzT":0,"breakerPosA":0}}  
{"gocbRef":"SUB_SEL451_FED2CFG/LLN0$G0$SUB_SEL451_FED2","datSet":"SUB_SEL451_FED2CFG/LLN0$8RDSet01","goID":"SUB_SEL451_FED2","appID":6,"srcMac":"00:30:A7:02:07:BF","dstMac":"01:0C:CD:01:00:06","stNum":6774071,"sqNum":0,"t":1638306305691,"allData":{"magCurrentPhaseA":0,"angCurrentPhaseA":0,"magCurrentPhaseB":0,"angCurrentPhaseB":0,"magCurrentPhaseC":0,"angCurrentPhaseC":0,"magFreqHz":60,"magVoltagePhaseA":0,"angVoltagePhaseA":0,"magVoltagePhaseB":0,"angVoltagePhaseB":0,"magVoltagePhaseC":0,"angVoltagePhaseC":0,"magTotVar":1.4164267270189157e-07,"magTotW":8.0048139352584258e-06,"magTotPF":0.99984347820281982,"HzT":0,"breakerPosA":0}}  
{"gocbRef":"SUB_SEL451_FED1CFG/LLN0$G0$SUB_SEL451_FED1","datSet":"SUB_SEL451_FED1CFG/LLN0$8RDSet01","goID":"SUB_SEL451_FED1","appID":4,"srcMac":"00:30:A7:02:2E:19","dstMac":"01:0C:CD:01:00:04","stNum":6769246,"sqNum":0,"t":1638306305828,"allData":{"magCurrentPhaseA":0,"angCurrentPhaseA":0,"magCurrentPhaseB":0,"angCurrentPhaseB":0,"magCurrentPhaseC":0,"angCurrentPhaseC":0,"magFreqHz":60,"magVoltagePhaseA":0,"angVoltagePhaseA":0,"magVoltagePhaseB":0,"angVoltagePhaseB":0,"magVoltagePhaseC":0,"angVoltagePhaseC":0,"magTotVar":-9.90937729028546892e-07,"magTotW":9.5690684247529134e-06,"magTotPF":0.99468088150024414,"HzT":0,"breakerPosA":0}}  
{"gocbRef":"SUB_SEL451_FED2CFG/LLN0$G0$SUB_SEL451_FED2","datSet":"SUB_SEL451_FED2CFG/LLN0$8RDSet01","goID":"SUB_SEL451_FED2","appID":6,"srcMac":"00:30:A7:02:07:BF","dstMac":"01:0C:CD:01:00:06","stNum":6774072,"sqNum":0,"t":1638306306161,"allData":{"magCurrentPhaseA":0,"angCurrentPhaseA":0,"magCurrentPhaseB":0,"angCurrentPhaseB":0,"magCurrentPhaseC":0,"angCurrentPhaseC":0,"magFreqHz":60,"magVoltagePhaseA":0,"angVoltagePhaseA":0,"magVoltagePhaseB":0,"angVoltagePhaseB":0,"magVoltagePhaseC":0,"angVoltagePhaseC":0,"magTotVar":2.0537729028546892e-07,"magTotW":7.9951660154620185e-06,"magTotPF":0.99967020750045776,"HzT":0,"breakerPosA":0}}  
{"gocbRef":"SUB_SEL451_FED1CFG/LLN0$G0$SUB_SEL451_FED1","datSet":"SUB_SEL451_FED1CFG/LLN0$8RDSet01","goID":"SUB_SEL451_FED1","appID":4,"srcMac":"00:30:A7:02:2E:19","dstMac":"01:0C:CD:01:00:04","stNum":6769247,"sqNum":0,"t":1638306306328,"allData":{"magCurrentPhaseA":0,"angCurrentPhaseA":0,"magCurrentPhaseB":0,"angCurrentPhaseB":0,"magCurrentPhaseC":0,"angCurrentPhaseC":0,"magFreqHz":60,"magVoltagePhaseA":0,"angVoltagePhaseA":0,"magVoltagePhaseB":0,"angVoltagePhaseB":0,"magVoltagePhaseC":0,"angVoltagePhaseC":0,"magTotVar":-9.6672908966866089e-07,"magTotW":9.5718914963072166e-06,"magTotPF":0.9949384331703186,"HzT":0,"breakerPosA":0}}  
{"gocbRef":"SUB_SEL451_FED2CFG/LLN0$G0$SUB_SEL451_FED2","datSet":"SUB_SEL451_FED2CFG/LLN0$8RDSet01","goID":"SUB_SEL451_FED2","appID":6,"srcMac":"00:30:A7:02:07:BF","dstMac":"01:0C:CD:01:00:06","stNum":6774073,"sqNum":0,"t":1638306306657,"allData":{"magCurrentPhaseA":0,"angCurrentPhaseA":0,"magCurrentPhaseB":0,"angCurrentPhaseB":0,"magCurrentPhaseC":0,"angCurrentPhaseC":0,"magFreqHz":60,"magVoltagePhaseA":0,"angVoltagePhaseA":0,"magVoltagePhaseB":0,"angVoltagePhaseB":0,"magVoltagePhaseC":0,"angVoltagePhaseC":0,"magTotVar":1.4158450767354225e-07,"magTotW":7.985218871908728e-06,"magTotPF":0.99984288215637207,"HzT":0,"breakerPosA":0}}  
{"gocbRef":"SUB_SEL451_FED1CFG/LLN0$G0$SUB_SEL451_FED1","datSet":"SUB_SEL451_FED1CFG/LLN0$8RDSet01","goID":"SUB_SEL451_FED1","appID":4,"srcMac":"00:30:A7:02:2E:19","dstMac":"01:0C:CD:01:00:04","stNum":6769248,"sqNum":0,"t":1638306306828,"allData":{"magCurrentPhaseA":0,"angCurrentPhaseA":0,"magCurrentPhaseB":0,"angCurrentPhaseB":0,"magCurrentPhaseC":0,"angCurrentPhaseC":0,"magFreqHz":60,"magVoltagePhaseA":0,"angVoltagePhaseA":0,"magVoltagePhaseB":0,"angVoltagePhaseB":0,"magVoltagePhaseC":0,"angVoltagePhaseC":0,"magTotVar":-1.0219938531008665e-06,"magTotW":9.3557873697136529e-06,"magTotPF":0.99408650398254395,"HzT":0,"breakerPosA":0}}  
[attestation:observer* 1:store- 2:iec61850_stats 3:dump_pcaps 4:netstattime 5:anomaly_detect 6:powersys_event_detect "dlt-5" 16:05 30-Nov-21  
11/30, 4:05 PM ~./nrl-dlt-network/scripts master •
```

Figure 58. IEC 61850 data displayed by one of the Attestation Framework modules.

7.2.4 Traffic network computer

A laptop computer was connected to the spanning port of the main Ethernet switch to collect overall traffic data from the experiments. These data packets can be used for later analysis to compare the voltage and current data embedded within the packets with the data produced by the real-time simulator. The data are also useful to study the behavior of various cyber events.

7.2.5 Control center and local HMI computers

The control center HMI computer was responsible for collecting IEC 61850 device data from the power meters and protective relays and displaying it in a dashboard to provide a central overview of all device states and current measurements. This was implemented on an OnLogic ML340G-51 Intel Core i5-based industrial computer running the Ubuntu Linux operating system. The IEC 61850 observer program ran on this computer to receive and format IEC 61850 packets from the test bed devices, the Telegraf agent to handle database ingestion [33], and a local InfluxDB database. Grafana was configured to provide a web-based dashboard displaying the most recent GOOSE and SV measurements from the database.

The control center HMI takes advantage of the current simplified network architecture of the test bed by using the IEC 61850 GOOSE and SV protocols to acquire data from the power meters and protective relays. In an operational configuration, the control center would not have direct access to data from these layer 2 protocols. This would necessitate setting up a gateway responsible for collecting and/or aggregating the IEC 61850 device data at the substation and sending the data to the control center. Future work should leverage IEC 61850 documents that provide specifications for protocol mappings to the MMS client-server protocol [34] and guidance for substation-to-control center communication [35] to create a more realistic configuration.

Another computer was responsible for acting as the local HMI, providing an overview of the current device state and displaying data for the relays inside the substation. This computer was set up similarly to the control center HMI with the same software but instead used a Raspberry Pi 3 single board computer for the hardware and ran the Raspbian Linux operating system. The Grafana dashboard for the local HMI was based on the control center dashboard but showed only data from the relay devices.

7.2.6 VM Blueframe computer

The Blueframe computer queried each device for artifacts and then stored the results in its internal database. A user may retrieve the data as described previously using the web server of the Blueframe computer and then proceeding to the appropriate application, the API.

7.2.7 The DLT master node

The DLT master node collected the GOOSE and SV packets of the IEC 61850 protocol and stored them in databases. Also, the DLT master node queried the internal database of the Blueframe computer to retrieve the raw data and the hash associated with it. The data in the databases may be exported as CSV files for later analysis.

7.2.8 EmSense high-speed SV emulator device

The EmSense device was on the main Ethernet network. This device emulates a high-resolution sensor for a power grid and is useful for generating SV packets because some SEL devices do not generate these packets. EmSense operated by using the raw sensor and voltage data derived from ORNL's signature library. EmSense then packaged the data in the form of IEC 61850 SV packets, which EmSense broadcasted on the network. In addition, the EmSense can generate artificial sinusoidal data that appears as waveforms for voltage and current. EmSense enables experimentation with the DarkNet infrastructure where a variety of sensors must be represented along with their typical communication traffic. The EmSense device was configured with software for receiving and processing packets from the DLT framework. This receiving software must be able to manage information that is high in velocity, variety, and volume. The EmSense device facilitates the development of such software in the DarkNet project.

8. BLUEFRAME OPERATING SYSTEM

This section describes the Blueframe operating system for the electrical substation-grid test bed. An overview of the architecture for the representative DLT, Blueframe platform, and IED devices with the physical connections is provided. Then, the operation and setup guidelines of the Blueframe computer are given.

8.1 OVERVIEW

The DLTs must be updated with artifacts from the SEL protective relays, power meters, RTACs, and other related IEDs in the test bed. The artifacts include details of configurations and settings for the devices. To update the DLTs, it is necessary to communicate with these IEDs to retrieve the artifacts. Blueframe, a product of SEL, enables us to perform the communication with these devices without having to write custom scripts. Blueframe is an operating system based on secure Linux.

In the Attestation and Anomaly Framework, Blueframe exists as an intermediary system between the IEDs and the DLT nodes and can run on either an SEL automation controller or a VM (Figure 59). In the case of the DarkNet test bed, the Blueframe software runs on a VM. The VM runs on an OnLogic MC850-40, which is referred to in this work as the “Blueframe computer” and is connected to the main network of the test bed. Blueframe retrieves the artifacts from the devices directly and then stores them in a database maintained by Blueframe inside the OnLogic MC850-40 (blue arrows in Figure 59). The DLT nodes have software that can access the database and store the relevant hashes in the ledger (red arrows in Figure 59). Figure 59 illustrates the architecture of a representative DLT master node as part of a larger network, Blueframe platform, and IED devices with the physical connections in addition to the logical connections and communications.

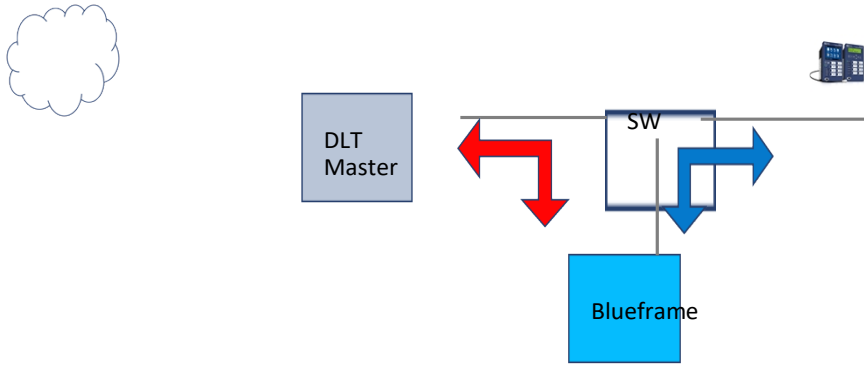


Figure 59. Architecture of a representative DLT, Blueframe platform, and IED devices with the physical connections in addition to the logical connections and communications.

8.2 OPERATION

For the DLT to retrieve the artifacts from the IEDs of the test bed, the framework must perform an operation consisting of two processes that involve network communication with specific protocols. First, Blueframe queries each device periodically according to a plan made by the user. The user can create the plan in the graphical user interface (GUI) of the Blueframe software. Second, Blueframe communicates with the IEDs over the network using the secure Telnet Protocol and Secure File Transfer Protocol.

8.3 SETTING UP BLUEFRAME

To enable the full operation described previously, users must configure Blueframe to retrieve the artifacts from specific devices, and specify the frequency for data collection. Blueframe has a GUI to allow users to configure it with various plans. The GUI is a website generated from a web server running on the Blueframe VM. Users can access the GUI by using a computer that is connected to the same network as the Blueframe platform and selecting the IP address of the Blueframe platform. Figure 60 shows the main screen of the GUI.

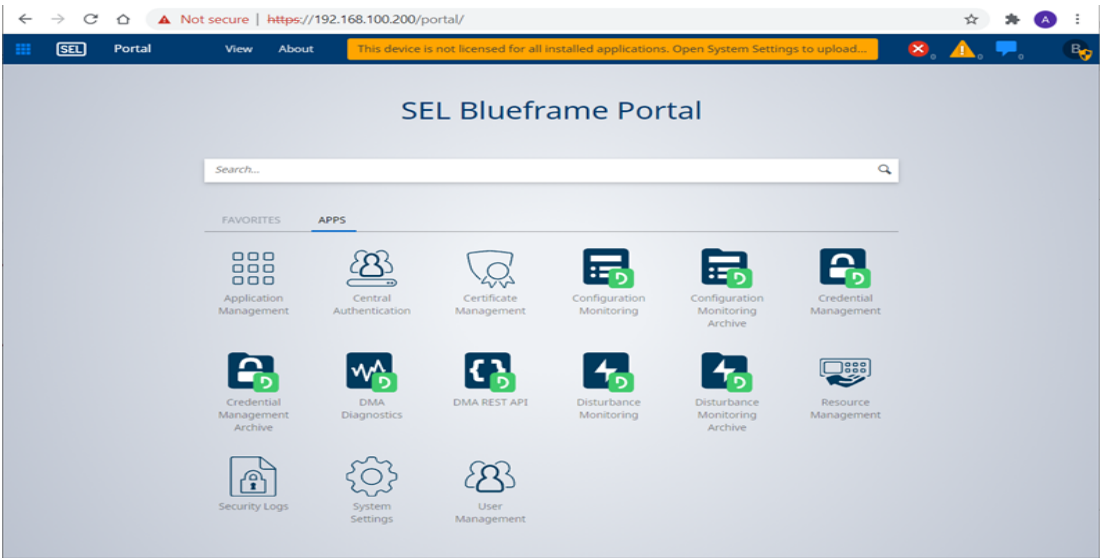


Figure 60. Main page of SEL Blueframe Portal after the user logs in.

Users must first access the Resource Management App and specify the SEL devices on the network for data retrieval. Once users have specified all the devices of interest, they then proceed to the Disturbance Monitoring App to set up a specific plan indicating how often Blueframe retrieves the data. The periods that may be selected are on the order of minutes with the smallest period being 1 min. Figure 61 shows the Disturbance Monitoring App with Plans from User.

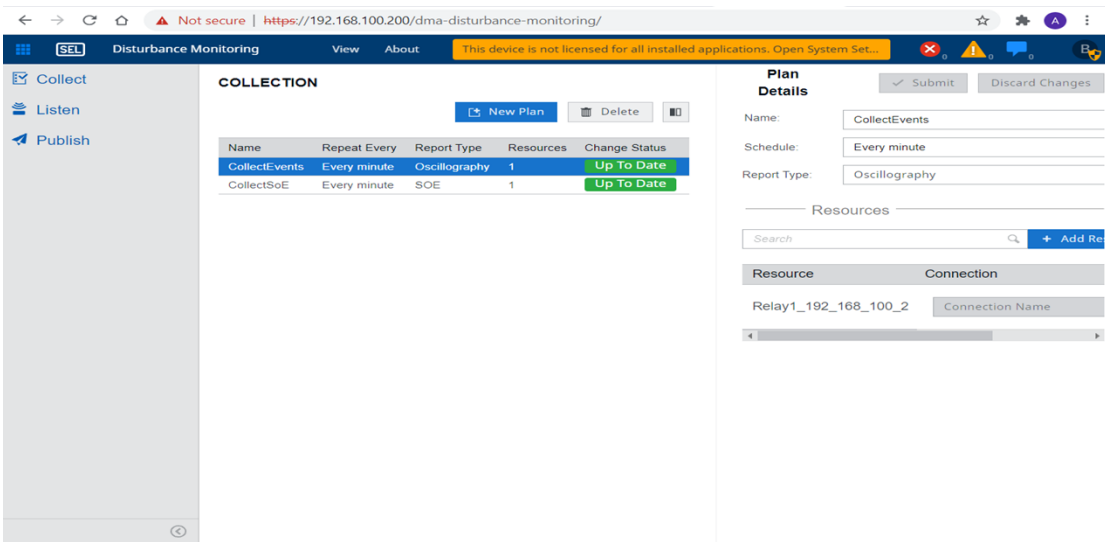


Figure 61. Disturbance Monitoring App with plans from a user.

Next, as a test is run, users go to the Directory Memory Access–API and chooses a source ID corresponding to a particular SEL device of interest, as shown in Figure 62. Then, users run the Execute command to retrieve an artifact from the database and view information about the artifact in the GUI. Also, the DLT has software to access the database through the network using Blueframe’s API. This software is triggered by the Anomaly Detection Module of the DLT Framework when the Anomaly Detection Module detects unusual behavior in the network or anomalous incoming packet data. Figure 62 shows the API App.

The screenshot shows a web browser window with the URL `https://192.168.100.200/dma-rest/api/v1/docs/rest-api/?urls.primaryName=sources#/Sources/getSource`. The browser's address bar also shows a "Not secure" warning. The page title is "DMA REST API" with "View" and "About" links. A yellow warning banner at the top states: "This device is not licensed for all installed applications. Open System Settings to upload license files." Below the banner, the main content area shows a "GET" request configuration for the endpoint `/sources/{source-id}` with the description "Gets a source with the ID value provided." A "Cancel" button is in the top right corner. The "Parameters" section is active, displaying a table with the following details:

Name	Description
source-id ★ <i>required</i>	The ID value of the source.
<code>string(\$uuid)</code> (path)	<input type="text" value="4bab557f-1c51-4bf0-aef6-120e050eb620"/>
X-SEL-Tracking-Id	The client request tracking identifier.
<code>string(\$uuid)</code> (header)	<input type="text" value="448c3e92-d4fd-443d-b1b0-6a110d4c8200"/>
X-SEL-Client-Instance-Id	The client instance tracking identifier.
<code>string(\$uuid)</code> (header)	<input type="text" value="9271278c-be68-41eb-850a-8715f59f8b84"/>

At the bottom of the configuration area is a large blue "Execute" button.

Figure 62. API App.

9. TEST BED RESULTS

In this section, the test bed results for the electrical substation-grid test bed are presented. For the analog signals, the phase primary currents and phase primary to neutral voltages from the HMI of the protective relays and power meters are compared. For the timing and synchronized sources, the steps to collect the time in the MM/DD/YYYY and HH:MM:SS format for the protective relays and power meters are presented. For the device messages, the processes to collect the data of the GOOSE and DNP messages from the protective relays and power meters are shown. Finally, the results of the relay events for the electrical fault tests are presented based on comparing the measured and calculated relay times for the protective relays, including the results from the electrical fault event detection with the DLT computer.

9.1 OVERVIEW

The results for the electrical substation-grid test bed were based on evaluating the analog signals, timing and synchronized sources, IEC 61850 and DNP messages, and electrical fault tests with DLT. Table 14 describes the types of assessments for the electrical substation-grid test bed with inside and outside substation devices.

Table 14. Results for the electrical substation-grid test bed

Assessment	Description
Analog signals	<ul style="list-style-type: none">• Verification of analog signals for the SEL-451 relays by calculating current and voltage gains, using the current and voltage scaling factors for the relay LLTI and comparing the magnitude of primary currents and voltages• Verification of analog signals for the SEL-734 and SEL-735 power meters by matching the magnitude and sinusoidal shape of primary currents and voltages from power meters and real time simulation, and adjusting the settings for the <i>CTRs</i> and <i>PTRs</i> on the power meters
Timing and synchronized sources	<ul style="list-style-type: none">• Verification of timing and synchronized signal sources for inside and outside substation devices by observing the time sources at the device display
IEC 61850 and DNP messages	<ul style="list-style-type: none">• Verification of map dataset points for IEC 61850 and DNP messages from power meters and relays with Wireshark
Electrical fault tests (with DLT)	<ul style="list-style-type: none">• Verification of SLG, LL, LLG, and 3L (or 3LG) electrical fault tests, running simulations for 10 s and placing an electrical fault at 5 s; after the electrical fault tests, collection of the COMTRADE events from the relays, and MATLAB simulation events from the host computer, to plot and compare the measured and theoretical relay time of electrical fault tests• Verification of the power system electrical fault event detection, collecting the DLT monitor screenshots for the SLG, LL, LLG, and 3L (or 3LG) electrical fault tests

9.2 RESULTS OF ANALOG SIGNALS

9.2.1 Analog signals for protective relays

The analog signals of the SEL-451 protective relays were represented by the A, B, and C phase secondary currents and A, B, and C phase to neutral secondary voltages that were fed at the LLTI, connecting the SEL-451 relays directly to the real-time simulator. In the electrical substation-grid test bed, the evaluation of analog signals was performed to compare the A, B, and C phase primary currents and A, B, and C phase to neutral primary voltages measured from the SEL-451 relays and real-time simulator. The

currents and voltage gains in Figure 63 were calculated and set based on measurement transformer ratios (CTR , PTR) and scaling factors for the LLTI of the SEL-451 protective relays [4]. In the electrical substation-grid test bed, the magnitudes of the phase primary currents and phase to neutral primary voltages were collected from the relay HMI with the AcSELeator Quickset software. The measured phase primary currents and phase to neutral primary voltages for the SUB_SEL451_FED1 (Figure 63A) and SUB_SEL451_FED2 (Figure 63B) protective relays were made using a CTR of 80 and PTR of 60. For these SEL-451 protective relays, the current and voltage scaling factors were 75 A/V and 150 V/V, respectively [4].

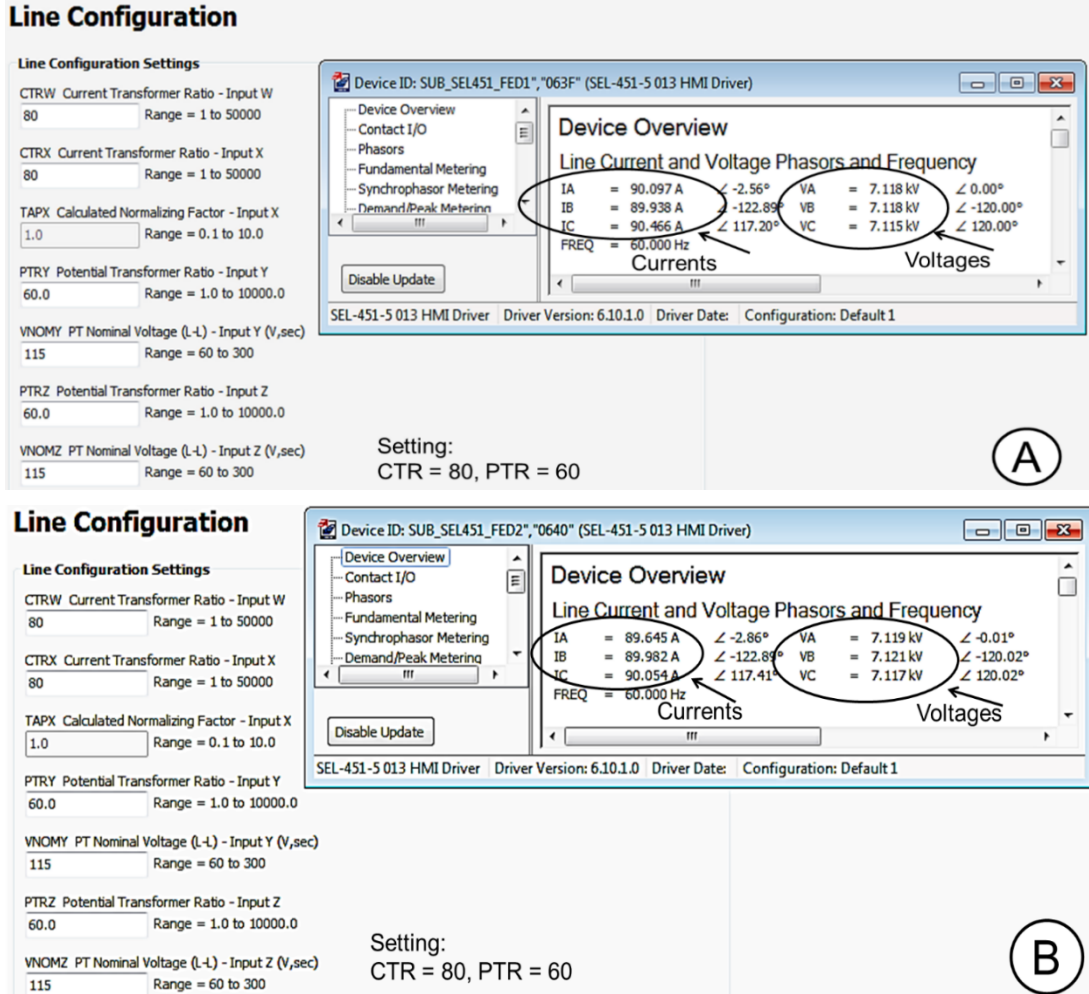


Figure 63. Measured currents and voltages of the SUB_SEL451_FED1 (A) and SUB_SEL451_FED2 (B) protective relays from the HMI with CTR of 80 and PTR of 60.

The analog signals for the SEL-451 protective relays were scaled using the simulated primary phase currents and phase to neutral voltages with current and voltage gain blocks, respectively (Figure 6). These current (1 V/6,000 A) and voltage (1 V/9,000 V) gains were calculated by Eqs. (7) and (8), respectively [9].

$$Gain_I = 1 / (CTR_{RTS} \times SF_A), \quad (7)$$

where $Gain_I$ is the current gain, CTR_{RTS} is the CTR of the relay (80) in real-time simulation, and SF_A is the relay's current scaling factor in amperes per volt.

$$Gain_V = 1/(PTR_{RTS} \times SF_V) , \quad (8)$$

where $Gain_V$ is the voltage gain, PTR_{RTS} is the PT ratio of the relay (60) in real-time simulation, and SF_V is the relay's voltage scaling factor in volts per volt.

Based on Eqs. (7) and (8), the calculated current and voltage gains are 1 V/6,000 A and 1 V/9,000 V, respectively. By running a test simulation, the A, B, and C phase primary currents and A, B, and C phase to neutral primary voltages were measured from the real-time simulator and relay HMI (Table 15).

Table 15. Measured currents and voltages of SEL-451 protective relays

Device name	Measurements from real-time simulator						Measurements from relay HMI					
	Current (A) of			Voltage (V) of			Current (A) of			Voltages (V) of		
	Phase A [IA]	Phase B [IB]	Phase C, [IC]	Phase A [VA]	Phase B [VB]	Phase C [VC]	Phase A [IA]	Phase B [IB]	Phase C [IC]	Phase A [VA]	Phase B [VB]	Phase C [VC]
SUB_SEL451_FED1	91.2	91.2	91.2	7,109	7,109	7,109	90.1	89.9	90.5	7,118	7,118	7,115
SUB_SEL451_FED2	91.2	91.2	91.2	7,109	7,109	7,109	89.6	90	90.1	7,119	7,121	7,117

Using the phase primary currents and phase to neutral primary voltages from Table 15, the percent errors of analog signals were calculated. The percent errors for the measured n (A, B, or C) phase primary currents ($E_{\%In}$) were calculated by Eq. (9),

$$E_{\%In} = \left(\frac{I_{nHMI} - I_{nRTS}}{I_{nRTS}} \right) \times 100 , \quad (9)$$

where I_{nRTS} was the n (A, B, or C) phase primary current collected from the real-time simulator in amperes, and I_{nHMI} was the n (A, B, or C) phase primary current collected from the device HMI in amperes.

The percent errors for measured n (A, B, or C) phase to neutral primary voltages ($E_{\%Vn}$) were calculated by Eq. (10),

$$E_{\%Vn} = \left(\frac{V_{nHMI} - V_{nRTS}}{V_{nRTS}} \right) \times 100 , \quad (10)$$

where V_{nRTS} was the n (A, B, or C) phase to neutral primary voltage collected from the real-time simulator in volts, and V_{nHMI} was the n (A, B, or C) phase to neutral primary voltage collected from the device HMI in volts.

The measurements at the electrical substations may provide vital information supporting decisions on service needs and grid control. Although the requirements for the electrical substation measurements on delivered power are rather strict, the precision related to generalized monitoring is less so. Often, an error margin of up to 5% on the absolute measurements is acceptable for monitoring [36]. Based on Table 15 and Table 16, the percent error for current and voltage magnitudes was calculated by Eqs. (9) and (10), respectively. The percent errors of the measured phase primary currents and phase to neutral primary voltages for the SEL-451 protective relays showed good performance. For the SEL-451 relays, the percent error range of the measured phase primary currents was -0.8% to -1.8% , and the percent error range of the measured phase to neutral primary voltages was $+0.2\%$ to $+0.1\%$.

Table 16. Percent errors of measured phase primary currents and phase to neutral primary voltages for the SEL-451 protective relays

Device name	Percent errors of measured currents and voltages for the SEL-451 relays					
	Phase primary current (%)			Phase to neutral primary voltage (%)		
	$E_{\% IA}$	$E_{\% IB}$	$E_{\% IC}$	$E_{\% VA}$	$E_{\% VB}$	$E_{\% VC}$
SUB_SEL451_FED1	-1.2	-1.4	-0.8	0.1	0.1	0.1
SUB_SEL451_FED2	-1.8	-1.3	-1.2	0.1	0.2	0.1

9.2.2 Analog signals for power meters

In the SEL-735 and SEL-734 power meters, the analog signals were not connected directly from the real-time simulator to the device LLTI because the current and voltage scaling factors were not available from the SEL-735 and SEL-734 power meter manuals [5, 6]. The SEL-734 and SEL-735 power meters were set with a *CTR* of 225 and *PTR* of 449 using the AcSELeRator Quickset software. In the SEL-734 and SEL-735 power meters, the analog signals were represented by the A, B, and C phase secondary currents and A, B, and C phase to neutral secondary voltages that were fed from current and voltage amplifiers, respectively. These current and voltage amplifiers were fed by the analog signals from the real-time simulator.

The calibration of the SEL-734 and SEL-735 power meters was important to determine not only the measured magnitude but also the sinusoidal shape for analog signals. In the electrical substation-grid test bed, the SEL-735 power meters were calibrated before the SEL-734 power meters because they had a front side display that plotted the current and voltage sine waves on the devices. The SEL-735 power meters were calibrated by adjusting the current and voltage gains (Figure 7). The SEL-735 power meter with a current gain of 1 V/2,000 A is shown in Figure 64A. The A, B, and C phase currents measured by the SEL-735 power meters resulted in a distortional analog signal because the current injected to the SEL-735 power meters were given by 0.02 A for a current gain of 1 V/2,000 A. Then, the current gains were set to 1 V/200 A (Figure 7) to increase the amplifier currents being injected at SEL-735 power meters. By placing a current gain of 1 V/200 A (Figure 7), the distortional analog signal for A, B, and C phase currents disappeared at SEL-735 power meter displays (Figure 64B).

The voltage gain for the SEL-735 power meters was set to 1 V/9,000 V (Figure 7). The A, B, and C phase voltages measured by the SEL-735 power meters were measured at the device display. The A, B, and C phase voltages measured by the SEL-735 power meters resulted in a non-distortional analog signal because the voltages injected to the SEL-735 power meters were given by 30 V for a voltage gain of 1 V/9,000 V (Figure 65). In Figure 64 and Figure 65, the sinusoidal currents and voltages plotted at the displays of the SEL-735 power meters had a resolution of 256 samples per cycle. This was effective for observing the shape of analog signals without collecting the events from the SEL-735 power meters.

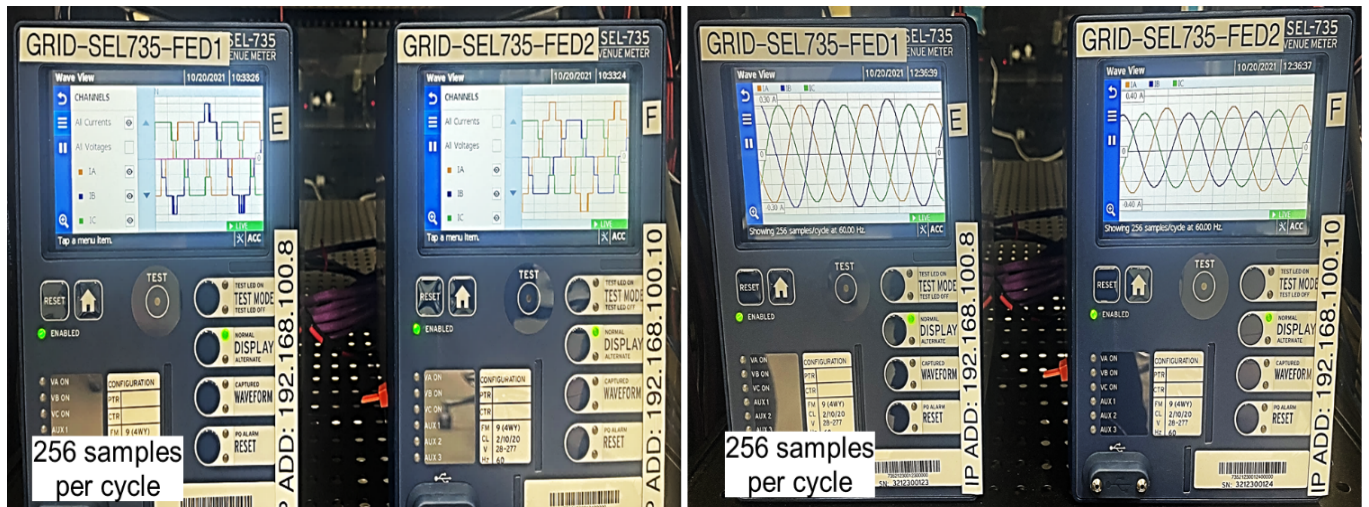


Figure 64. SEL-735 power meters with a current gain of 1 V/2,000 A (A) and 1 V/200 A (B) in the RT-LAB project.

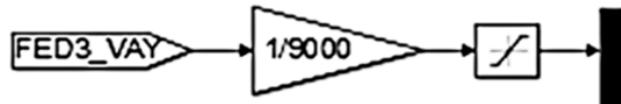
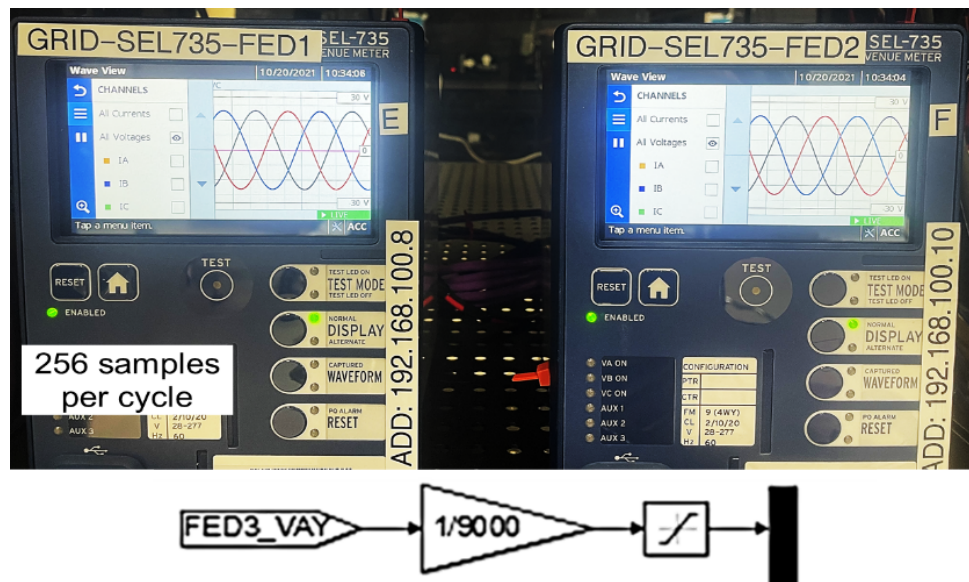


Figure 65. SEL-735 power meters with a voltage gain of 1 V/9,000 V in the RT-LAB project.

The magnitudes of analog signals from the SEL-735 power meters were collected. The A, B, and C phase primary currents and A, B, and C phase to neutral primary voltages were measured with the device HMI using the AcSELeator Quickset software. The measured currents and voltages of the GRID_SEL735_FED1 (Figure 66A) and GRID_SEL735_FED2 (Figure 66B) power meters from the device HMI with *CTR* of 225 and *PTR* of 449 are shown.

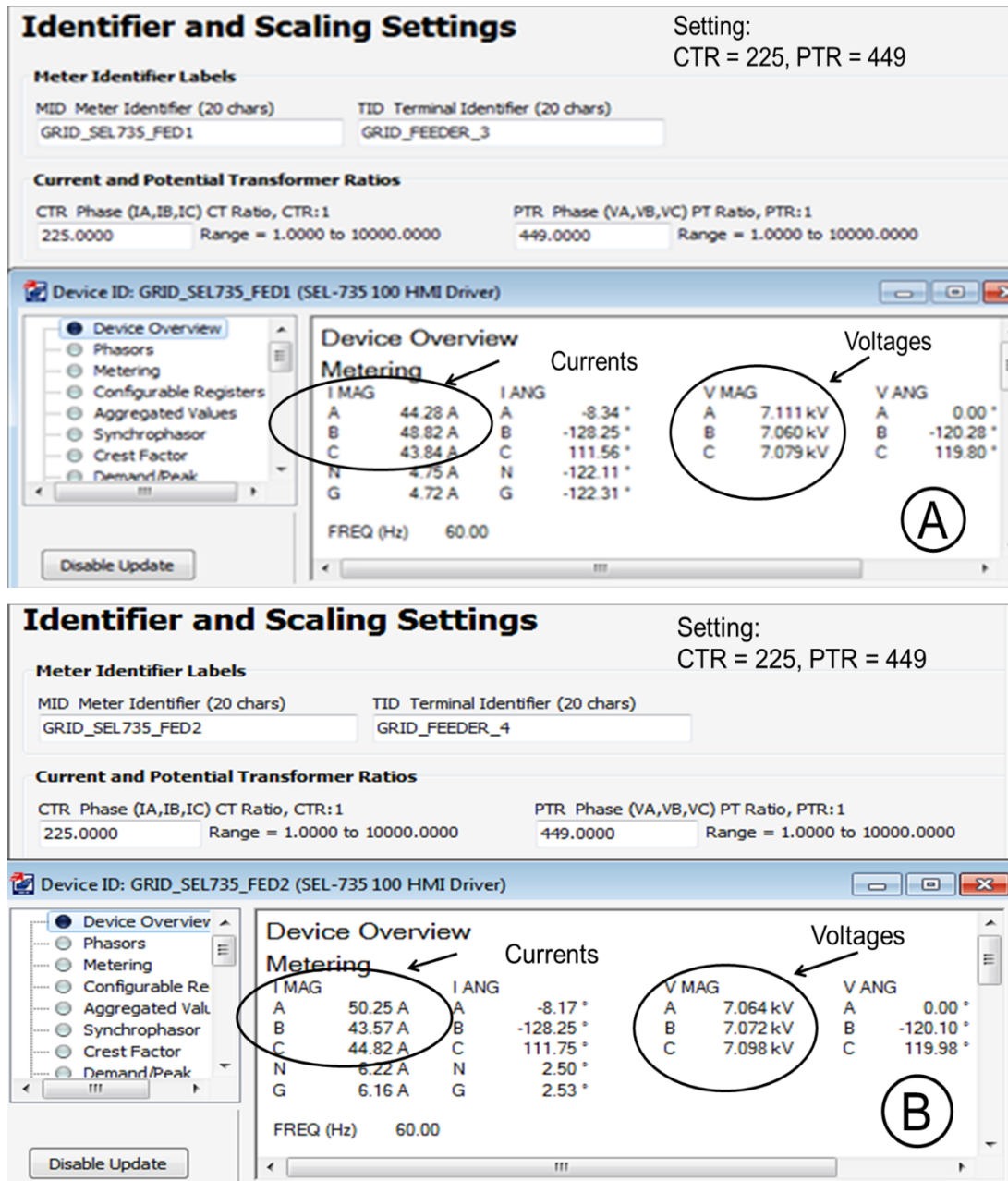


Figure 66. Measured currents and voltages of the GRID_SEL735_FED1 (A) and GRID_SEL735_FED2 (B) power meters from HMI with CTR of 225 and PTR of 449.

The SEL-734 power meters do not have front side displays that plot the wave shape from the analog signals. Therefore, the current and voltage gains for the SEL-734 power meters were set like the SEL-735 power meters. The SEL-734 power meter current and voltage gains were set to 1 V/200 A and 1 V/9,000 V, respectively (Figure 7). In addition, the CTR and PTR for the SEL-734 power meters were set like the SEL-735 power meters. The A, B, and C phase primary currents and A, B, and C phase to neutral primary voltages were measured with the device HMI using the AcSElator Quickset software. The measured currents and voltages of the GRID_SEL734_FED1 (Figure 67A) and GRID_SEL734_FED2 (Figure 67B) power meters from the device HMI with CTR of 225 and PTR of 449 are shown.

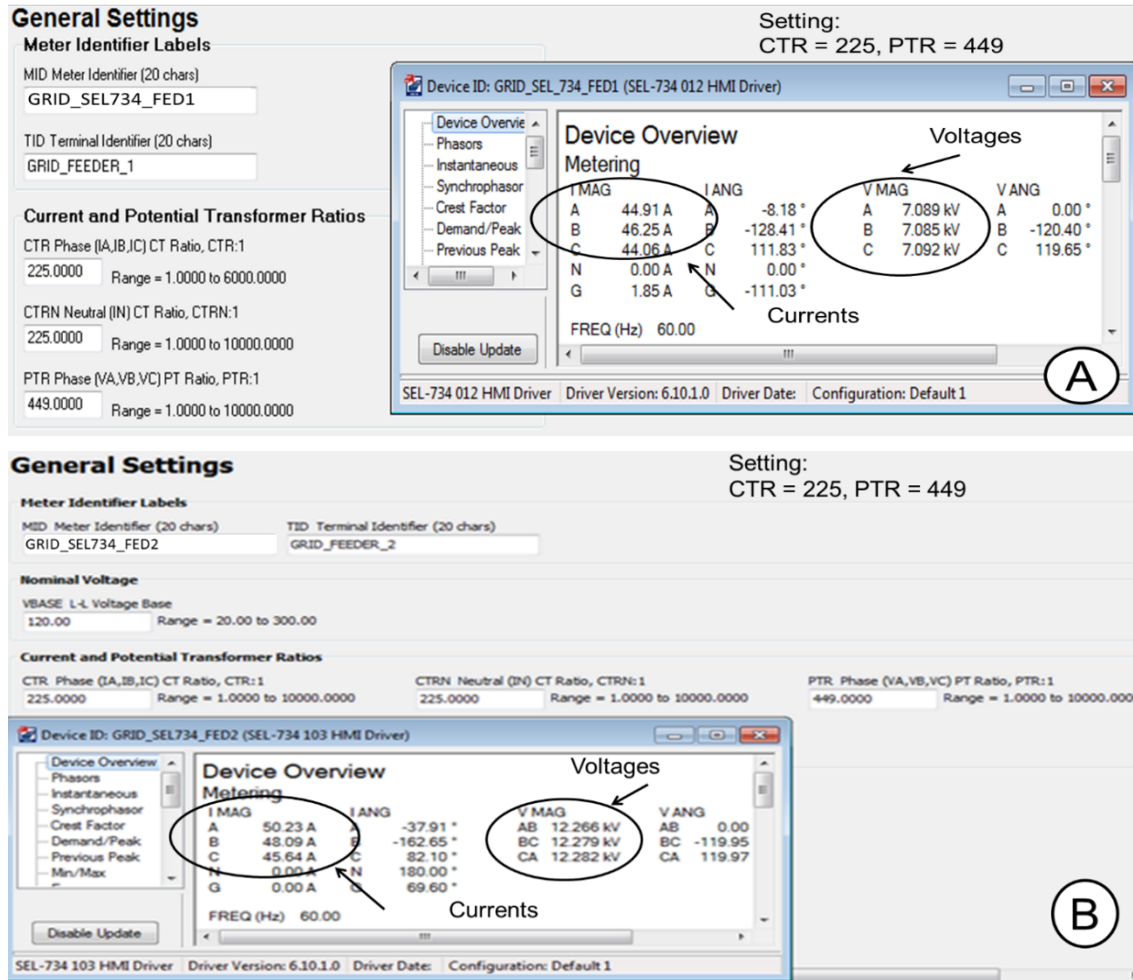


Figure 67. Measure currents and voltages of the GRID_SEL734_FED1 (A) and GRID_SEL734_FED2 (B) power meters from HMI with CTR of 225 and PTR of 449.

The SEL-734 and SEL-735 power meters were assessed via a simulation test. The measured magnitudes of the primary currents and voltages from the power meters and real-time simulator were collected. Table 17 shows the measured currents and voltages of the SEL-735 and SEL-734 power meters from the real-time simulator and device HMI (Figure 66 and Figure 67).

Table 17. Measured primary currents and voltages of SEL-734 and SEL-735 power meters

Device name	Measurements from real-time simulator						Measurements from device HMI					
	Current (A) of			Voltage (V) of			Current (A) of			Voltage (V) of		
	Phase A [IA]	Phase B [IB]	Phase C [IC]	Phase A [VA]	Phase B [VB]	Phase C [VC]	Phase A [IA]	Phase B [IB]	Phase C [IC]	Phase A [VA]	Phase B [VB]	Phase C [VC]
GRID_SEL734_FED1 (HORIZONTAL)	45.6	45.6	45.6	7,091	7,091	7,091	44.91	46.25	44.06	7,089	7,085	7,092
GRID_SEL734_FED2 (VERTICAL)	45.6	45.6	45.6	12,267*	12,267*	12,267*	50.23	48.09	45.64	12,266*	12,279*	12,282*
GRID_SEL735_FED1	45.6	45.6	45.6	7,091	7,091	7,091	44.28	48.82	43.84	7,111	7,060	7,079
GRID_SEL735_FED2	45.6	45.6	45.6	7,091	7,091	7,091	50.25	43.57	44.82	7,064	7,072	7,098

*Phase to neutral voltages

From Table 17 and Table 18, the percent error for the current and voltage magnitudes was calculated by Eqs. (9) and (10), respectively. For the SEL-734 power meters, the percent error range of the measured phase primary current was +9.2% to -3.5%, and the percent error range of the measured phase primary voltages was +0.1% to -0.1%. For the SEL-735 power meters, the percent error range of the measured phase primary currents was +9.3% to -4.7%, and the percent error range of the measured phase primary voltages was +0.3% to -0.4%. The measurements at electrical substations may provide vital information supporting decisions on service needs and grid control. Although the requirements for the electrical substation measurements on delivered power are rather strict, the precision related to generalized monitoring is less so. Often, an error margin of up to 5% on the absolute measurements is acceptable [36]. The calculated percent errors between the measurements of current magnitudes from the real-time simulator and device HMI had indicated an error margin greater than 5% (underlined values in Table 18). However, these power meters are outside substation devices and are used for metering applications instead of protection applications because feeder fuses were set at the SEL-734 and SEL-735 power meter locations. This error could be acceptable for these devices at the electrical substation-grid test bed. In addition, these percent errors could be reduced by adjusting the current gains of the A and B phase currents for these devices in Figure 7A and B.

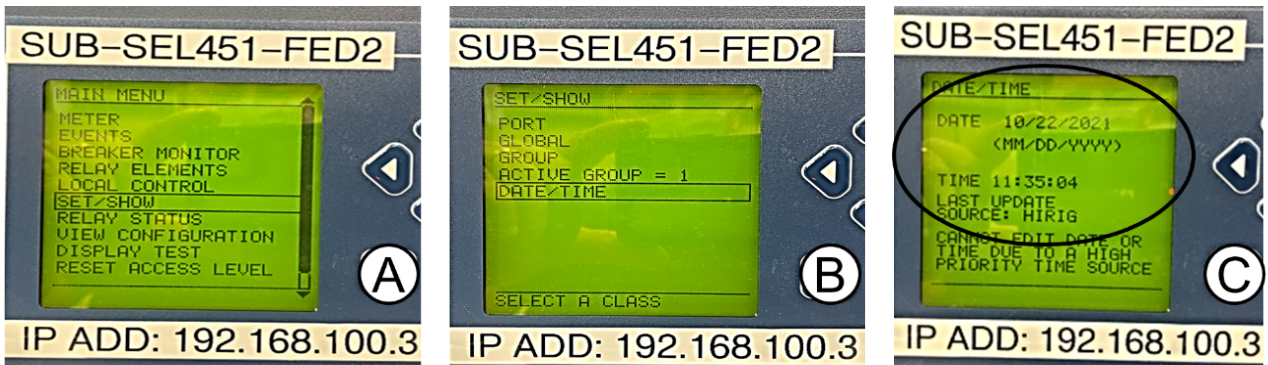
Table 18. Percent error of measured primary current and voltage of SEL-734 and SEL-735 power meters

Device name	Percent errors from measured					
	Phase currents (%)			Phase voltages (%)		
	$E\%_{IA}$	$E\%_{IB}$	$E\%_{IC}$	$E\%_{VA}$	$E\%_{VB}$	$E\%_{VC}$
GRID_SEL734_FED1 (HORIZONTAL)	-1.5	1.4	-3.5	0.0	-0.1	0.0
GRID_SEL734_FED2 (VERTICAL)	9.2	5.2	0.1	0.0*	0.1*	0.1*
GRID_SEL735_FED1	-3.0	6.6	-4.0	0.3	-0.4	-0.2
GRID_SEL735_FED2	9.3	-4.7	-1.7	-0.4	-0.3	0.1

*Phase to neutral voltages

9.3 RESULTS OF TIMING AND SYNCHRONIZED SOURCE

For the assessment of the timing and synchronized source, the SEL-451 protective relays and SEL-734 and SEL-735 power meters were set with the IRIG-B protocol because the PTP Ethernet port 5A for timing synchronized signals was not available for the SEL-451 protective relays [4]. The SEL-735 and SEL-734 power meters did not have the PTP based on their manufacturer manuals [5, 6]. The results of the timing and synchronized sources for protective relays and power meters were verified from each device display. The steps to observe the time source from the SEL-451 relay display are shown in Figure 68. From the front side display of the SEL-451 protective relays, the MAIN MENU was selected, and then the SET/SHOW option was selected (Figure 68A). Next, the DATE/TIME option (Figure 68B) was selected, and then the date and time in the MM/DD/YYYY and HH:MM:SS formats, respectively. The IRIG sources were observed on SEL-451 relay display (Figure 68C)



- 1- Select from the relay display the MAIN MENU => SET/SHOW 2- Select from the relay display the SET/SHOW => DATE/TIME 3- From the DATE/ TIME, the date, time and HIRIG source are shown

Figure 68. Steps to evaluate the time source from SEL-451 relay display.

The SEL-734 power meter automatically switched time source inputs from internal to IRIG-B if a valid IRIG signal was connected [6]. If the IRIG-B time source was unavailable, the power meter switched to the internal source. The power meter automatically switched to a higher-priority time source (IRIG-B) when the power meter measured an acceptable time source stability and reliability. In the SEL-734 power meters, the timing and synchronized source and date/time could be observed from the device display.

From the display at the SEL-734 power meter, the MAIN Menu and SET/SHOW options were selected. Then, the DATE/TIME option was selected to observe the date and time in the MM/DD/YYYY and HH:MM:SS formats, respectively. The SEL-735 power meter has a color touch screen display [5] that shows the Date and Time from the Home screen (Table 19). By selecting the Settings from the Home screen, the Date and Time option was then selected. The Date and Time for the SEL-735 power meters could be observed from the color touchscreen display to evaluate the timing synchronized source for the SEL-735 power meters.

Table 19. Home screen and level menu settings for the date/time of the SEL-735 power meters

Home screen for the SEL-735 power meter	Level 2 menu	Level 3 menu	Level 4 menu
	Settings	Port	Port F Port 1 Port 2 Port 3 Port 4
		General	
		Energy Preload	
		Front Panel	
		Date and Time	Date and Time
		Touchscreen	
		Change Password	

9.4 RESULTS OF THE IEC 61850 AND DNP MESSAGES

In the electrical substation-grid test bed, communication messages from the SEL-451 protective relays and SEL-734 and SEL-735 power meters were evaluated by running a simulation test with the real-time simulator and collecting the IEC 61850 and DNP messages from the devices using the Wireshark software [37, 38].

9.4.1 IEC 61850 for the SEL-451 protective relays

In the electrical substation-grid test bed, the SEL-451 protective relays were set with the IEC 61850 protocol. Then, the GOOSE messages from the devices were transmitted. The GOOSE Dataset that was transmitted from the SEL-451 protective relays was stored in the CID file that was downloaded at the devices. Figure 69 shows the steps to observe the GOOSE Dataset that was downloaded to the SEL-451 protective relays based on the project created with the AcSELErator Architect software.

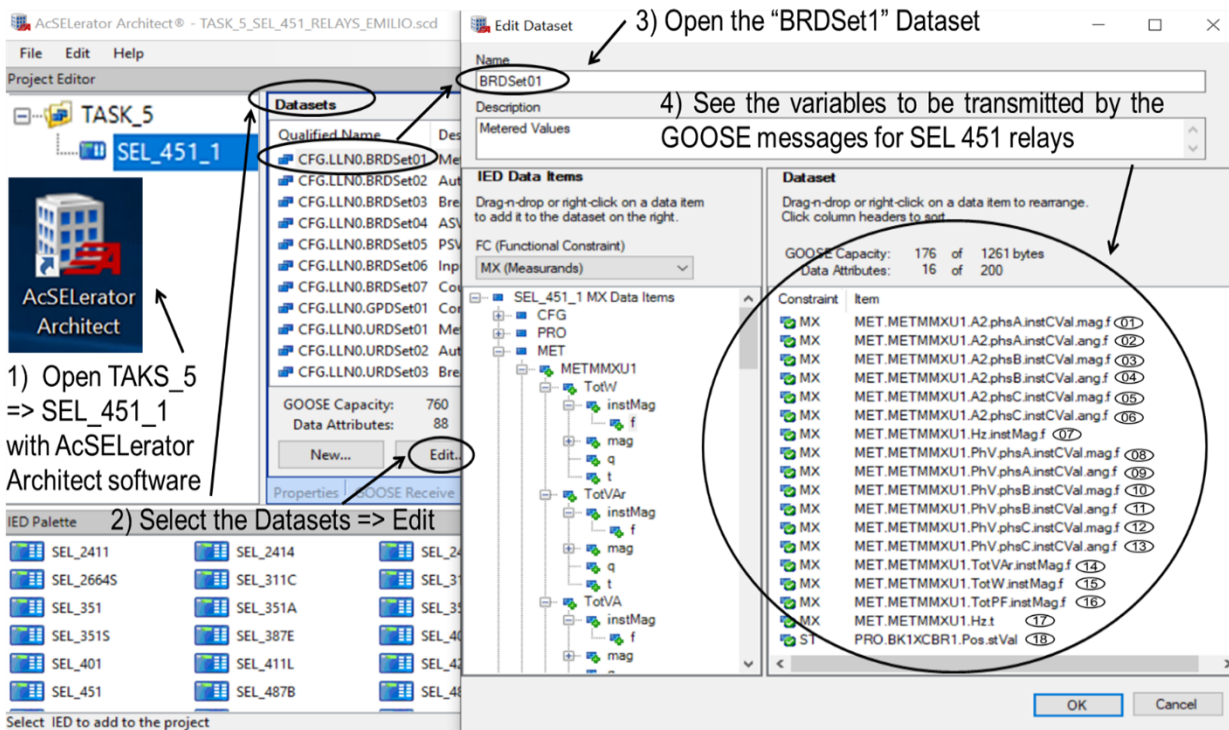


Figure 69. GOOSE Dataset of SEL-451 relays generated with the AcSELErator Architect software.

As shown in Figure 70, the items of the GOOSE Dataset for the SEL-451 protective relays were numbered from 01 to 18. These items were evaluated by running a simulation test with the real-time simulator and collecting the GOOSE messages from the SEL-451 protective relay using the Wireshark software. Figure 70 shows the steps to display the GOOSE messages for the SEL-451 protective relays. These data had been recorded with the Wireshark software. Frame 3594 for the Data_Nov3 file was selected. Then, the View menu and Expand All option were selected, identifying the 18 data floating points (Figure 70) that corresponded to the 18 items of the GOOSE Dataset (Figure 69).

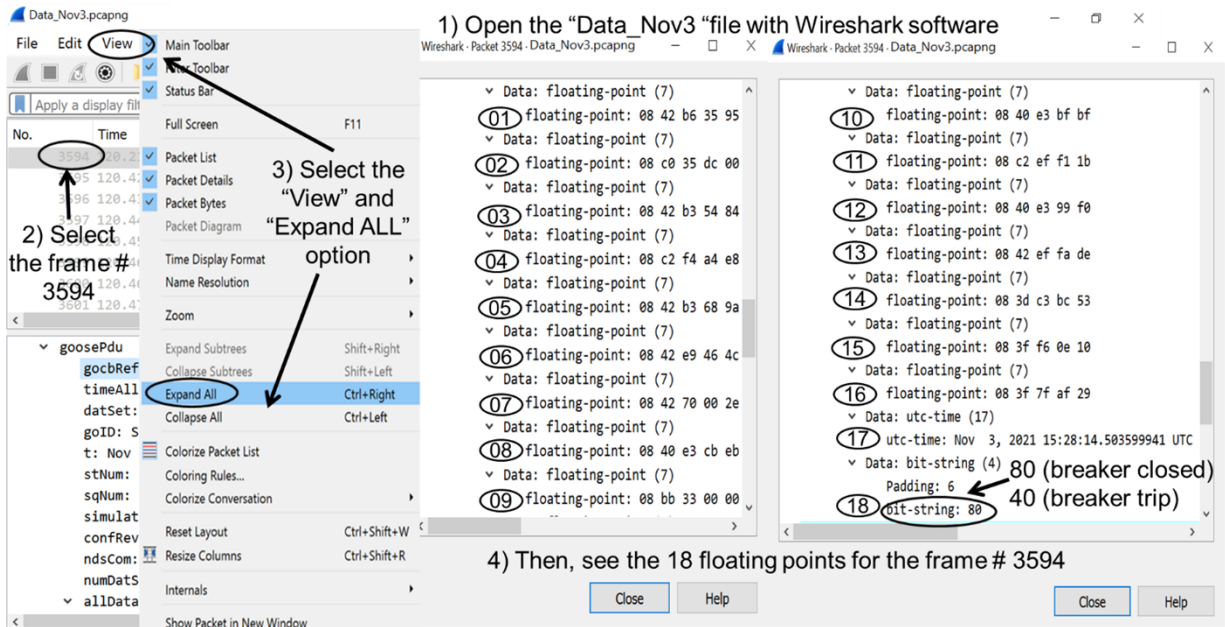
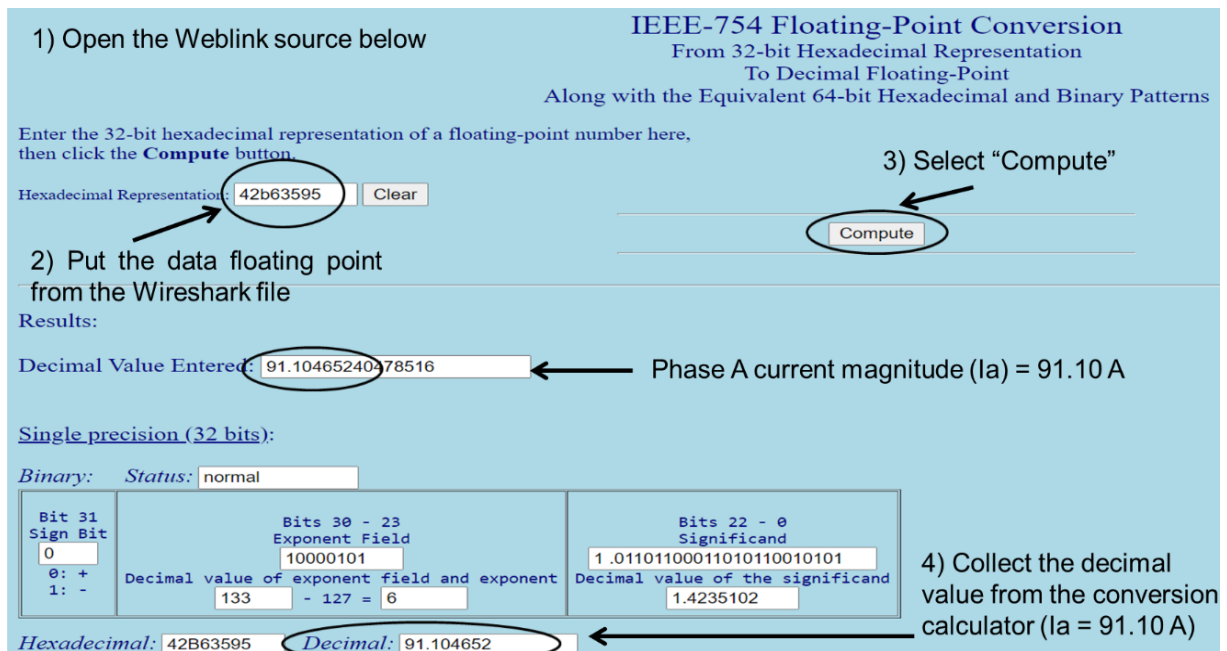


Figure 70. GOOSE messages of SEL-451 protective relays collected with Wireshark software.

As shown in Figure 70, the data floating points from 01 to 16 were represented by hexadecimal numbers. The last 8 numbers from the data floating points were converted from hexadecimal to decimal numbers using an IEEE-754 floating-point converter (<https://babbage.cs.qc.cuny.edu/ieee-754.old/32bit.html>), to obtain the measured values simulated during the time simulation tests. Figure 71 shows the steps to convert the data floating points from 01 to 16 in hexadecimal to decimal numbers.



Weblink source: IEEE-754 Floating-Point Conversion from 32-bit Hexadecimal to Floating-Point (cuny.edu)

Figure 71. IEEE-754 floating-point converter website.

The data floating points of the GOOSE messages for the SEL-451 protective relay from Frame 3594 of the Data_Nov3 file captured with Wireshark are shown in Table A.1. The GOOSE Dataset from the CID file, item descriptions from the SEL-451 protective relay manual [4], and measured data floating points from the GOOSE messages were set as described in Table A.1. In this case, the simulation test was based on a three-phase balanced power system of 7.2 kV, with A, B, and C phase currents of 90 A. The assessment of the GOOSE data floating points was based on converting the hexadecimal to decimal values, observing that the GOOSE data floating points represented the simulated three-phase balanced power system.

In the simulation, the breaker controlled by the SEL-451 protective relay was closed. In Table A.1, the measured circuit breaker 1 (pole A closed/open) state was 80 (data floating point 18), and the breaker pole state was open or closed for the 40 and 80 measured states, respectively. The collected data floating points (Table A.1) from the SEL-451 relays represented a balanced power system of 60.00 Hz (data floating point 07). The measured magnitude/angle for A (data floating point 01/02), B (data floating point 03/04), and C (data floating point 05/06) phase primary currents were $91.1^\circ/-2.84^\circ$, $89.6^\circ/-122.32^\circ$, and $89.7^\circ/116.63^\circ$, respectively. The measured magnitude/angle for A (data floating point 08/09), B (data floating point 10/11), and C (data floating point 12/13) phase to neutral primary voltages were $7.11^\circ/0.00^\circ$, $7.11^\circ/-119.97^\circ$, and $7.11^\circ/119.98^\circ$, respectively. The measured fundamental three-phase reactive power (data floating point 14) and real power (data floating point 15) were 0.095 MVAR and 1.922 MW, respectively, and the measured three-phase displacement power factor (data floating point 16) was 0.998 at a date/time (data floating point 18) of November 3, 2021/15:28:14.503599941 UTC.

9.4.2 IEC 61850 for the SEL-735 power meters

In the electrical substation-grid test bed, the SEL-735 power meters were set with the IEC 61850 protocol. Then, the GOOSE messages from the devices were transmitted. The steps to see the GOOSE Dataset that were transmitted from the SEL-735 power meters was given by the CID file that was downloaded at the devices. Figure 72 shows the steps to observe the GOOSE Dataset that was downloaded at SEL-735 power meters based on the project created with the AcSELeator Architect software.

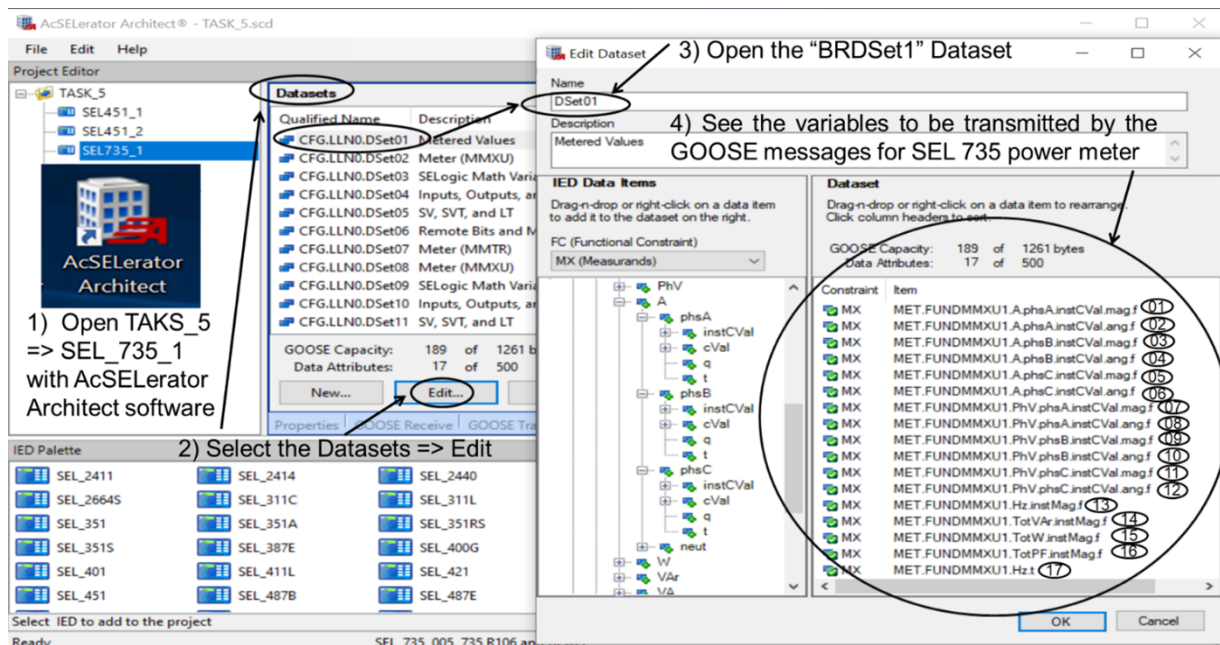


Figure 72. GOOSE Dataset of SEL-735 power meters generated with the AcSELeator Architect software.

As shown in Figure 72, the items of the GOOSE Dataset for the SEL-735 power meters were numbered from 01 to 17. These items were evaluated by running a simulation test with the real-time simulator and collecting the IEC 61850 messages from the SEL-735 power meters using the Wireshark software. Figure 73 shows the steps to observe the GOOSE message for the SEL-735 power meters, which had been recording the traffic from the device with Wireshark software. Frame 3428 for the Data_Nov22 file was selected. Then, the View menu and Expand All option were selected, identifying the 17 data floating points (Figure 73) that corresponded to the 17 items of the GOOSE Dataset (Figure 72).

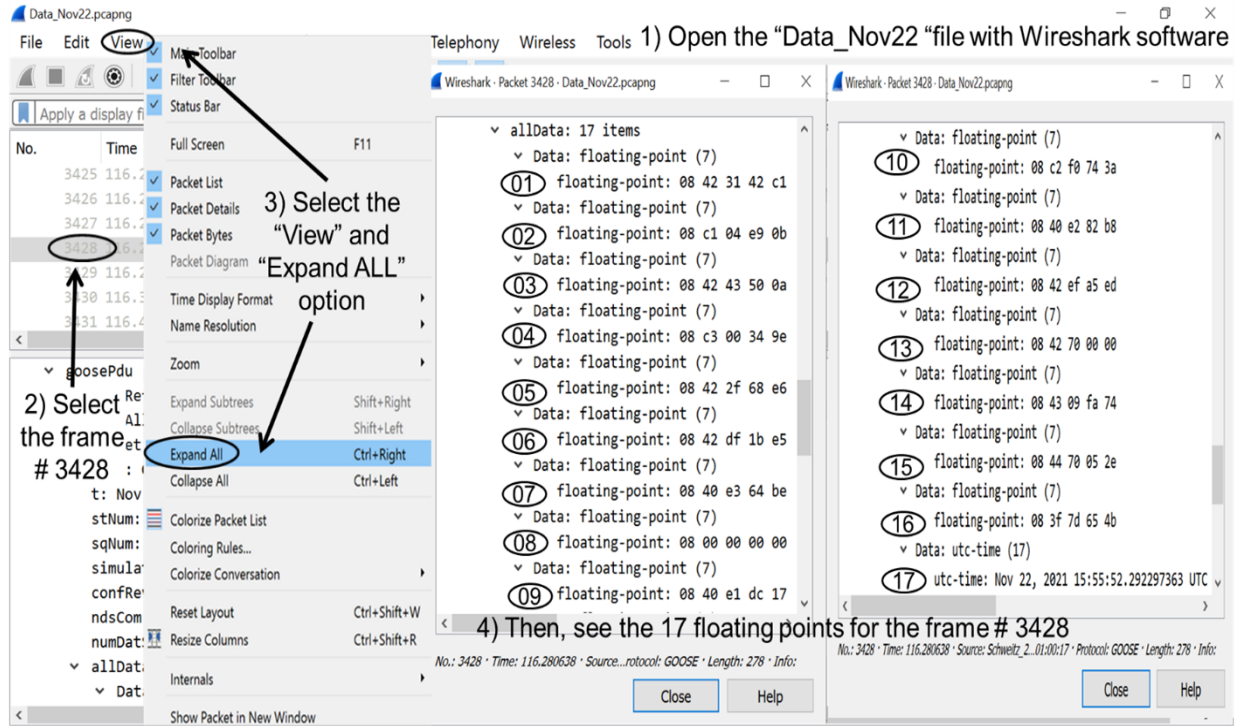


Figure 73. GOOSE message of SEL-735 power meters collected with Wireshark software.

The data floating points from 01 to 16 were represented by hexadecimal numbers. The last 8 numbers from the data floating points were converted from hexadecimal to decimal numbers using an IEEE-754 floating-point converter (<https://babbage.cs.qc.cuny.edu/ieee-754.old/32bit.html>), to obtain the measured values simulated during the simulation tests.

The data floating points of GOOSE messages for the SEL-735 power meters from Frame 3428 of the Data_Nov22 file captured with Wireshark software are shown in Table A.2. The GOOSE Dataset from the CID file, item descriptions from the SEL-735 power meter manual [5], and measured data floating points from the GOOSE messages are described in Table A.2. The simulation test was based on a three-phase balanced power system of 7.2 kV, with A, B, and C phase currents of 45 A. The evaluation of GOOSE data floating points was based on converting the hexadecimal to decimal values, observing the GOOSE data floating points represented the simulated three-phase balanced power system. Based on Table A.2, the data floating points from the SEL-735 power meter represented a balanced power system with a measured power system frequency of 60.00 Hz (data floating point 13). The measured magnitude/angle for A (data floating point 01/02), B (data floating point 03/04), and C (data floating point 05/06) phase primary currents were $44.31^\circ/-8.30^\circ$, $48.82^\circ/-128.20^\circ$, and $43.85^\circ/111.55^\circ$, respectively. The measured magnitude/angle for A (data floating point 07/08), B (data floating point 09/10), and C (data floating point 11/12) phase to neutral primary voltages were $7.10^\circ/-0.00^\circ$, $7.05^\circ/-120.22^\circ$, and $7.07^\circ/119.82^\circ$, respectively. The measured fundamental three-phase reactive power

(data floating point 14) and real power (data floating point 15) were 137.97 kVAR and 960.08 kW, respectively, and the measured three-phase displacement power factor (data floating point 16) was 0.9898 at a date/time (data floating point 17) of November 22, 2021/15:55:52.292297363 UTC.

9.4.3 DNP for the SEL-734 power meters

In the electrical substation-grid test bed, the SEL-734 power meters were set with the DNP communication. The SEL-734 power meters were connected to a SEL-3530-4 RTAC that polled the DNP map points transmitted by the SEL-734 power meters. To collect the DNP messages from the SEL-734 power meters, a computer with the AcSELeRator RTAC software and Wireshark software was used. Then, the SEL-3530-4 RTAC was connected to the computer, and the DNP messages from the SEL-734 power meters were collected through the SEL-3530-4 RTAC. Figure 74A shows the steps to log in to the SEL-3530-4 RTAC, and Figure 74B shows the steps to capture the SEL-734 power meter messages. The Go Online option was selected, and the User Name and Password were set to log in at the SEL-3530-4 RTAC. The Comm Monitor option was selected, and then the Live-Ethernet and Tunneled Serial Devices option from the Capture Source menu was selected (Figure 74A). Next, the Start tab was selected to capture the traffic from the devices (Figure 74B), and the Open Capture in Wireshark option was selected to save the DNP messages from the SEL-734 power meters.

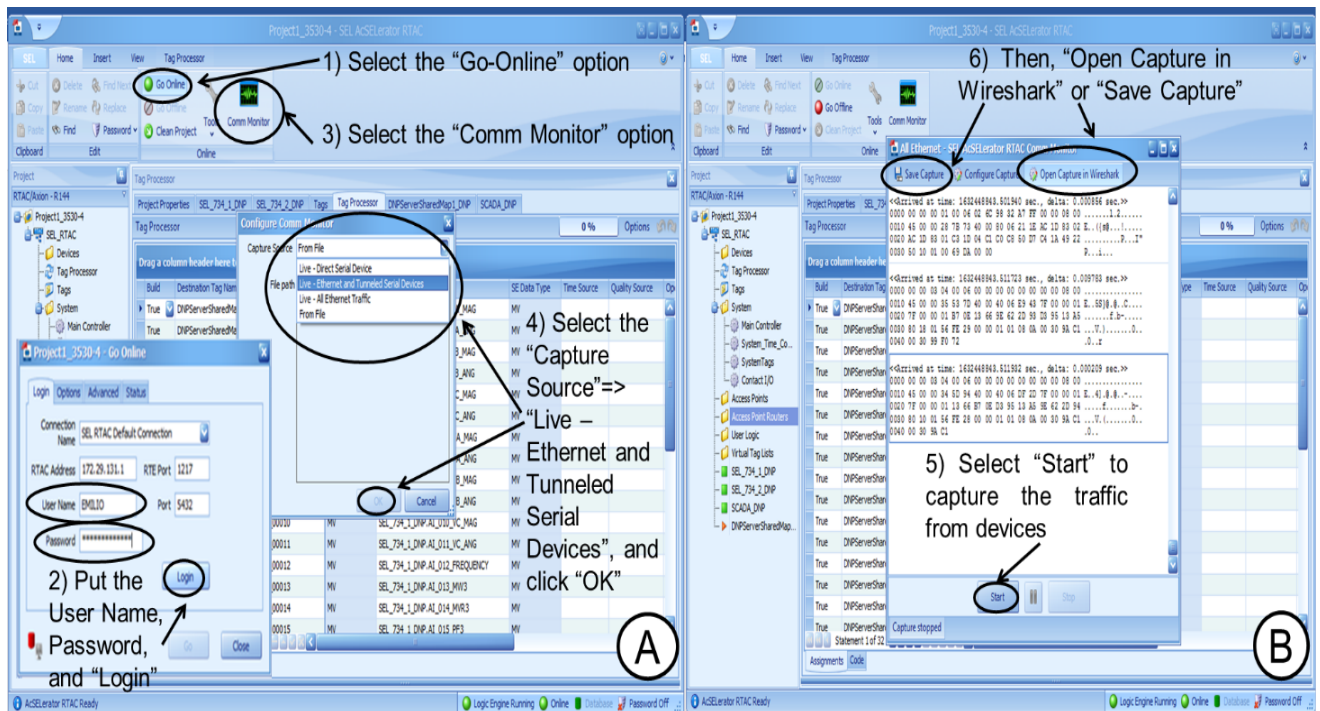


Figure 74. Steps to log in with the SEL-3530-4 RTAC (A) and capture SEL-734 power meter messages (B).

The DNP points for the SEL-734 power meters were numbered from 01 to 16 (Figure 75). These DNP points were evaluated by running a simulation test with the real-time simulator and collecting the DNP messages from the SEL-734 power meters connected to the SEL-3530-4 RTAC.

Figure 75 shows the steps to display the DNP messages for the SEL-734 power meter. These had been captured from the device with the AcSELeRator RTAC software. Frame 43 for the RTAC_WITH_SEL_734_POWER_METERS file was selected. Then, the View menu and Expand All options were selected, identifying the 16 DNP points (Figure 75) that corresponded to the 16 analog

inputs of the DNP map set on the target processor for the SEL-3530-4 RTAC, and for the SEL-734 power meter (Table A.3).

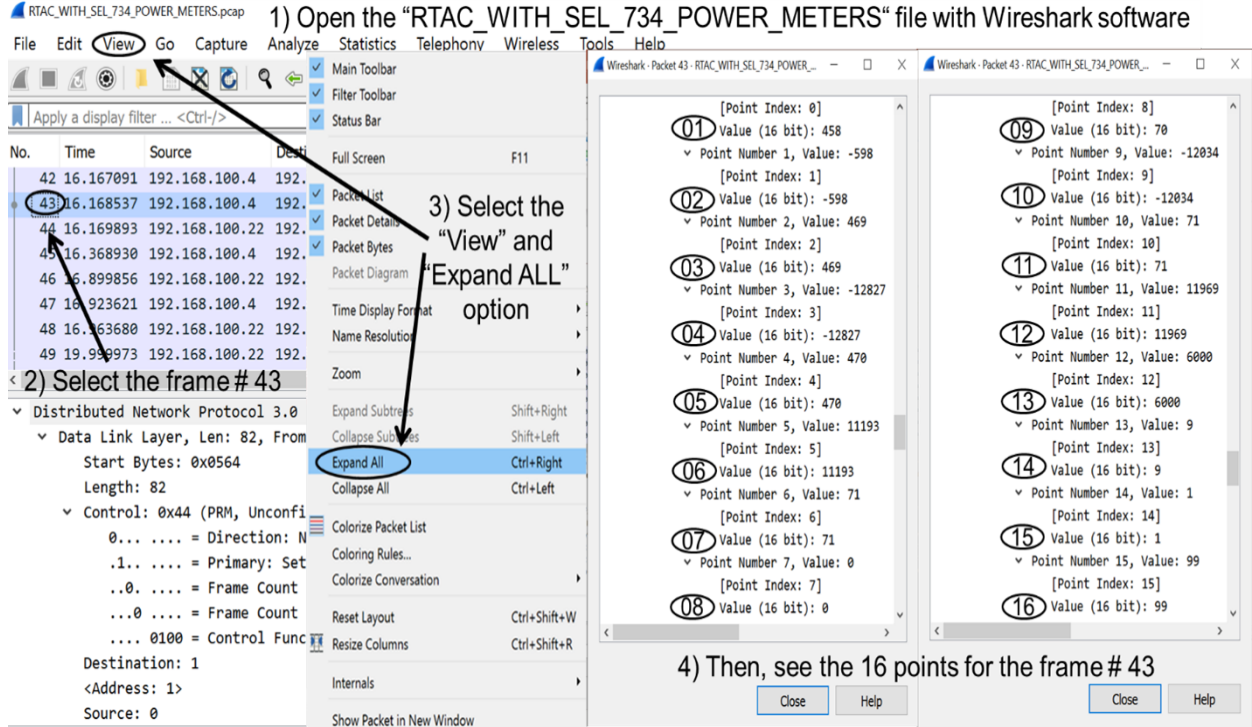


Figure 75. DNP message of SEL-734 power meter collected with Wireshark software.

The data floating points of DNP messages for the SEL-734 power meters from Frame 43 of the RTAC_WITH_SEL_734_POWER_METERS file captured with the AcSElerator RTAC and Wireshark software are shown in Table A.3. The measured data floating points from the DNP messages were multiplied by a factor to obtain the real measured values at the electrical substation-grid test bed. The real measured value (M_V) is calculated by Eq. (11),

$$M_V = F \times DP_V, \quad (11)$$

where M_V is the measured real value, DP_V is the measured data floating point value, and F is the factor to convert the measured data floating point value into the measured real value. The units for the measured real values are shown in the last column of Table A.3.

In the electrical substation-grid test bed, the simulation was based on a three-phase balanced power system of 7.2 kV, with A, B, and C phase currents of 45 A. Based on Table A.3, the measured real values from the SEL-734 power meter have shown a balanced power system of 60.00 Hz (data floating point 13) given by A (data floating points 01/02), B (data floating points 03/04), and C (data floating points 05/06) phase currents of $45.8^\circ/-5.98^\circ$, $46.9^\circ/-128.27^\circ$, and $47.0^\circ/111.93^\circ$, respectively, and A (data floating points 07/08), B (data floating points 09/10), and C (data floating points 11/12) phase to neutral voltages of $7.1^\circ/0.00^\circ$, $7.0^\circ/-120.34^\circ$, and $7.1^\circ/119.69^\circ$, respectively. The measured fundamental three-phase reactive power (data floating point 14) and real power (data floating point 15) were 100 kVAR and 900 kW, respectively, and the measured three-phase displacement power factor (data floating point 14) was 0.99.

9.5 RESULTS OF ELECTRICAL FAULT TESTS

9.5.1 Electrical fault test events

The assessment of electrical fault test events was based on comparing the measured and calculated relay times for the SEL-451 protective relays. In the electrical substation-grid test bed, both SEL-451 protective relays were connected to similar radial power lines and power load feeders. Therefore, the evaluation was performed for one device, simulating the AG, AB, ABG, and ABC (or ABCG) electrical faults. These types of electrical faults were set on the fault block (Figure 5D) that was triggered by the fault signals block (Figure 5C) at 5 s. The electrical fault tests were simulated for 10 s and triggering the electrical fault at 5 s. After each electrical fault test was run, the COMTRADE events from the SEL-451 relay, and MATLAB simulation events from the host computer, were collected to compare the calculated and measured relay time at electrical fault tests. The calculated relay time (T_R) was estimated by Eq. (12) that depends on Eq. (4), and from placing the time dial setting at 2 s, CTR at 80, and relay current pickup at 5 A (from the SEL-451 protective relay setting). The simulated maximum primary electrical fault currents (I) were collected from Table 4.

$$T_R = 2 \times \left(0.0963 + \frac{3.88}{(I/80/5)^2 - 1} \right) \times 60 . \quad (12)$$

The measured relay time was obtained from the relay events collected at the electrical fault tests. The COMTRADE events for the AG, AB, ABG, and ABC (or ABCG) electrical faults were collected from the SEL-451 relays, and the trip signals and phase primary currents were plotted. Then, the measured relay time from the relay event was calculated by Eq. (13).

$$T_{Rm} = T_{TRIPm} - T_{Ifm} , \quad (13)$$

where T_{Rm} is the measured relay time in cycles, T_{TRIPm} is the measured relay trip time in cycles, and T_{Ifm} is the measured initial electrical fault state time in cycles.

The electrical fault tests were assessed by calculating the percent relay time error for all electrical fault tests. The percent relay time error was calculated by collecting the calculated and measured relay time in cycles, and by using Eq. (14).

$$E_{\%RT} = \left(\frac{T_{Rm} - T_R}{T_R} \right) \times 100 , \quad (14)$$

where $E_{\%RT}$ is the percent relay time error, T_R is the calculated relay time in cycles, and T_{Rm} is the measured relay time cycles.

Table 20 describes the results of the assessment for the electrical fault tests at the electrical substation-grid test bed, comparing the calculated relay time vs. measured relay time for the SEL-451 protective relay at the AG, AB, ABG, and ABC (or ABCG) electrical faults, located at the SEL-734 power meter site (Figure 5). The percent error range for the relay time at electrical fault tests was +6.08% to -0.45%.

In Table 20, the calculated relay time (T_R) was estimated by Eq. (12), and the measured relay time values for electrical fault tests were calculated by collecting the measured relay trip time (T_{TRIPm}) and measured initial fault state time (T_{Ifm}) from the relay events and using Eq. (13). Figure 76, Figure 77, Figure 78, and Figure 79 show the relay events for the SEL-734_AG-FAULT, SEL-734_AB-FAULT, SEL-734_ABG-FAULT, and SEL-734_ABC-FAULT tests, respectively. The phase primary currents and digital signals were plotted there.

Table 20. Comparison of calculated relay time vs. measured relay time for the SEL-451 relay

Test name (fault location – type of fault)	Fault type	Maximum primary RMS electrical fault current, from Table 4 I (A)	Calculated relay time T_R (cycles) Eq. (12)	SEL-451 relay events			Percent relay time error (%) Eq. (14)
				Measured maximum primary RMS electrical fault current (A)	Measured relay time T_{Rm} (cycles)	Figure	
SEL-734_AG-FAULT	SLG	751	195.95	755	195.71	Figure 76	-0.12
SEL-734_AB-FAULT	LL	1,005	99.20	1,028	105.23	Figure 77	6.08
SEL-734_ABG-FAULT	LLG	1,080	85.58	1,081	85.19	Figure 78	-0.45
SEL-734_ABC-FAULT (SEL-734_ABCG- FAULT)	3L (3LG)	1,134	77.72	1,136	77.17	Figure 79	-0.71

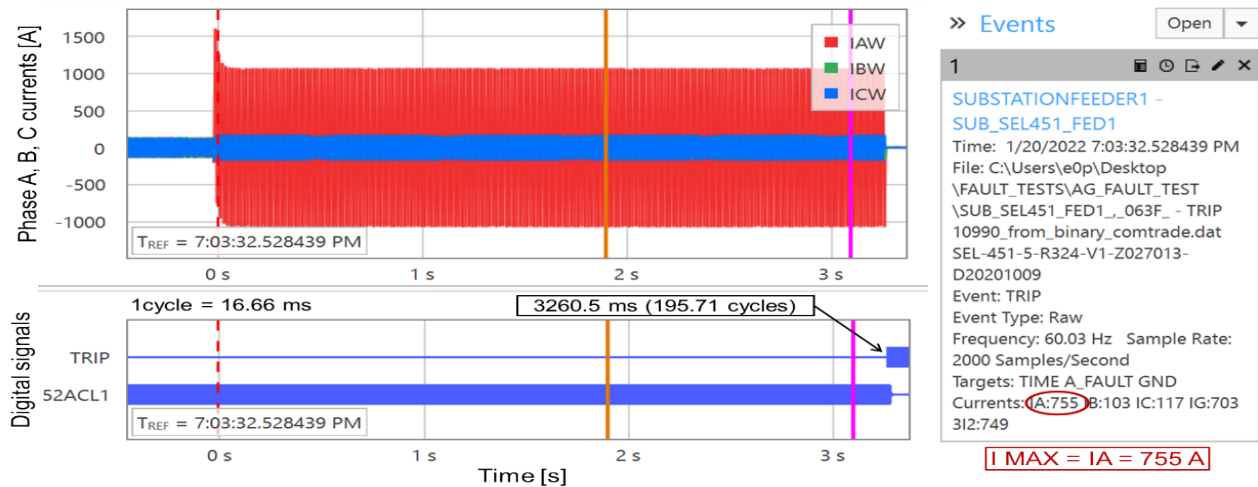


Figure 76. SEL-451 protective relay event for the SEL-734_AG-FAULT test.

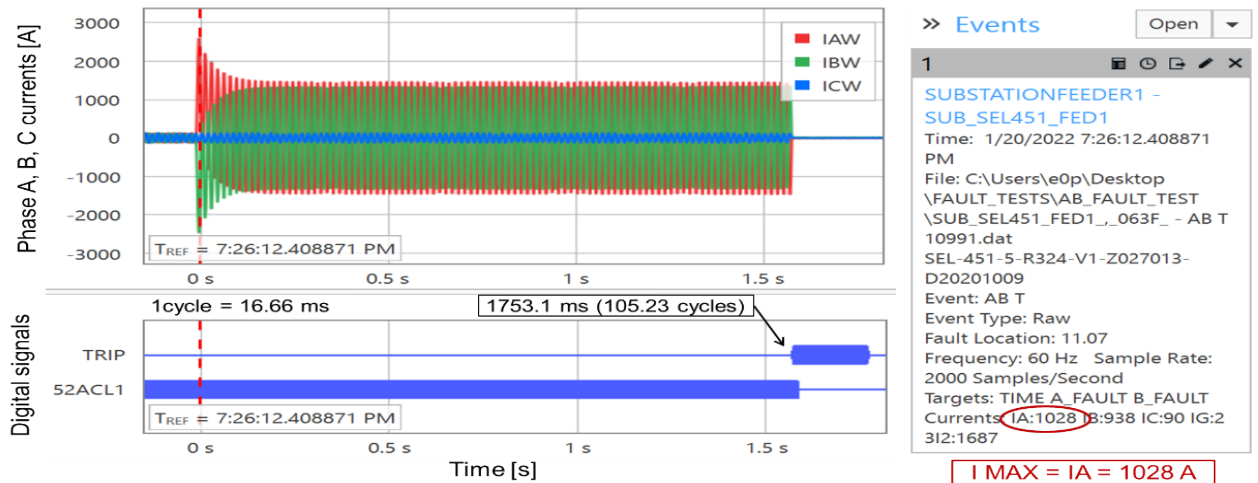


Figure 77. SEL-451 protective relay event for the SEL-734_AB-FAULT test.

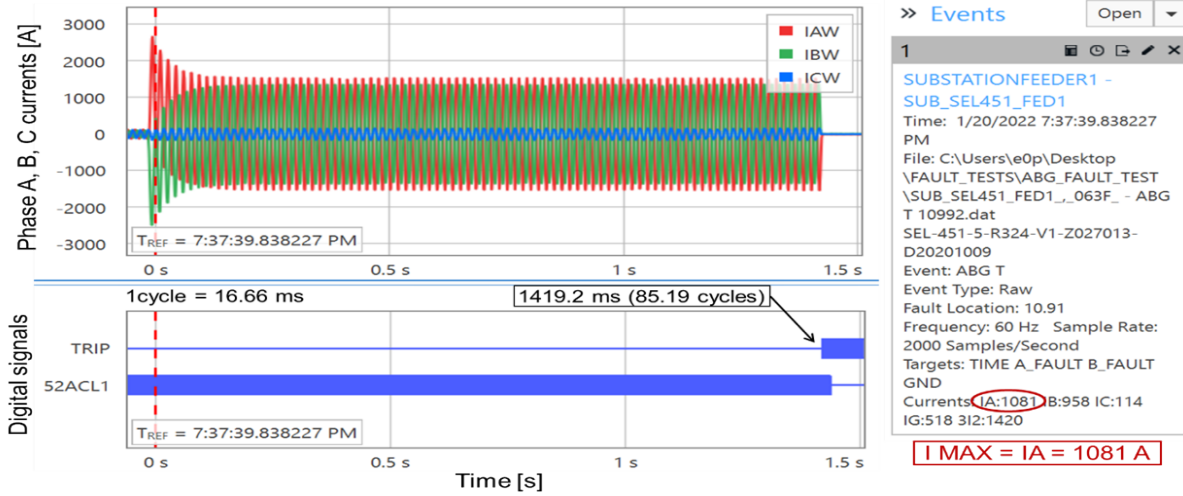


Figure 78. SEL-451 protective relay event for the SEL-734_ABG-FAULT test.

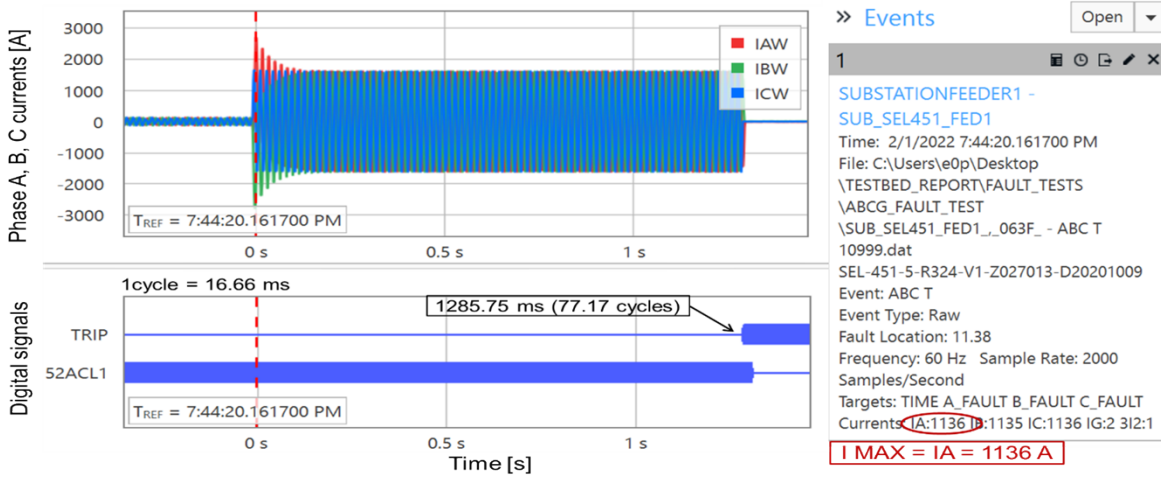



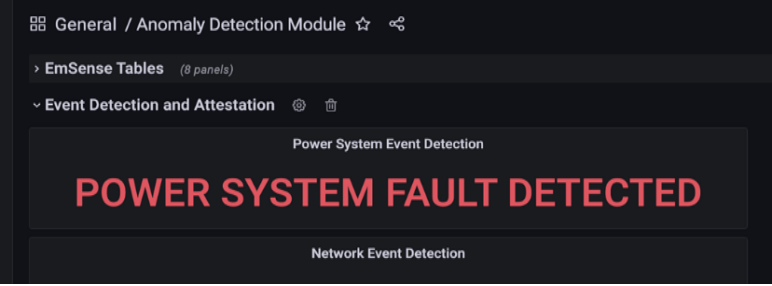
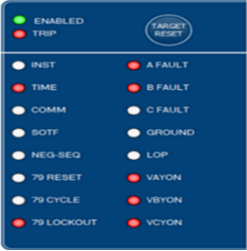


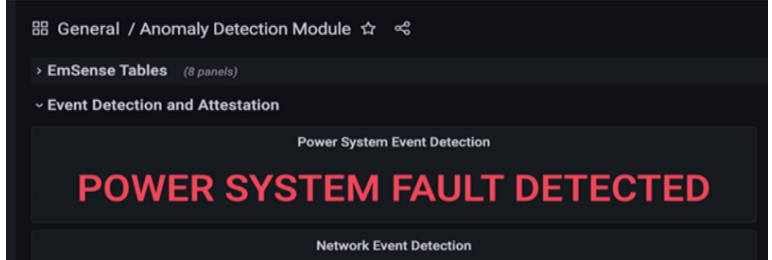

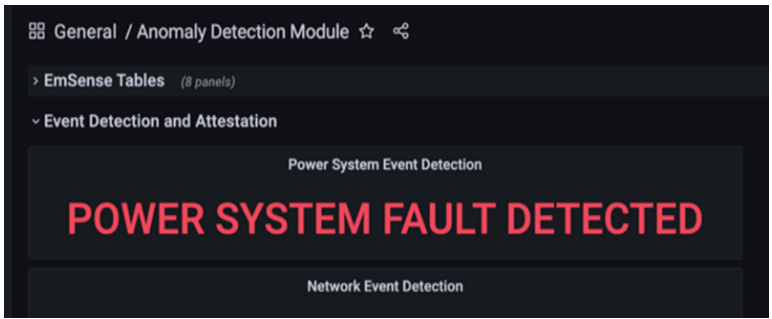
Figure 79. SEL-451 protective relay event for the SEL-734_ABC-FAULT test.

9.5.2 Electrical fault event detection with DLT

The assessment of the electrical fault event detection with DLT was based on using an algorithm to identify the power system fault events at the electrical substation-grid test bed. For the anomaly detection concerning electrical faults, the DLT framework uses the following process. First, the observer in the framework receives the IEC 61850 packets coming from devices in the network and determines if they are SV messages or GOOSE messages. If the observer encounters SV packets that contain raw current and voltage data, which is typically sinusoidal in nature, the observer calculates the RMS value. RMS is a more compact format for storage and contains only the essential information. If the observer encounters GOOSE messages that contain current and voltage data, then these data already use RMS values. The resulting RMS values are stored into databases. Also, the anomaly detection unit processes the databases and performs a threshold check on certain current data. If the data exceed a given threshold, then the electrical fault alarm is triggered. By using the algorithm to identify the power system electrical fault events at the electrical substation-grid test bed, the SLG, LL, LLG, and 3L (or 3LG) electrical fault tests were run at the test bed. The electrical faults were set on the fault block (Figure 5D) that was triggered by the fault signals block (Figure 5C) at 5 s. The electrical fault tests were simulated for 10 s and triggering the electrical fault at 5 s. After each electrical fault test was run, the COMTRADE events and HMI

screenshot from the SEL-451 relay that tripped were collected from the HMI computer, and the screenshots of the DLT-SCADA computer detecting the power system fault events were collected. The electrical fault detection results from the SEL-451 relay and the DLT system were compared to evaluate the electrical fault event detection with the DLT at the electrical substation-grid test bed. The results of the assessment of the electrical fault event detection with the DLT-SCADA computer and SEL-451 relay light indicators from the HMI are described in Table 21. The results collected from the SEL-451 relay and the DLT computer were compared. The power system fault events were detected satisfactorily for the SEL-734_AG-FAULT, SEL-734_AB-FAULT, SEL-734_ABG-FAULT, and SEL-734_ABC-FAULT tests. The SEL-451 relay light indicators from the HMI that were collected with the AcSELeator Quickset software are shown in the left column of Table 21. These light indicators presented the type of electrical faults that were detected by the SEL-451 relay for the A phase to ground electrical fault, A-B phase electrical fault, A-B phase to ground electrical fault, and A-B-C phase electrical fault tests.

Table 21. Assessment of electrical fault event detection with the relay HMI and DLT computer

Test	SEL-451 relay front side	DLT computer screenshot
SEL-734_AG-FAULT		
SEL-734_AB-FAULT		
SEL-734_ABG-FAULT		
SEL-734_ABC-FAULT		

10. DISCUSSION AND CONCLUSIONS

In this section, the discussion and conclusions of test results for the electrical substation-grid test bed with inside/outside substation devices and DLT communication are presented. The percent errors of the measured phase primary currents and phase to neutral primary voltages for the protective relays and power meters at the electrical substation-grid test bed are discussed. The three-phase phasor diagrams of the measured phase primary currents and phase to neutral primary voltages for the protective relays and power meters are plotted with the data collected from the IEC 61850 and DNP messages, verifying the simulated three-phase balance power system generated by the real-time simulator. The relay time percent error values with the results from the electrical fault detection with DLT and protective relay HMIs are presented. Finally, the conclusions and future work for the electrical substation-grid test bed are presented.

10.1 ELECTRICAL SUBSTATION-GRID TEST BED DISCUSSIONS

The assessment of the electrical substation-grid test bed with inside and outside substation devices (using DLT and a synchronized time system) was performed for the analog signals, date/time and synchronized sources, GOOSE and DNP messages, and electrical fault tests with DLT results. These results were collected and analyzed to evaluate the design of the electrical substation-grid test bed with inside/outside devices and DLT.

In the assessment of the analog signals for the inside and outside substation devices, the measured and simulated phase to ground primary voltages and phase primary currents for the SEL-451 protective relays and SEL-734 and SEL-735 power meters were compared. The percent errors for the A, B, and C phase to neutral primary voltages were calculated with Eq. (10) and plotted in Figure 80A. The percent errors for the A, B, and C phase primary currents were calculated with Eq. (9) and plotted in Figure 80B. The percent errors of the phase to neutral primary voltages and phase primary currents for the protective relays were smaller than for the power meters, comparing Figure 80A and B. This could be because the protective relays need to have a better accuracy than the power meters, and protective relays are used for protection and monitoring, whereas power meters are only used for monitoring.

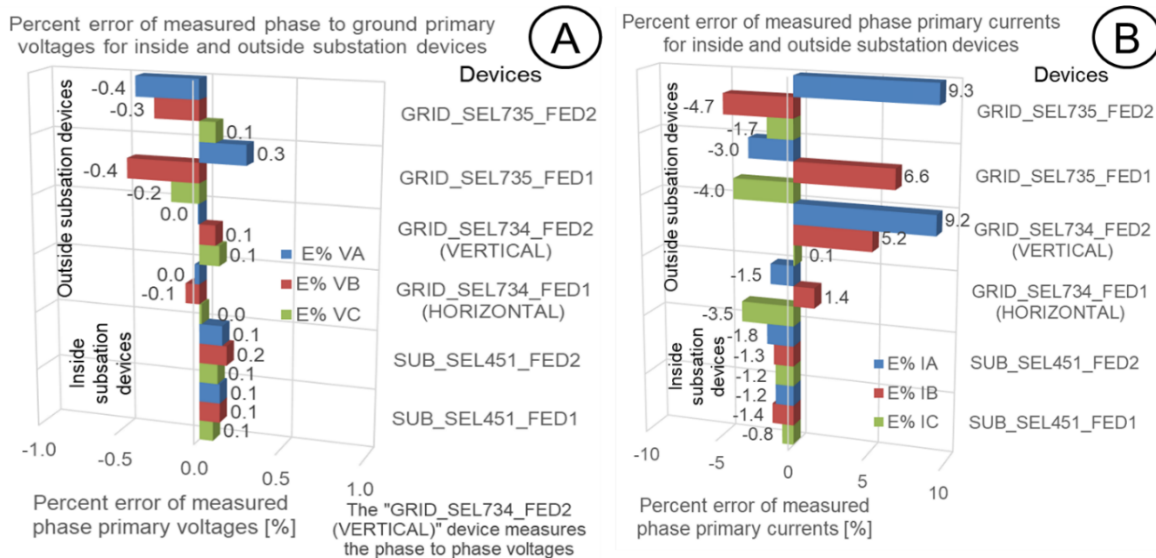


Figure 80. Percent error of measured voltages (A) and currents (B) for inside and outside substation devices at the electrical substation-grid test bed.

The measurements at the electrical substations may provide vital information supporting decisions on service needs and grid control. Although the requirements for the electrical substation measurements on delivered power are rather strict, the precision related to generalized monitoring is less so. Often, an error margin of up to 5% on the absolute measurements is acceptable [36]. The percent error of the measured phase to ground primary voltages for the protective relays and power meters showed good performance (Figure 80A). In addition, the percent error of the measured phase primary currents for the protective relays also showed good performance (Figure 80B).

However, the percent error of the measured A/B phase primary currents for some power meters, such as the GRID_SEL735_FED2, GRID_SEL735_FED1, and GRID_SEL_734_FED2 (VERTICAL) devices, indicated an error margin greater than 5% (Figure 80B). Because the power meters are outside substation devices and are used for metering applications instead of protection applications (fuses are set at the power meter locations), then this error could be accepted for the electrical substation-grid test bed, or the error could be reduced by adjusting the current gains (A/B phase currents) of the interface circuits for the electrical substation-grid power system in the MATLAB/Simulink model (Figure 7A, B).

In the assessment of date/time and synchronized sources for inside and outside substation devices, the date/time and sources were measured at the device displays. IRIG-B is the most common synchronized time protocol because not all protective relays and power meters could have an enabled Ethernet port with the PTP. The IRIG-B communication was set at the protective relays and power meters, whereas the PTP was set at the DLT system at the electrical substation-grid test bed.

In the assessment of the GOOSE and DNP messages for the protective relays and power meters, Wireshark software was used to collect the messages from the devices, and collect the magnitudes and angles of the A, B, and C phase primary currents and A, B, and C phase to neutral primary voltages. Then, from Table A.1, Table A.2, and Table A.3, the three-phasor diagrams for the phase primary currents and phase to neutral primary voltages were plotted to observe the simulated three-phase balanced power system that was created by the real-time simulator, and to check that the wiring connection for the positive and neutral connectors of the inside and outside substation devices was made correctly. The phasor diagrams for the phase primary currents and phase to neutral primary voltages for the SEL-451 relays and SEL-734 and SEL-735 power meters are shown in Figure 81, verifying the measured phase balanced power system from the GOOSE and DNP messages at the electrical substation-grid test bed.

In the assessment of the electrical fault tests with the DLT at the electrical substation-grid test bed, the AG, AB, ABG, and ABC (or ABCG) electrical fault tests were simulated. The simulated electrical fault tests at the electrical substation-grid test bed were evaluated with the SEL-451 relay HMI (Figure 82A) versus the DLT-SCADA computer using the DLT algorithm to detect the power system electrical fault events, and the electrical fault events from the DLT-SCADA computer (Figure 82B) were assessed. The percent relay time error for the SEL-451 relays (Table 20) was plotted in Figure 82C to evaluate the SEL-451 relay at electrical fault tests.

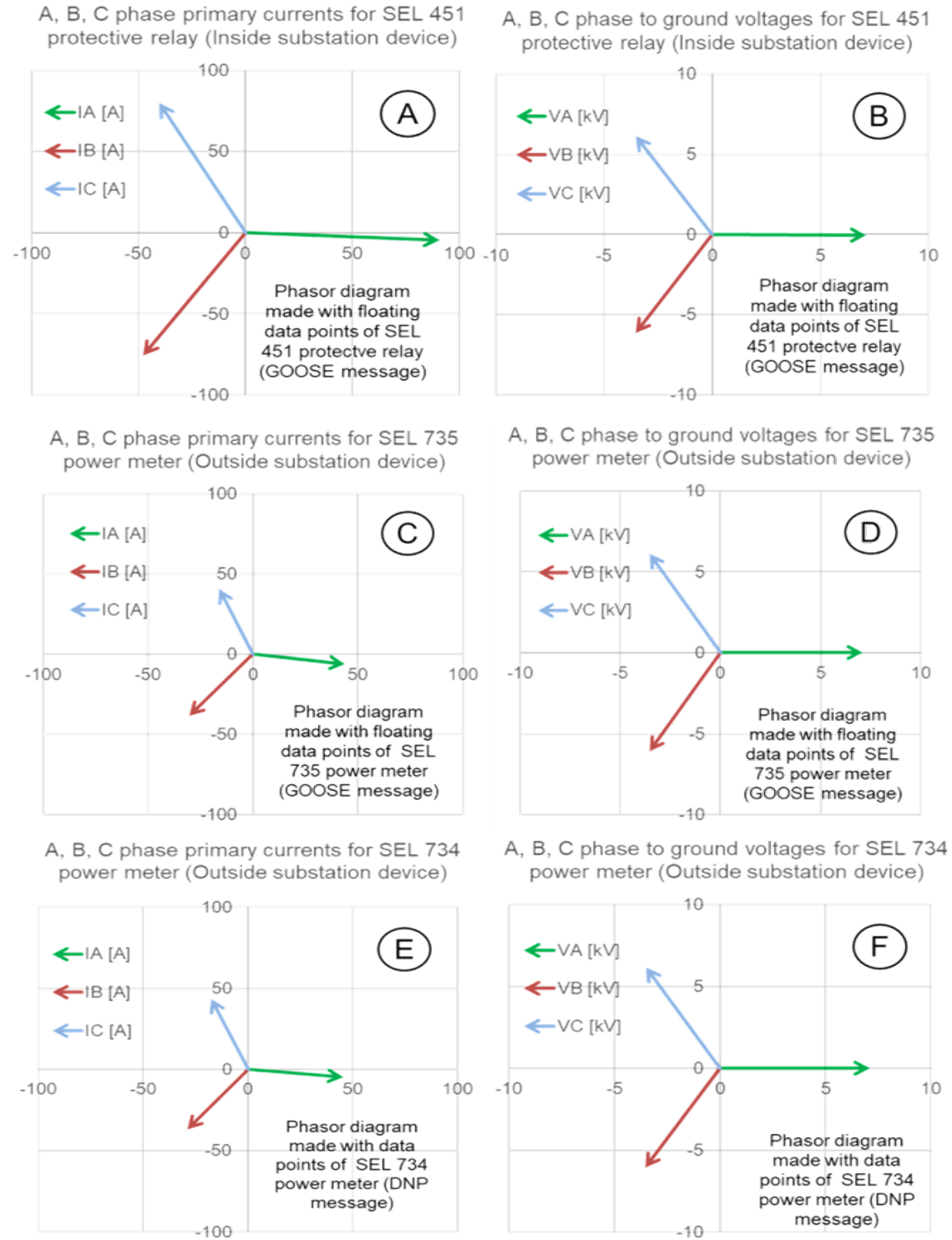


Figure 81. Phasor diagrams of measured currents and voltages for the SEL-451 protective relays (A, B), SEL-735 power meters (C, D) and SEL-734 power meters (E, F) from GOOSE and DNP messages at the electrical substation-grid test bed.

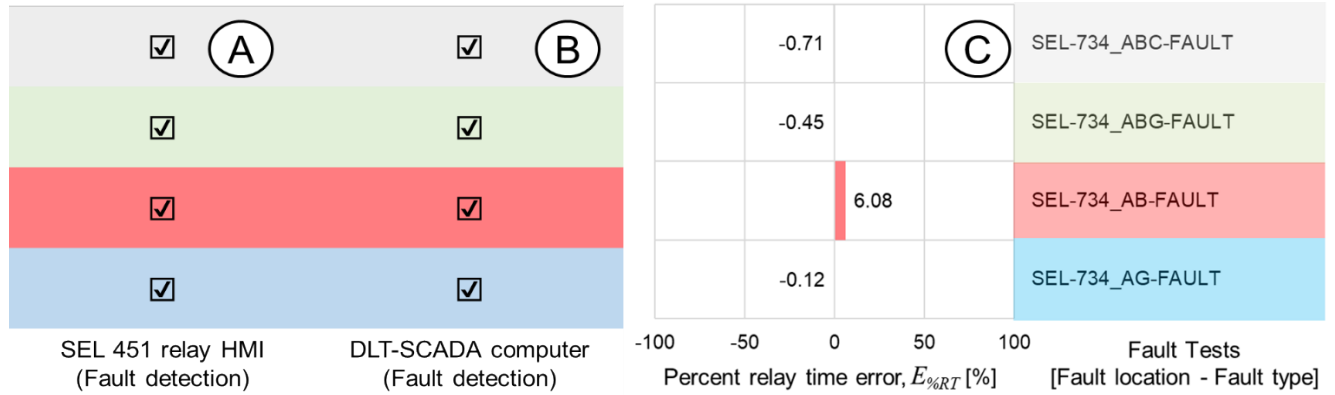


Figure 82. Electrical fault detection of SEL-451 relay (A) vs. DLT (B) and relay time percent error (C).

10.2 CONCLUSIONS

In this study, the electrical substation-grid test bed with protective relays and power meters using DLT communication was satisfactorily integrated with GOOSE messages. The assessments of the electrical substation-grid test bed with inside and outside substation devices using DLT and a synchronized time system were performed for the analog signals, date/time and synchronized sources, GOOSE and DNP messages, and electrical fault tests with DLT results.

- In the assessment of the analog signals, the measured and simulated magnitudes for the phase to neutral primary voltages and phase primary currents for the SEL-451 protective relays and SEL-734 and SEL-735 power meters were compared. Although the requirements for the electrical substation measurements on delivered power are rather strict, the precision related to generalized monitoring is less so. Often, an error margin of up to 5% on the absolute measurements is acceptable [36]. The measured primary voltages of the protective relays and power meters had absolute percent errors up to 0.2% and 0.4%, respectively. The measured phase primary currents of the protective relays had an absolute percent error up to 1.8%. However, for the A/B phase primary currents of some power meters had an absolute percent error up to 9.2%, which could be reduced by adjusting the current gains (A/B phase currents) of the interface circuits for the electrical substation-grid power system in the MATLAB/Simulink model (Figure 7A, B).
- In the assessment of date/time and synchronized sources for inside and outside substation devices, the date/time and sources were measured at the device displays. IRIG-B is the most common synchronized time protocol because not all protective relays and power meters could have an enabled Ethernet port with PTP. The IRIG-B communication was set at the protective relays and power meters, whereas the PTP was set at the DLT system at the electrical substation-grid test bed.
- In the assessment of the GOOSE and DNP messages for the protective relays and power meters, the collected magnitudes and angles of the A, B, and C phase primary currents and A, B, and C phase to neutral primary voltages had shown three-phasing diagrams to observe the simulated three-phase balanced power system that was created by the real-time simulator, and to check that the wiring connection for the positive and neutral connectors of the inside and outside substation devices was made correctly.
- In the assessment of the electrical fault tests with the DLT at the electrical substation-grid test bed, the AG, AB, ABG, and ABC (or ABCG) electrical fault tests were simulated, and the SEL-451 relay tripped by clearing the electrical faults. The calculated and measured relay time values were

compared with relay time percent errors for the electrical fault tests, demonstrating good performance of the protection system. The electrical faults at the electrical substation-grid test bed were detected with the DLT-SCADA computer that had a DLT algorithm to detect the electrical fault events.

In future work for the electrical substation-grid test bed with inside/outside substation devices and DLT with a synchronized time source from DarkNet, studies will be performed to determine the effect of potential cyber events on inside/outside substation devices using advanced algorithms for detecting potential cyber events produced by unwanted protective relay settings to improve the detection and reliability of protection, control, and communication systems at electrical substations and power grids.

11. REFERENCES

- [1] Edvard, C., Six common bus configurations in substations up to 354 kV, Power Substation/Transmission and Distribution, March 18, 2019. Electrical Engineering Portal. Available online: <https://electrical-engineering-portal.com/bus-configurations-substations-345-kv> Accessed: December 18, 2021.
- [2] Piesciorovsky, E. C., and Schulz, N. N., Comparison of Programmable Logic and Setting Group Methods for adaptive overcurrent protection in microgrids, *Electric Power Systems Research* 151, 273–282, 2017. <https://doi.org/10.1016/j.epsr.2017.05.035>.
- [3] Piesciorovsky, E. C., and Schulz, N. N., Fuse relay adaptive overcurrent protection scheme for microgrid with distributed generators, *IET Generation, Transmission, & Distribution* 11, 540–549, 2017. <https://doi.org/10.1049/iet-gtd.2016.1144>.
- [4] SEL-451-5 Protection, Automation, and Bay Control System and SEL-400 Series Relays Instruction Manual, Schweitzer Engineering Laboratories Inc. Available online: <https://selinc.com/products/451/docs/>. Accessed: December 18, 2021.
- [5] SEL-735 Power Quality and Revenue Meter Instruction Manual, Schweitzer Engineering Laboratories Inc. Available online: <https://selinc.com/products/735/docs/>. Accessed: December 18, 2021.
- [6] SEL-734 Advanced Metering System Instruction Manual, Schweitzer Engineering Laboratories Inc. Available online: <https://selinc.com/products/734/docs/>. Accessed: December 18, 2021.
- [7] SEL-3530 Real-Time Automation Controller (RTAC) Instruction Manual, Schweitzer Engineering Laboratories Inc. Available online: <https://selinc.com/products/3530/docs/>. Accessed: December 18, 2021.
- [8] Total Clearing Time-Current Characteristic Curves, Positrol® Fuse Links–S&C “T” Speed (TCC 170-6-2). Available online: <https://www.sandc.com/en/products--services/products/positrol-fuse-links/#Construction>. Accessed December 18, 2021.
- [9] Piesciorovsky, E. C., and Schulz, N. N., Comparison of non-real-time and real-time simulators with relays in-the-loop for adaptive overcurrent protection, *Electric Power Systems Research* 143, 657–668, 2017. <https://doi.org/10.1016/j.epsr.2016.10.049>.
- [10] Fuseology. Littelfuse POWR-GARDTM. 2005. Available online: https://stevenengineering.com/tech_support/PDFs/28FUSE.pdf. Accessed: December 18, 2021.
- [11] IEEE Std. C37.112-1996: IEEE Standard Inverse-Time Characteristic Equations for Overcurrent Relays. 1996:1-19.
- [12] TCC Number 170-6-2 (Excel), Positrol Fuse Links, S&C “T” Speed, Total Clearing. Available online: <https://www.sandc.com/en/contact-us/time-current-characteristic-curves/>. Accessed: December 18, 2021.
- [13] IEEE Std. 242-2001: IEEE Recommended Practice for Protection and Coordination of Industrial and Commercial Power Systems. 2001.
- [14] SEL-2488 Satellite-Synchronized Network Clock Instruction Manual, Schweitzer Engineering Laboratories Inc. Available online: <https://selinc.com/products/2488/docs/>. Accessed: December 18, 2021.
- [15] IEEE 1588-2019. IEEE Standard for a Precision Clock Synchronization Protocol for Networked Measurement and Control Systems.

- [16] DNP3 protocol and IEC 61850, Copadata. Available online: <https://www.copadata.com/en/industries/energy-infrastructure/energy-insights/dnp3-distributed-network-protocol/>. Accessed: December 18, 2021.
- [17] Atienza, E., Testing and Troubleshooting IEC 61850 GOOSE-Based Control and Protection Schemes, *12th Annual Western Power Delivery Automation Conference*, Spokane, Washington, April 13–15, 2010.
- [18] El Ioini, N., and Pahl, C., A Review of Distributed Ledger Technologies. In: Panetto, H., Debruyne, C., Proper, H., Ardagna, C., Roman, D., and Meersman, R. (eds.), *On the Move to Meaningful Internet Systems*. OTM 2018 Conferences. 2018. Lecture Notes in Computer Science, 11230. Springer, Cham. https://doi.org/10.1007/978-3-030-02671-4_16.
- [19] Hyperleger Fabric, Ledgers, Facts, and States. Available online: <https://hyperledger-fabric.readthedocs.io/en/release-2.2/ledger/ledger.html#ledgers-facts-and-states>. Accessed: December 18, 2021.
- [20] Hyperledger Fabric, hyperledger/fabric, GitHub. Available online: <https://github.com/hyperledger/fabric>. Accessed: December 18, 2021.
- [21] Hyperledger Fabric, Ledger Features. Available online: https://hyperledger-fabric.readthedocs.io/en/release-2.2/fabric_model.html#ledger-features. Accessed: December 18, 2021.
- [22] Hyperleger Fabric, The Ordering Service. Available online: https://hyperledger-fabric.readthedocs.io/en/release-2.2/orderer/ordering_service.html. Accessed: December 18, 2021.
- [23] Hyperleger Fabric, Smart Contracts. Available online: <https://hyperledger-fabric.readthedocs.io/en/release-2.2/whatis.html#smart-contracts>. Accessed: December 18, 2021.
- [24] Schweitzer Engineering Laboratories, RTAC SEL-3555 Real-Time Automation Controller. Available online: https://cms-cdn.selinc.com/assets/Literature/Product%20Literature/Data%20Sheets/3555_DS_20200224.pdf. Accessed: December 18, 2021.
- [25] Schweitzer Engineering Laboratories, SEL-3555-2 Real-Time Automation Controller (RTAC). Available online: https://cms-cdn.selinc.com/assets/Literature/Product%20Literature/Data%20Sheets/3555-2_DS_20210720.pdf. Accessed: December 18, 2021.
- [26] Cisco, Cisco Catalyst IE3400 Rugged Series Data Sheet, August 31, 2021. Available online: <https://www.cisco.com/c/en/us/products/collateral/switches/catalyst-ie3400-rugged-series/cat-ie3400-rugged-series-ds.html>. Accessed: December 18, 2021.
- [27] Linux PTP, The Linux PTP Project. Available online: <http://linuxptp.sourceforge.net/>. Accessed: December 18, 2021.
- [28] Whitehead, D. E., Owens, K., Gammel, D., and Smith, J. Ukraine Cyber-Induced Power Outage: Analysis and Practical Mitigation Strategies, *2017 70th Annual Conference for Protective Relay Engineers (CPRE)*, College Station, Texas, April 3–6, 2017, 1–8. <https://doi.org/10.1109/CPRE.2017.8090056>.
- [29] Pyinfra, pyinfra. Available online: <https://pyinfra.com/>. Accessed: December 18, 2021.
- [30] Tmux, tmux/tmux, GitHub. Available online: <https://github.com/tmux/tmux>. Accessed: December 18, 2021.
- [31] Grafana Labs, Grafana documentation. Available online: <https://grafana.com/docs/grafana/latest/>. Accessed: December 18, 2021.

- [32] Prometheus, Prometheus - Monitoring System & Time Series Database. Available online: <https://prometheus.io/>. Accessed: December 18, 2021.
- [33] InfluxData, Telegraf Open Source Server Agent: Influxdb, 2021. Available online: <https://www.influxdata.com/time-series-platform/telegraf/>. Accessed: December 18, 2021.
- [34] IEC 61850-8-1:2011+AMD1:2020 CSV. Available online: <https://webstore.iec.ch/publication/66585>. Accessed: December 18, 2021.
- [35] IEC 61850-90-2. IEC TR 61850-90-2:2016. Available online: <https://webstore.iec.ch/publication/24249>. Accessed: December 18, 2021.
- [36] Johansen, P., Substation monitoring and control, Part 1: Capacitive voltage measurement. <http://jomitek.dk/downloads/Substation%20monitoring%20and%20control.pdf>. Accessed: December 18, 2021.
- [37] Firouzia, S. R., Vanfretti, L., Ruiz-Alvarez, A., Hooshyar, H., and Mahmood, F., Interpreting and implementing IEC 61850-90-5 Routed-Sampled Value and Routed-GOOSE protocols for IEEE C37.118.2 compliant wide-area synchrophasor data transfer, *Electric Power Systems Research*, 144, 255–267, 2017. <https://doi.org/10.1016/j.epsr.2016.12.006>.
- [38] Kriger, C., Behardien, S., and Retonda-Modiya, J., A Detailed Analysis of the GOOSE Message Structure in an IEC 61850 Standard-Based Substation Automation System, *International Journal of Computers Communications & Control* 8(5), 708–721, 2013. <https://doi.org/10.15837/IJCCC.2013.5.329>.

APPENDIX A. Data floating points of protective relays and power meters

Table A. 1. Assessment of data floating points converted from hexadecimal to decimal values for the SEL-451 protective relays

N°	Item from dataset	Item description from the SEL-451 relay manual	Measurements from Wireshark file (Data_Nov3, Frame 3594)	
			08-hexadecimal	Decimal ^c
01	MET.METMMXU1.A2.phsA.instCVal.mag.f	Breaker 1 10-cycle average fundamental A phase current (magnitude) in amperes	08-42b63595	91.104652
02	MET.METMMXU1.A2.phsA.instCVal.ang.f	Breaker 1 10-cycle average fundamental A phase current (angle) in degrees	08-c035dc00	-2.8415527
03	MET.METMMXU1.A2.phsB.instCVal.mag.f	Breaker 1 10-cycle average fundamental B phase current (magnitude) in amperes	08-42b35484	89.665070
04	MET.METMMXU1.A2.phsB.instCVal.ang.f	Breaker 1 10-cycle average fundamental B phase current (angle) in degrees	08-c2f4a4e8	-122.32208
05	MET.METMMXU1.A2.phsC.instCVal.mag.f	Breaker 1 10-cycle average fundamental C phase current (magnitude) in amperes	08-42b3689a	89.704300
06	MET.METMMXU1.A2.phsC.instCVal.ang.f	Breaker 1 10-cycle average fundamental C phase current (angle) in degrees	08-42e9464c	116.63730
07	MET.METMMXU1.Hz.instMag.f	Measured system frequency in hertz	08-4270002e	60.000175
08	MET.METMMXU1.PhV.phsA.instCVal.mag.f	10-cycle average fundamental A phase voltage (magnitude) in kilovolts	08-40e3cbeb	7.1186423
09	MET.METMMXU1.PhV.phsA.instCVal.ang.f	10-cycle average fundamental A phase voltage (angle) in degrees	08-bb330000	-0.002731
10	MET.METMMXU1.PhV.phsB.instCVal.mag.f	10-cycle average fundamental B phase voltage (magnitude) in kilovolts	08-40e3bfbf	7.1171565
11	MET.METMMXU1.PhV.phsB.instCVal.ang.f	10-cycle average fundamental B phase voltage (angle) in degrees	08-c2eff11b	-119.97091
12	MET.METMMXU1.PhV.phsC.instCVal.mag.f	10-cycle average fundamental C phase voltage (magnitude) in kilovolts	08-40e399f0	7.1125412
13	MET.METMMXU1.PhV.phsC.instCVal.ang.f	10-cycle average fundamental C phase voltage (angle) in degrees	08-42effade	119.98997
14	MET.METMMXU1.TotVAr.instMag.f	Fundamental reactive three-phase power in megavolt amps reactive	08-3dc3bc53	0.0955740
15	MET.METMMXU1.TotW.instMag.f	Fundamental real three-phase power in megawatts	08-3ff60e10	1.9223042
16	MET.METMMXU1.TotPF.instMag.f	Three-phase displacement power factor (unity)	08-3f7faf29	0.9987664
17	MET.METMMXU1.Hz.t	Time stamp from measured system frequency ^a	Nov 3, 2021, 15:28:14.503599941 UTC	
18	PRO.BK1XCBR1.Pos.stVal	Circuit Breaker 1, Pole A closed/open ^b	80	

^aThe time stamp is not set as hexadecimal value, and it was collected from the frequency for the SEL-451 relays

^bThe circuit breaker states are not set as hexadecimal values (80 = closed breaker, 40 = open breaker)

^cThe decimal values were calculated from [IEEE-754 Floating-Point Conversion from 32-bit Hexadecimal to Floating-Point \(cuny.edu\)](http://IEEE-754 Floating-Point Conversion from 32-bit Hexadecimal to Floating-Point (cuny.edu))

Table A. 2. Assessment of data floating points converted from hexadecimal to decimal values for the SEL-735 power meters

N°	Item from dataset	Item description from the SEL-735 power meter manual	Measurements from Wireshark file (Data_Nov22, Frame 3428)	
			08-hexadecimal	Decimal ^b
01	MET.FUNDMMXU1.A.phsA.instCVal.mag.f	I_a current magnitude in amperes	08-423142c1	44.315189
02	MET.FUNDMMXU1.A.phsA.instCVal.ang.f	I_a current angle in degrees	08-c104e90b	-8.3068953
03	MET.FUNDMMXU1.A.phsB.instCVal.mag.f	I_b current magnitude in amperes	08-4243500a	48.828163
04	MET.FUNDMMXU1.A.phsB.instCVal.ang.f	I_b current angle in degrees	08-c300349e	-128.20554
05	MET.FUNDMMXU1.A.phsC.instCVal.mag.f	I_c current magnitude in amperes	08-422f68e6	43.852440
06	MET.FUNDMMXU1.A.phsC.instCVal.ang.f	I_c current angle in degrees	08-42df1be5	111.55448
07	MET.FUNDMMXU1.PhV.phsA.instCVal.mag.f	V_{an} voltage magnitude in kilovolts	08-40e364be	7.1060476
08	MET.FUNDMMXU1.PhV.phsA.instCVal.ang.f	V_{an} voltage angle in degrees	08-00000000	0.0000000
09	MET.FUNDMMXU1.PhV.phsB.instCVal.mag.f	V_{bn} voltage magnitude in kilovolts	08-40e1dc17	7.0581164
10	MET.FUNDMMXU1.PhV.phsB.instCVal.ang.f	V_{bn} voltage angle in degrees	08-c2f0743a	-120.22701
11	MET.FUNDMMXU1.PhV.phsC.instCVal.mag.f	V_{cn} voltage magnitude in kilovolts	08-40e282b8	7.0784569
12	MET.FUNDMMXU1.PhV.phsC.instCVal.ang.f	V_{cn} voltage angle in degrees	08-42efa5ed	119.82407
13	MET.FUNDMMXU1.Hz.instMag.f	Measured system frequency in hertz	08-42700000	60.000000
14	MET.FUNDMMXU1.TotVAr.instMag.f	Fundamental reactive three-phase power in kilovolt amps reactive	08-4309fa74	137.97833
15	MET.FUNDMMXU1.TotW.instMag.f	Fundamental real three-phase power in watts	08-4470052e	960.08093
16	MET.FUNDMMXU1.TotPF.instMag.f	Three-phase displacement power factor	08-3f7d654b	0.9898268
17	MET.FUNDMMXU1.Hz.t	Time stamp from measured system frequency ^a	Nov 22, 2021, 15:55:52.292297363 UTC	

^aThe time stamp is not set as hexadecimal value, and it was collected from the frequency for the SEL-735 power meters

^bThe decimal values were calculated from [IEEE-754 Floating-Point Conversion from 32-bit Hexadecimal to Floating-Point \(cuny.edu\)](https://www.cuny.edu/~math/ieee-754-floating-point-conversion-from-32-bit-hexadecimal-to-floating-point/)

Table A. 3. Assessment of data floating points converted to measured values for the SEL-734 power meters

Nº	Tag name from target processor of the SEL-3530-4 RTAC	Item description from SEL-734 power meter manual	Measurements from Wireshark file (RTAC_WITH_SEL_734_POWER_METERS – Frame 43)		
			Multiply by F	Data floating point value (DP_V)	Measured value ($M_V = DP_V \times F$)
01	SEL_734_1_DNP.AI_000_IA_MAG	I_a current magnitude in amperes	0.1	458	45.8
02	SEL_734_1_DNP.AI_001_IA_ANG	I_a current angle in degrees	0.01	–598	–5.98
03	SEL_734_1_DNP.AI_002_IB_MAG	I_b current magnitude in amperes	0.1	469	46.9
04	SEL_734_1_DNP.AI_003_IB_ANG	I_b current angle in degrees	0.01	–12,827	–128.27
05	SEL_734_1_DNP.AI_004_IC_MAG	I_c current magnitude in amperes	0.1	470	47.0
06	SEL_734_1_DNP.AI_005_IC_ANG	I_c current angle in degrees	0.01	11,193	111.93
07	SEL_734_1_DNP.AI_006_VA_MAG	V_{an} voltage magnitude in kilovolts	0.1	71	7.1
08	SEL_734_1_DNP.AI_007_VA_ANG	V_{an} voltage angle in degrees	0.01	0	0.00
09	SEL_734_1_DNP.AI_008_VB_MAG	V_{bn} voltage magnitude in kilovolts	0.1	70	7.0
10	SEL_734_1_DNP.AI_009_VB_ANG	V_{bn} voltage angle in degrees	0.01	–12,034	–120.34
11	SEL_734_1_DNP.AI_010_VC_MAG	V_{cn} voltage magnitude in kilovolts	0.1	71	7.1
12	SEL_734_1_DNP.AI_011_VC_ANG	V_{cn} voltage angle in degrees	0.01	11,969	119.69
13	SEL_734_1_DNP.AI_012_FREQUENCY	Measured system frequency in hertz	0.01	6,000	60.00
14	SEL_734_1_DNP.AI_013_MW3	Fundamental real three-phase power in watts	100	9	900
15	SEL_734_1_DNP.AI_014_MVR3	Fundamental reactive three-phase power in kilovolt amps reactive	100	1	100
16	SEL_734_1_DNP.AI_015_PF3	Three-phase displacement power factor (unity)	0.01	99	0.99